

Available online at [www.sciencedirect.com](http://www.sciencedirect.com)

SCIENCE @ DIRECT®

Science of the Total Environment xx (2006) xxx–xxx

Science of the  
Total EnvironmentAn International Journal for Scientific Research  
into the Environment and its Relationship with Humankind[www.elsevier.com/locate/scitotenv](http://www.elsevier.com/locate/scitotenv)

Review

## Quantifying submarine groundwater discharge in the coastal zone via multiple methods

W.C. Burnett <sup>a,\*</sup>, P.K. Aggarwal <sup>b</sup>, A. Aureli <sup>c</sup>, H. Bokuniewicz <sup>d</sup>, J.E. Cable <sup>e</sup>,  
M.A. Charette <sup>f</sup>, E. Kontar <sup>g</sup>, S. Krupa <sup>h</sup>, K.M. Kulkarni <sup>b</sup>, A. Loveless <sup>i</sup>, W.S. Moore <sup>j</sup>,  
J.A. Oberdorfer <sup>k</sup>, J. Oliveira <sup>l</sup>, N. Ozyurt <sup>m</sup>, P. Povinec <sup>n,1</sup>, A.M.G. Privitera <sup>o</sup>, R. Rajar <sup>p</sup>,  
R.T. Ramessur <sup>q</sup>, J. Scholten <sup>n</sup>, T. Stieglitz <sup>r,s</sup>, M. Taniguchi <sup>t</sup>, J.V. Turner <sup>u</sup>

<sup>a</sup> Department of Oceanography, Florida State University, Tallahassee, FL 32306, USA<sup>b</sup> Isotope Hydrology Section, International Atomic Energy Agency, Austria<sup>c</sup> Department Water Resources Management, University of Palermo, Catania, Italy<sup>d</sup> Marine Science Research Center, Stony Brook University, USA<sup>e</sup> Department Oceanography, Louisiana State University, USA<sup>f</sup> Department Marine Chemistry, Woods Hole Oceanographic Institution, USA<sup>g</sup> Shirshov Institute of Oceanology, Russia<sup>h</sup> South Florida Water Management District, USA<sup>i</sup> University of Western Australia, Australia<sup>j</sup> Department Geological Sciences, University of South Carolina, USA<sup>k</sup> Department Geology, San Jose State University, USA<sup>l</sup> Instituto de Pesquisas Energéticas e Nucleares, Brazil<sup>m</sup> Department Geological Engineering, Hacettepe, Turkey<sup>n</sup> Marine Environment Laboratory, International Atomic Energy Agency, Monaco<sup>o</sup> U.O. 4.17 of the G.N.D.C.I., National Research Council, Italy<sup>p</sup> Faculty of Civil and Geodetic Engineering, University of Ljubljana, Slovenia<sup>q</sup> Department Chemistry, University of Mauritius, Mauritius<sup>r</sup> Mathematical and Physical Sciences, James Cook University, Australia<sup>s</sup> Australian Institute of Marine Sciences, Townsville, Australia<sup>t</sup> Research Institute for Humanity and Nature, Japan<sup>u</sup> CSIRO, Land and Water, Perth, Australia

Received 3 February 2006; received in revised form 1 May 2006; accepted 4 May 2006

### Abstract

Submarine groundwater discharge (SGD) is now recognized as an important pathway between land and sea. As such, this flow may contribute to the biogeochemical and other marine budgets of near-shore waters. These discharges typically display significant spatial and temporal variability making assessments difficult. Groundwater seepage is patchy, diffuse, temporally variable, and may involve multiple aquifers. Thus, the measurement of its magnitude and associated chemical fluxes is a challenging enterprise.

\* Corresponding author. Tel.: +1 850 644 6703; fax: +1 850 644 2581.

E-mail address: [wburnett@mail.fsu.edu](mailto:wburnett@mail.fsu.edu) (W.C. Burnett).

<sup>1</sup> Present address: Comenius University, Bratislava, Slovakia.

A joint project of UNESCO and the International Atomic Energy Agency (IAEA) has examined several methods of SGD assessment and carried out a series of five intercomparison experiments in different hydrogeologic environments (coastal plain, karst, glacial till, fractured crystalline rock, and volcanic terrains). This report reviews the scientific and management significance of SGD, measurement approaches, and the results of the intercomparison experiments. We conclude that while the process is essentially ubiquitous in coastal areas, the assessment of its magnitude at any one location is subject to enough variability that measurements should be made by a variety of techniques and over large enough spatial and temporal scales to capture the majority of these changing conditions.

We feel that all the measurement techniques described here are valid although they each have their own advantages and disadvantages. It is recommended that multiple approaches be applied whenever possible. In addition, a continuing effort is required in order to capture long-period tidal fluctuations, storm effects, and seasonal variations.

© 2006 Elsevier B.V. All rights reserved.

**Keywords:** Submarine groundwater discharge; Coastal zone management; Seepage meters; Radon; Radium isotopes; Tracers

## Contents

|        |   |   |
|--------|---|---|
| 1.     | Introduction . . . . .  | 0 |
| 1.1.   | Background . . . . .  | 0 |
| 1.2.   | Significance of SGD . . . . .                                 | 0 |
| 1.3.   | Definition of submarine groundwater discharge . . . . .       | 0 |
| 1.4.   | Drivers of SGD . . . . .                                      | 0 |
| 2.     | A short history of SGD research . . . . .                     | 0 |
| 2.1.   | Overview. . . . .   | 0 |
| 2.2.   | Worldwide studies . . . . .                                   | 0 |
| 2.3.   | The IAEA/UNESCO SGD initiative. . . . .                       | 0 |
| 3.     | Methods used to measure SGD . . . . .                         | 0 |
| 3.1.   | Seepage meters . . . . .                                      | 0 |
| 3.2.   | Piezometers . . . . .   | 0 |
| 3.3.   | Natural tracers . . . . .                                     | 0 |
| 3.4.   | Water balance approaches . . . . .                            | 0 |
| 3.5.   | Hydrograph separation techniques . . . . .                    | 0 |
| 3.6.   | Theoretical analysis and numerical simulations . . . . .      | 0 |
| 4.     | Coastal zone management implications of SGD . . . . .         | 0 |
| 5.     | The UNESCO/IAEA joint SGD intercomparison activities. . . . . | 0 |
| 5.1.   | Cockburn Sound, Australia . . . . .                           | 0 |
| 5.1.1. | Introduction. . . . .   | 0 |
| 5.1.2. | Seepage meters . . . . .                                      | 0 |
| 5.1.3. | Radium isotopes . . . . .                                     | 0 |
| 5.1.4. | Radon. . . . .  | 0 |
| 5.1.5. | Summary . . . . .   | 0 |
| 5.2.   | Donnalucata, Sicily . . . . .                                 | 0 |
| 5.2.1. | Introduction. . . . .   | 0 |
| 5.2.2. | Study area and geophysical characterization . . . . .         | 0 |
| 5.2.3. | Isotopic analyses . . . . .                                   | 0 |
| 5.2.4. | SGD evaluations . . . . .                                     | 0 |
| 5.3.   | Shelter Island, New York . . . . .                            | 0 |
| 5.3.1. | Introduction. . . . .   | 0 |
| 5.3.2. | Seepage meters . . . . .                                      | 0 |
| 5.3.3. | Radon and radium isotopes. . . . .                            | 0 |
| 5.3.4. | Geophysical studies. . . . .                                  | 0 |
| 5.3.5. | Summary . . . . .   | 0 |
| 5.4.   | Ubatuba, Brazil . . . . .                                     | 0 |
| 5.4.1. | Introduction. . . . .   | 0 |
| 5.4.2. | Geophysical studies. . . . .                                  | 0 |
| 5.4.3. | Seepage meters . . . . .                                      | 0 |

|        |   |   |
|--------|---|---|
| 5.4.4. | Artificial tracer approach. . . . .           | 0 |
| 5.4.5. | Radon and radium isotopes . . . . .           | 0 |
| 5.4.6. | Summary. . . . .                              | 0 |
| 5.5.   | Mauritius . . . . .                           | 0 |
| 5.5.1. | Introduction . . . . .                        | 0 |
| 5.5.2. | Water balance estimate. . . . .               | 0 |
| 5.5.3. | Seepage meters. . . . .                       | 0 |
| 5.5.4. | Radon . . . . .                               | 0 |
| 5.5.5. | Summary. . . . .                              | 0 |
| 6.     | Overall findings and recommendations. . . . . | 0 |
|        | Acknowledgments . . . . .                     | 0 |
|        | References . . . . .                          | 0 |

## 1. Introduction

### 1.1. Background

Submarine groundwater discharge (SGD) has been recognized as an important pathway for material transport to the marine environment. It is important for the marine geochemical cycles of elements and can lead to environmental deterioration of coastal zones. While inputs from major rivers are gauged and well analyzed, thus allowing relatively precise estimates of freshwater and contaminant inputs to the ocean, assessing groundwater fluxes and their impacts on the near-shore marine environment is much more difficult, as there is no simple means to gauge these fluxes to the sea. In addition, there are cultural and disciplinary differences between hydrogeologists and coastal oceanographers which have inhibited interactions.

The direct discharge of groundwater into the near-shore marine environment may have significant environmental consequences because groundwater in many areas has become contaminated with a variety of substances like nutrients, heavy metals, radionuclides and organic compounds. As almost all coastal zones are subject to flow of groundwater either as submarine springs or disseminated seepage, coastal areas are likely to experience environmental degradation. Transport of nutrients to coastal waters may trigger algae blooms, including harmful algae blooms, having negative impacts on the economy of coastal zones (LaRoche et al., 1997).

We present here a review of the subject and the results of a recently completed project initiated as a concerted effort to improve the measurement situation by development of an expert group to: (1) assess the importance of SGD in different environments; and (2) to organize a series of “intercomparison experiments” involving both hydrological and oceanographic personnel and techniques.

### 1.2. Significance of SGD

It is now recognized that subterranean non-point pathways of material transport may be very important in some coastal areas (Moore, 1999; Charette and Sholkovitz, 2002). Because the slow, yet persistent seepage of groundwater through sediments will occur anywhere that an aquifer with a positive head relative to sea level is hydraulically connected to a surface water body, almost all coastal zones are subject to such flow (Johannes, 1980; Fanning et al., 1981; Church, 1996; Moore, 1996; Li et al., 1999; Hussain et al., 1999; Taniguchi and Iwakawa, 2001; Kim and Hwang, 2002). Groundwater seepage is patchy, diffuse, temporally variable, and may involve multiple aquifers. Reliable methods to measure these fluxes need to be refined and the relative importance of the processes driving the flow needs clarification and quantification.

Specific examples of the ecological impact of groundwater flow into coastal zones have been given by Valiela et al. (1978, 1992, 2002), who showed that groundwater inputs of nitrogen are critical to the overall nutrient economy of salt marshes. Corbett et al. (1999, 2000) estimated that groundwater nutrient inputs are approximately equal to nutrient inputs via surface freshwater runoff in eastern Florida Bay. Krest et al. (2000) estimated that SGD to salt marshes on the South Carolina coast supplies a higher flux of nutrients than that derived from all South Carolina rivers. Bokuniewicz (1980) and Bokuniewicz and Pavlik (1990) showed that subsurface discharge accounts for greater than 20% of the freshwater input into the Great South Bay, New York. Follow-up studies by Capone and Bautista (1985) and Capone and Slater (1990) showed that groundwater is a significant source (~50%) of nitrate to the bay. Lapointe et al. (1990) found significant groundwater inputs of nitrogen and dissolved organic phosphorus to canals and surface waters in the

Florida Keys and suggested this may be a key factor for initiating the phytoplankton blooms observed in that area. Nitrogen-rich groundwater is also suspected of nourishing *Cladophora* algal mats in Harrington Sound, Bermuda (Lapointe and O'Connell, 1989). One possible hypothesis for the triggering mechanism of Harmful Algal Blooms (HABs) is increased nutrient supply via SGD (LaRoche et al., 1997; Hwang et al., 2005). In many of the cases cited above, shallow groundwaters were enriched in nitrogen because of contamination from septic systems. In a more pristine environment, submarine springs were shown to cause measurable dilution of salinity and enrichment of nitrogen in Discovery Bay, Jamaica (D'Elia et al., 1981). Groundwater was also shown to be a significant component of terrestrial nutrient and freshwater loading to Tomales Bay, California (Oberdorfer et al., 1990). Johannes (1980), investigating coastal waters in Western Australia, stated that "it is ... clear that submarine groundwater discharge is widespread and, in some areas, of greater ecological significance than surface runoff."

### 1.3. Definition of submarine groundwater discharge

We have noted confusion in the literature concerning use of the term "groundwater discharge" (e.g., see comment to Moore, 1996 by Younger, 1996 and subsequent reply on whether groundwater<sup>2</sup> is meteorically derived or "any water in the ground"). The most general and frequently cited definition of groundwater is water within the saturated zone of geologic material (e.g., Freeze and Cherry, 1979; Jackson, 1977); in other words, water in the pores of submerged sediments ("pore water") is synonymous with "groundwater." We thus consider "submarine groundwater discharge" to be any flow of water out across the sea floor. We define SGD without regard to its composition (e.g., salinity), its origin, or the mechanism(s) driving the flow (Burnett et al., 2003a). Although our broad definition of SGD would technically allow inclusion of such processes as deep-sea hydrothermal circulation, fluid expulsion at convergent margins, and density-driven cold seeps on

continental slopes, we restrict the term here (and thus focus our attention) to fluid circulation through continental shelf sediments with emphasis on the coastal zone (Fig. 1).

Traditional hydrology, however, has been concerned with terrestrial freshwater. As a result, some definitions identify groundwater as rainwater that has infiltrated and percolated to the water table, or put on some similar qualifications, consistent with the applications to freshwater, terrestrial systems (e.g., Considine, 1995; Stieglar, 1977). Such qualifications on the definition of groundwater are too restrictive and lead to conceptual problems when dealing with submarine discharges. In our view, SGD does not have to be terrestrially derived, although it can be and is in many important situations. It may be legitimate to require water classified as "groundwater" to move, when it does move, according to Darcy's Law,<sup>3</sup> but even that is too restrictive in some highly channelized (e.g. karst) situations. At least one definition of groundwater specifically excludes underground streams (Wyatt, 1986) while another specifically includes underground streams (Bates and Jackson, 1984; Jackson, 1977). Since karst is such an important setting for SGD, we think it best to include "underground streams."

So we have a system of terminology as follows. The flow of water across the sea floor can be divided into SGD, a discharging flow *out* across the sea floor, or submarine groundwater recharge (SGR), a recharging flow *in* across the sea floor. The two terms do not have to balance, however, because SGD can, and often will, include a component of terrestrially recharged water. Alternatively, some or all of the SGR can penetrate the subaerial aquifer, raising the water table or discharging as terrestrial surface waters (e.g., saline springs) rather

<sup>2</sup> The modern convention is to write "groundwater" as one word. The early practice was to write it as two words and hyphenated (or compounded) when used as an adjective. This usage is becoming more rare, although it is still the convention of the U.S. Geological Survey and the journal Ground Water. Writing it as one word may be done to emphasize "the fact that it is a technical term with a particular meaning" (Todd, 1980).

<sup>3</sup> Whose law is it anyway? Darcy's? D'Arcy's? d'Arcy's? D'Arcys'? Darcys'? D'Arcys? Darcys? Or even, Darcies? You will find them all in the literature or on the WEB. The correct version is "Darcy's" (Brown et al., 2000). Although the man was born d'Arcy, his Jacobin tutor compelled him to change it to Darcy at an early age, a convention he permanently adopted (Darcy, 1957 as cited in Brown et al., 2000). "Darcy" is the name on his tombstone, although we have it on good authority that Elvis Presley's name is misspelled on his tombstone so perhaps the grave marker is not necessarily definitive. (But, then again, maybe Elvis's not really dead either). We are indebted to Glenn Brown for his scholarship in sorting this all out. There might be a slim case made for "Darcys" based on the convention in geography to drop the possessive apostrophe (e.g. "Gardiners Island" not "Gardiner's Island"). However, this is not the convention in physics and chemistry (e.g. Newton's Laws or Henry's Law). You, and Henry Darcy, apparently can possess a law.

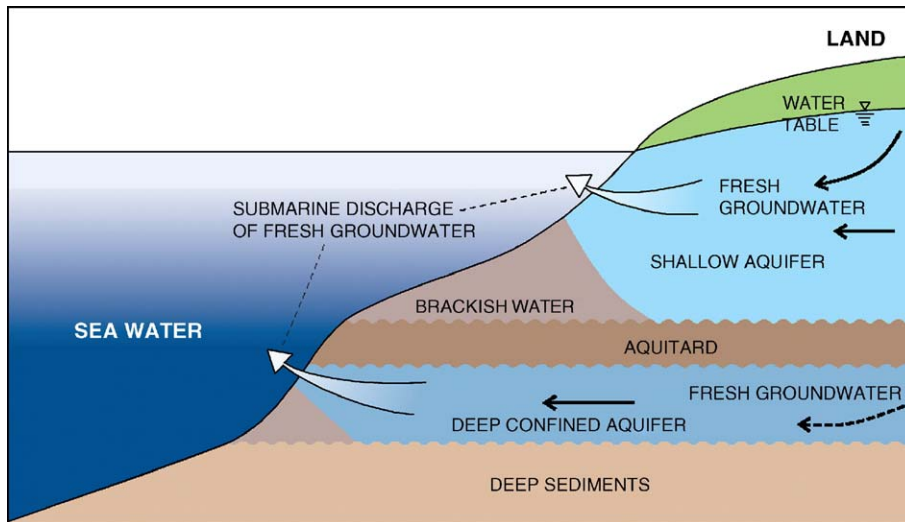


Fig. 1. Schematic depiction (no scale) of processes associated with SGD. Arrows indicate fluid movement.

than discharging out across the sea floor. The net discharge is the difference between these two components.

Coastal aquifers may consist of complicated arrays of confined, semi-confined, and unconfined systems. Simple hydrologic models do not consider the anisotropic nature of coastal sediments, dispersion, and tidal pumping. Moreover, cycling of seawater through the coastal aquifer may be driven by the flow of freshwater from coastal uplands (Destouni and Prieto, 2003). As freshwater flows through an aquifer driven by an inland hydraulic head, it can entrain seawater that is diffusing and dispersing up from the salty aquifer that underlies it. Superimposed upon this terrestrially driven circulation are a variety of marine-induced forces that result in flow into and out of the seabed even in the absence of a hydraulic head. Such “subterranean estuaries” (Moore, 1999) will be characterized by biogeochemical reactions that influence the transfer of nutrients to the coastal zone in a manner similar to that of surface estuaries (Nixon et al., 1996; Charette and Sholkovitz, 2002; Talbot et al., 2003).

#### 1.4. Drivers of SGD

SGD forcing has both terrestrial and marine components. The following drivers of fluid flow through shelf sediments may be considered: (1) the terrestrial hydraulic gradient (gravity) that results in water flowing downhill; (2) water level differences across a permeable barrier; (3) tide, wave, storm, or current-induced pressure gradients in the near-shore zone; (4) convection (salt-fingering) induced by salty water overlying fresh

groundwater in some near-shore environments; (5) seasonal inflow and outflow of seawater into the aquifer resulting from the movement of the freshwater–seawater interface in response to annual recharge cycles; and (6) geothermal heating.

Hydrologists have traditionally applied Darcy’s Law to describe the freshwater flow resulting from measured hydraulic gradients. However, when comparisons have been made, the modeled outflow is often much less than what is actually measured (e.g., Smith and Zawadzki, 2003). Differences in water levels across permeable narrow reefs such as the Florida Keys (Reich et al., 2002; Chanton et al., 2003) or barrier islands such as Fire Island, New York (Bokuniewicz and Pavlik, 1990) are also known to induce subterranean flow. Such differences in sea level could be the result of tidal fluctuations, wave set-up, or wind forcing. Pressure gradients due to wave set-up at the shore (Li et al., 1999), tidal pumping at the shore (Riedl et al., 1972; Nielsen, 1990), large storms (Moore and Wilson, 2005), or current-induced gradients over topographic expressions such as sand ripples also result in SGD (Huettel and Gust, 1992; Huettel et al., 1996). If the density of the ocean water increases above that of the pore water for any reason, pore water can float out of the sediment by gravitational convection in an exchange with denser seawater without a net discharge (Webster et al., 1996). Moore and Wilson (2005) documented the exchange of pore water to a depth of 1.5 m following an intrusion of cold water onto the shelf.

An annual recharge cycle causing a seasonal inflow and outflow of seawater within an unconfined coastal aquifer is a new concept introduced by a team at MIT



(Michael et al., 2005). This group had shown earlier via a seepage meter survey of Waquoit Bay that the groundwater discharge was largely saline (Michael et al., 2003). To explain the source and timing of the high flux of salty water (highest discharge in early summer), these investigators proposed a seasonal shift in the freshwater–seawater interface in response to the annual recharge cycle (highest recharge in the early spring). As the water table rises in response to enhanced recharge, more freshwater is drawn from further inland displacing salty groundwater and causing it to be discharged offshore (Fig. 2). The opposite pattern occurs during the period of maximum evapotranspiration in the summer and saltwater flows into the aquifer. A numerical model predicted that there would be a time lag of up to 3 months for the interface to move through the aquifer. So the observed maximum discharge in the early summer is thought to have been generated by the maximum water table thickness that occurred following greatest recharge in the early spring.

From an oceanographic point of view, the total (fresh + seawater) SGD flux is important because all flow enhances biogeochemical inputs. Hydrologists have typically been concerned with the freshwater flow and seawater intrusion along the coast. The terrestrial and oceanic forces overlap in space and time; thus, measured fluid flow through coastal sediments is a result of composite forcing.

Seepage meter records that display temporal trends in near-shore regions typically show variations that correspond to the tidal period in that area. For example, Lee (1977) showed that seepage rates were distinctly higher at low tide. While some correspondence between tides and seepage flux is typical for near-shore

environments, the timing of the seepage maximum relative to the tidal stage varies depending upon the hydrologic setting at each location. Some areas show a direct inverse correlation between seepage rate and tidal stage, probably reflecting a modulation of a terrestrially driven flow by changing hydrostatic pressure. In other situations, tidal pumping or wave set-up recharges the coastal aquifer with seawater on the flood tide that discharges seaward at a later time, complicating this simple picture (Nielsen, 1990).

Recent investigations have reported longer-term (weeks to months) tidally modulated cycles in seepage based on continuous measurements of the groundwater tracers radon and methane (Kim and Hwang, 2002) and automated seepage meter observations. Taniguchi (2002) continuously recorded seepage flux rates in Osaka Bay, Japan, from May to August 2001 and analyzed these data via the Fast Fourier Transfer (FFT) method to discern the dominant periods of variation (Fig. 3). Both studies showed that there is not only a semi-diurnal to diurnal tidal relationship to SGD but also a semi-monthly variation in flow reflecting the neap–spring lunar cycle. Superimposed on this predictable behavior in tidally driven response, are variations in terrestrial hydrologic parameters (water table height, etc.). This terrestrial influence showed up in tracer data from Korea, where Kim and Hwang (2002) noted that groundwater discharge was more limited in the dry season when the aquifer was not recharging. These results demonstrate the overlapping nature between terrestrial and marine SGD forcing components.

In the coastal zone, discharges influenced by terrestrial and marine forces are typically coincident in time and space but may differ significantly in

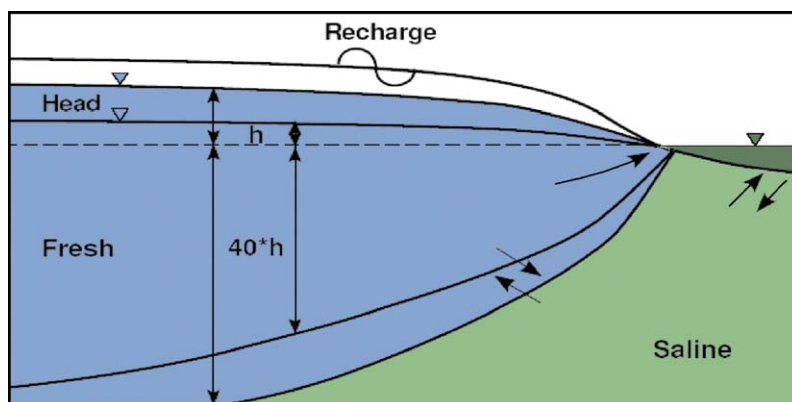


Fig. 2. Schematic showing how interface position may shift within an unconsolidated aquifer in response to aquifer head level according to Ghyben–Herzberg relation. Because of differences in density between freshwater and seawater, seasonal changes in recharge will generate corresponding changes in the interface that would be magnified by  $\sim 40\times$  (density of fresh water divided by the difference in densities). Diagram from Michael et al. (2005).

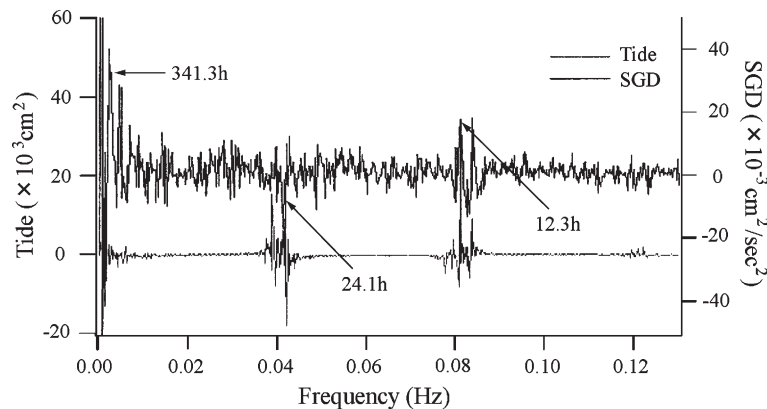


Fig. 3. Time series analysis (FFT method) of long-term SGD measurements and tides in Osaka Bay, Japan, from May 29 to August 23, 2001. The main SGD frequencies correspond to semi-diurnal (12.3 h), diurnal (24.1 h), and bi-weekly (341.3 h) lunar cycles (Taniguchi, 2002).

magnitude. Since the hydraulic gradient of a coastal aquifer, tidal range, and position of the freshwater–seawater interface change over time; it is possible that the situation in any one area could shift (e.g., seasonally) between terrestrially governed and marine dominated systems.

## 2. A short history of SGD research

### 2.1. Overview

Knowledge concerning the undersea discharge of fresh groundwater has existed for many centuries. According to Kohout (1966), the Roman geographer, Strabo, who lived from 63 BC to 21 AD, mentioned a submarine spring 2.5 miles offshore from Latakia, Syria, near the island of Aradus in the Mediterranean. Water from this spring was collected from a boat, utilizing a lead funnel and leather tube, and transported to the city as a source of freshwater. Other historical accounts tell of water vendors in Bahrain collecting potable water from offshore submarine springs for shipboard and land use (Williams, 1946), Etruscan citizens using coastal springs for “hot baths” (Pausanias, ca. 2nd century AD), and submarine “springs bubbling freshwater as if from pipes” along the Black Sea (Pliny the Elder, ca. 1st century AD).

The offshore discharge of freshwater has been investigated and used in a number of cases for water resource purposes. One particularly spectacular example of such use involved the construction of dams in the sea near the southeastern coast of Greece. The resulting “fence” allowed the formation of a freshwater lake in the sea that was then used for irrigation on the adjacent coastal lands (Zektser, 1996). Thus, while the existence of the direct discharge of groundwater into the sea has been realized for many years, the impetus was largely

from water resource considerations and much of the information was anecdotal.

Groundwater hydrologists have traditionally been primarily concerned with identifying and maintaining potable groundwater reserves. At the shoreline, their interest is naturally directed landward and attention has been focused only on the identification of the saltwater/freshwater “interface” in coastal aquifers. The classic Ghyben–Herzberg relationship sufficed in many practical applications in unconfined aquifers (Baydon-Ghyben, 1888–1889; Herzberg, 1901 both as cited in Bear et al., 1999) even though it represented an unrealistic, hydrostatic situation. The gravitational balance between the fresh groundwater and the underlying salty groundwater cannot predict the geometry of the freshwater lens but only estimate the depth of the saltwater/freshwater interface if the elevation of the water table is measured. A truly stable, hydrostatic distribution, however, would find saline groundwater everywhere below sea level. Maintaining a freshwater lens requires a dynamic equilibrium supported by freshwater recharge. The Dupuit approximation (Dupuit, 1888, as cited in Freeze and Cherry, 1979) was incorporated to account for this equilibrium. The assumption is essentially that the flow of groundwater is entirely horizontal. In that treatment, the saltwater/freshwater interface is a sharp boundary across which there is no flow and which intersects the shoreline; the salty groundwater is stationary. None of this is strictly true and the Dupuit–Ghyben–Herzberg relationship leads to the awkward, but not debilitating, result that all the freshwater recharge had to escape exactly at the shoreline. Hubbert (1940) removed this awkwardness by introducing the concept of an outflow gap. The saltwater/freshwater interface was still sharp and was considered a boundary of no flow. The saline groundwater was still stationary, but the interface did not

intersect the shoreline. Rather it intersected the sea floor at some distance from shore leaving, a band or gap through which the fresh groundwater could escape into the sea. If the depth of the saltwater/freshwater interface at the shoreline is measured, the Dupuit–Ghyben–Herzberg methodology can be used, with this as a boundary condition, to calculate the width of the outflow gap (Vacher, 1988). Potential theory (Henry, 1964) and the Glover solution (Glover, 1964) provided independent means to calculate the size of this gap and the position of the saltwater/freshwater interface. These representations, simplified for calculational necessity, unfortunately could lead one to the mistaken impression that SGD is entirely freshwater derived from land. Hubbert (1940) had also pointed out that the interface was not necessarily sharp and that the cyclic flow of salty groundwater needed to maintain a transition zone must be driven by the presence of hydraulic gradients in the saline groundwater. It thus became recognized that the saline groundwater is not necessarily stationary.

With the development of numerical models, it became possible to calculate more realistic hydrodynamics. One early numerical model calculated the groundwater seepage into lakes (McBride and Pfannkuch, 1975). While this lacustrine seepage had nothing to do with the saltwater/freshwater interface, it is noteworthy because it was the first use of the notion of an exponential decrease to approximate the distribution of seepage rates offshore.

The next generations of models allowed the saline groundwater to circulate in response to hydraulic gradients but still prohibited flow across the “interface” although the interface itself might move. Modern, two-phase models recognize that water can cross isohalines and can track both salt and water in the continuum, and they allow density driven circulation as well as flows driven by other hydraulic gradients onshore. Bear et al. (1999) provide a review of the complex array of modern models. There is, however, a serious lack of data to calibrate and verify such models. In addition, dispersion is usually incorporated in a single parameter although it is recognized that numerous processes can cause salt dispersion on a wide range of time and space scales.

It is important to recognize that the Ghyben–Herzberg relationship cannot be used to estimate the width of the fresh–salt interface for semi-confined artesian aquifers. Such aquifers can leak freshwater or salt–freshwater mixtures for considerable distances from shore.

SGD was neglected scientifically for many years because of the difficulty in assessment and the perception that the process was unimportant. This perception is changing. Within the last several years there has

emerged recognition that in some cases, groundwater discharge into the sea may be both volumetrically and chemically important (Johannes, 1980). A decade after Johannes’ benchmark paper, Valiela and D’Elia (1990) published a compilation on the subject and stated, “We are very much in the exploratory stage of this field.” The exploration has continued and there is now growing agreement that groundwater inputs can be chemically and ecologically important to coastal waters.

As a result of this increased interest, the Scientific Committee on Oceanic Research (SCOR) formed two working groups (WG) to examine this emerging field more closely. SCOR WG-112 (“Magnitude of Submarine Groundwater Discharge and its Influence on Coastal Oceanographic Processes”) was established in 1997 to “define more accurately and completely how submarine groundwater discharge influences chemical and biological processes in the coastal ocean” (Burnett, 1999). This group published a special issue of *Biogeochemistry* on SGD in 2003 as their final product (Burnett et al., 2003b). WG-114 (“Transport and Reaction in Permeable Marine Sediments”) was established in 1999 to investigate the importance of fluid flow through permeable sediments to local and global biogeochemical cycling and its influence on surrounding environments (Boudreau et al., 2001). That group completed its work in 2003 with the introduction of a continuing conference on the subject, the “Gordon Research Conference on Permeable Sediments”.

## 2.2. Worldwide studies

Taniguchi et al. (2002) presented a review of all available studies that have attempted to estimate the magnitude of SGD or indicated that SGD in the area studied was significant. This compilation was limited to literature citations of discharge estimates using seepage meters, piezometers, and/or geochemical/geophysical tracers.

Locations of specific SGD estimates showed that many independent studies have been performed on the east coast of the United States, Europe, Japan, and Oceania (Fig. 4). Fewer studies have been done on the west coast of the US, South America, and Hawaii. They were unable to find any quantitative data from Africa, India, or China, though indications of groundwater discharge have been reported for Bangladesh (Moore, 1997) and Kenya (Kitheka, 1988).

## 2.3. The IAEA/UNESCO SGD initiative

An initiative on SGD was developed by the International Atomic Energy Agency (IAEA) and



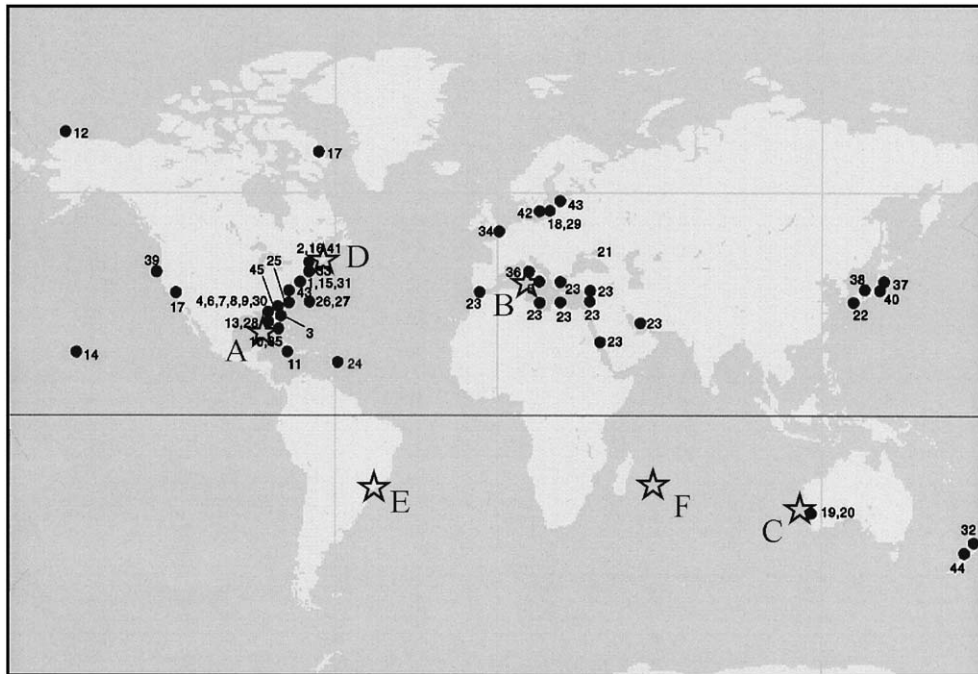


Fig. 4. Location of published investigations of submarine groundwater discharge (SGD). All studies used provided SGD estimations using seepage meters, piezometers, or geochemical/geophysical (temperature) tracers. Sites labeled “A” through “F” are locations where SGD assessment intercomparisons have been carried out. Site “A” was an initial experiment in Florida (Burnett et al., 2002) and “B” through “F” represent the five experiments reported in this paper. The numbers refer to 45 sites where SGD evaluations were identified by Taniguchi et al. (2002).

UNESCO in 2000 as a 5-year plan to assess methodologies and importance of SGD for coastal zone management. The IAEA component included a Coordinated Research Project (CRP) on “Nuclear and Isotopic Techniques for the Characterization of Submarine Groundwater Discharge (SGD) in Coastal Zones” carried out jointly by IAEA’s Isotope Hydrology Section in Vienna and the Marine Environment Laboratory in Monaco, together with nine laboratories from eight countries. The activities have included joint meetings (Vienna 2000, 2002, and 2005; Syracuse, Sicily 2001; and Monaco 2004), sampling expeditions (Australia 2000; Sicily 2001 and 2002; New York 2002; Brazil 2003; and Mauritius 2005), joint analytical work, data evaluation and preparation of joint publications. The objectives of the CRP included the improvement of capabilities for water resources and environmental management of coastal zones; application of recently developed nuclear and isotopic techniques suitable for quantitative estimation of various components of SGD; understanding of the influence of SGD on coastal processes and on groundwater regimes; a better management of groundwater resources in coastal areas; and development of numerical models of SGD.

The UNESCO component included sponsorship from the Intergovernmental Oceanographic Commission (IOC) and the International Hydrological Program (IHP). The

main objective of this aspect of the project was to provide both the scientific and coastal zone management communities with the tools and skills necessary to evaluate the influence of SGD in the coastal zone. A central part of this program was to define and test the most appropriate SGD assessment techniques via carefully designed intercomparison experiments. The plan was to run one experiment per year over approximately 5 years. The sites were selected based on a variety of criteria including logistics, background information, amount of SGD expected, hydrological and geological characteristics, etc. The intention was to include as many different hydrogeologic environments as possible (e.g., karst, coastal plain, volcanic, crystalline bedrock, glacial, etc.). Each systematic intercomparison exercise involved as many methodologies as possible including modeling approaches, “direct” measurements (e.g., seepage meters of varying design, piezometers), and natural tracer studies (e.g., radium isotopes, radon, methane, artificial tracers, etc.).

Because of differences in the nature and scale of each of these approaches, the final experimental design necessarily varied from site to site. The general experimental plan consisted of transects of piezometers (to measure the hydraulic gradients and conductivities), transects of bulk ground conductivity measurements, manual and automated seepage meters (to measure flow

directly), with specialized experiments and water sampling at appropriate points within the study area. Various seepage meter designs were evaluated during the field experiments. Water sampling for tracer studies was conducted while the hydrological measurements were in progress with most analyses being performed at the field site. Samples for geochemical tracers were collected from both the water column as well as from the aquifer itself. The specific sampling plan for tracer samples was determined by the spatial and temporal variations expected at each site.

The IAEA/UNESCO group developed the following list of desirable characteristics for “flagship” site(s) to perform such intercomparisons. These were not intended to be representative sites of SGD, but rather sites where the processes could be evaluated and methods compared with minor complications.

- (1) *General characteristics*: Known occurrence of SGD at the site, and preferably, some prior assessments including some understanding of the temporal and spatial variability. In addition, the study site should have a significant amount of SGD and a large ratio of groundwater discharge to other inputs (streams, precipitation).
- (2) *Geology/hydrogeology*: A reasonable understanding of the local hydrogeology. Good access to historical and current records (potentiometric levels, hydraulic conductivity, rainfall, etc.). Uniform geology and bottom type (sandy or silt, but not rocky is best for seepage meters).
- (3) *Climate*: Good local/regional ancillary data such as climate, coastal oceanography, water budget, hydrologic cycle, etc.
- (4) *Site geometry/oceanography*: A sheltered enclosed or semi-enclosed basin with a small adjacent drainage basin would be easier to handle in many ways than an open shelf environment with tidal currents, and other complicating factors.
- (5) *Logistics*: Good access to the site, both local and long distance; local logistical support (vans, support personnel, housing, etc.), proximity to laboratory facilities (perhaps a marine laboratory), easy access to electric power for such things as data loggers, etc., local sponsor or coordinator.

### 3. Methods used to measure SGD

#### 3.1. Seepage meters

Measurements of groundwater seepage rates into surface water bodies are often made using manual

“seepage meters.” Israelsen and Reeve (1944) first developed this device to measure the water loss from irrigation canals. Lee (1977) designed a seepage meter consisting of one end of a 55-gal (208 L) steel drum that is fitted with a sample port and a plastic collection bag (Fig. 5). The drum forms a chamber that is inserted open end down into the sediment. Water seeping through the sediment will displace water trapped in the chamber forcing it up through the port into the plastic bag. The change in volume of water in the bag over a measured time interval provides the flux measurement.

Studies involving seepage meters have reached the following general conclusions: (1) many seepage meters are needed because of the natural spatial and temporal variability of seepage flow rates (Shaw and Prepas, 1990a,b); (2) the resistance of the tube (Fellows and Brezonik, 1980) and bag (Shaw and Prepas, 1989; Belanger and Montgomery, 1992) should be minimized to the degree possible to prevent artifacts; (3) use of a cover for the collection bag may reduce the effects of surface water movements due to wave, current or stream flow activity (Libelo and MacIntyre, 1994); (4) the bag should initially contain a measured volume of water; thus, positive and negative seepage may be determined; (5) caution should be applied when operating near the seepage meter detection limit, i.e., a few  $\text{cm}^3/\text{cm}^2$  day (Cable et al., 1997a,b); and (6) artifacts occasionally exist from pressure gradients developed by uni-directional currents passing over the meter (Shinn et al., 2002). In a recent rebuttal to the criticism concerning pressure-induced flow, Corbett and Cable (2002) question whether sufficient evidence was presented to support the conclusion that seepage meters are not a practical instrument to use in coastal environments.

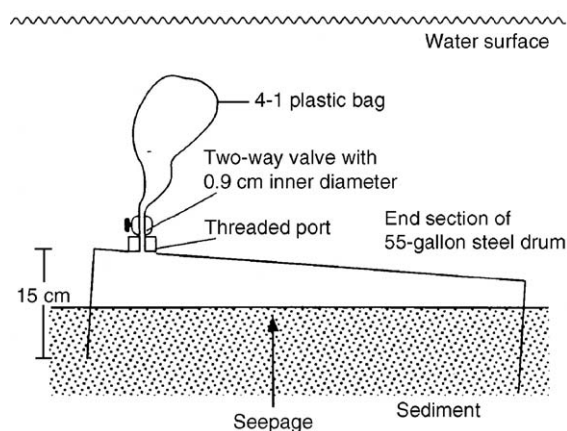


Fig. 5. Sketch of a simple “Lee-type” manual seepage meter (Lee, 1977).

Perhaps the most serious disadvantage for coastal zone studies is that manual seepage meters are very labor intensive. In order to obtain the groundwater discharge rate automatically and continuously, various types of automated seepage meters have been developed. Fukuo (1986), Cherkauer and McBride (1988), and Boyle (1994) describe remote installations of seepage meters from the surface of various water bodies. Sayles and Dickinson (1990) constructed a seepage meter that was a benthic chamber for the sampling and analysis of seepage through sediments associated with hydrothermal vents. Another example of an automated approach for measurement of SGD seepage is the heat-pulse device described by Taniguchi and Fukuo (1993) and a similar meter constructed by Krupa et al. (1998).

The “Taniguchi-type (heat-pulse type)” automated seepage meter is based on the travel time of a heat pulse down a narrow tube. The device uses a string of thermistors in a column positioned above an inverted funnel covering a known area of sediment (Fig. 6;

Taniguchi and Fukuo, 1993). The method involves measuring the travel time of a heat pulse generated within the column by a Nichrome wire induction heater. Since heat is a conservative property, the travel time is a function of the advective velocity of the water flowing through the column. Thus, once the system is calibrated in the laboratory, measurements of seepage flow at a field site can be made automatically on a near-continuous basis. The Taniguchi meter has successfully measured seepage up to several days at a rate of about one measurement every 5 min (Taniguchi and Fukuo, 1996).

Taniguchi and Iwakawa (2001) more recently developed a “continuous-heat type automated seepage meter” (Fig. 7). This design makes it possible to measure the temperature gradient of the water flowing between the downstream (sensor A) and upstream (sensor B) positions in a flow tube with a diameter of 1.3 cm. The temperature gradient is caused by the heat continuously generated within the column, the so-called “Granier method” (Granier, 1985). When there is no water flow,

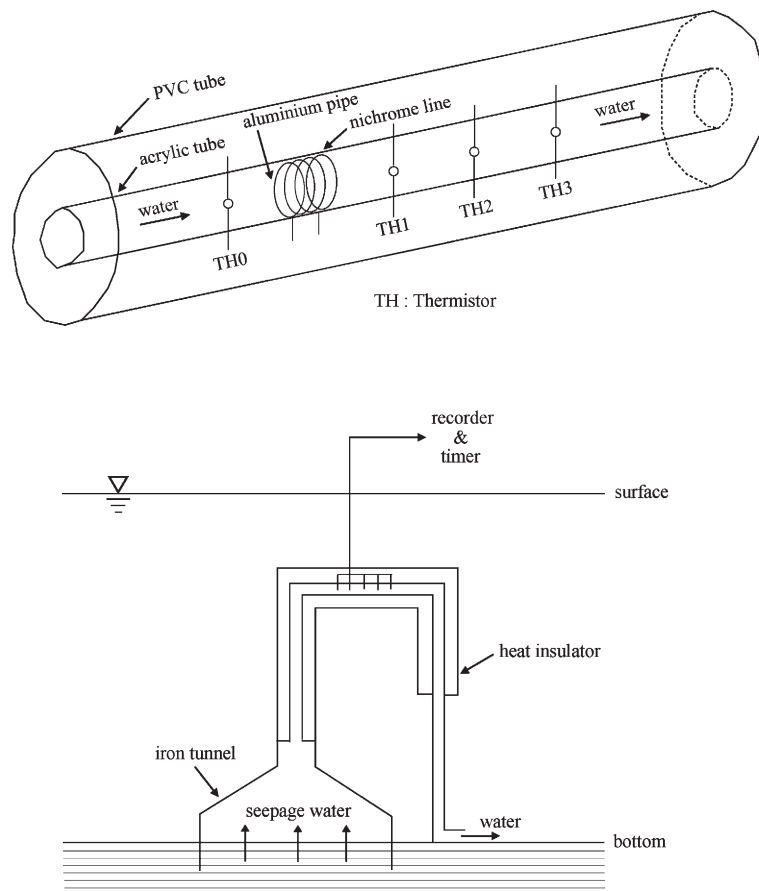


Fig. 6. Taniguchi-type (heat pulse) automated seepage meter (Taniguchi and Fukuo, 1993).

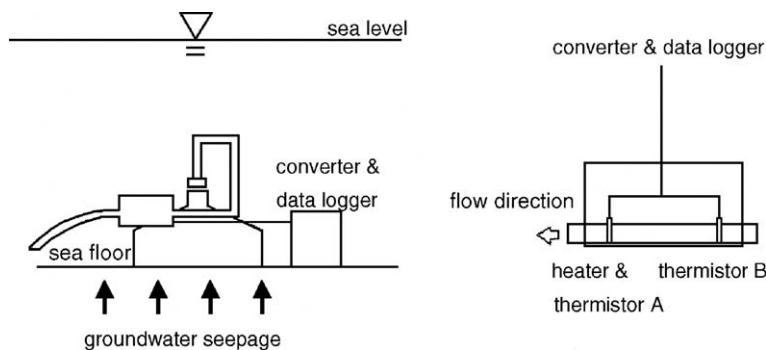


Fig. 7. Continuous heat-type automated seepage meter (Taniguchi and Iwakawa, 2001).

the temperature difference between sensors A and B in the column is the maximum, and it decreases with increasing the water flow velocity (Taniguchi et al., 2003a).

The “dye-dilution seepage meter,” developed at Woods Hole Oceanographic Institution, involves the injection of a colored dye into a mixing chamber attached to a seepage meter and the subsequent measurement of the dye absorbance in the mixing chamber over time. Typically, dye is injected every hour into a mixing chamber of known volume (usually 0.5 L), and the absorbance is recorded every 5 min. The rate at which the dye is diluted by the inflowing seepage water is used to calculate the flow-rate. In order to avoid the cost and complexity of a dedicated spectrophotometer, a nitrate analyzer is used to inject the dye and make the absorbance measurements (Sholkovitz et al., 2003).

Flow meters based on ultrasonic measurements are also used to evaluate seepage flow (Paulsen et al., 2001). The benthic chamber uses a commercially-available, acoustic flow meter to monitor the SGD. Since the speed of sound depends on salinity, the same sensor output can be used to continuously calculate the salinity of SGD as well as the flow rates.

A serious limitation of seepage meters is the requirement that they be deployed in a relatively calm environment. Breaking waves dislodge seepage meters and strong currents induce flow through the seabed when passing over and around large objects (Huetzel et al., 1996).

### 3.2. Piezometers

Another method for assessing groundwater seepage rates is the use of multi-level piezometer nests. With this approach, the groundwater potential in the sediments can be measured at several depths (Freeze and Cherry, 1979). Using observations or estimates of the aquifer

hydraulic conductivity (here assumed constant), one can then easily calculate the groundwater discharge rate into the ocean by use of a one-dimensional form of Darcy’s Law:

$$q = -Kdh/dL \quad (1)$$

where  $q$  is Darcian flux (groundwater discharge volume per unit area per unit time),  $K$  is hydraulic conductivity, and  $dh/dL$  is the hydraulic gradient in which  $h$  is hydraulic head and  $L$  is distance.

Piezometer nests suffer from the natural variability in seepage rates due to heterogeneity in the local geology. Typically, it is difficult to obtain representative values of hydraulic conductivity, which often varies over several orders of magnitude within an aquifer. Therefore, accurate evaluations of SGD using piezometers depend largely on the estimate of the aquifer’s hydraulic conductivity. Therefore, piezometer nests are often used in conjunction with seepage meters to estimate the hydraulic conductivity from observed seepage rates and the hydraulic gradient (Barwell and Lee, 1981; Taniguchi, 1995).

### 3.3. Natural tracers

One approach for local to regional-scale estimation of groundwater inputs into the ocean uses naturally occurring geochemical tracers. An advantage of groundwater tracers is that they present an integrated signal as they enter the marine water column via various pathways in the aquifer. Although small-scale variability is a serious drawback for the use of seepage meters or piezometers, such small spatial scale variations tend to be smoothed out over time and space in the case of tracer methods (Burnett et al., 2001a). On the other hand, natural tracers require that all other tracer sources and sinks except groundwater be evaluated, an often difficult exercise.



Natural geochemical tracers have been applied in two ways to evaluate groundwater discharge rates into the ocean. First is the use of enriched geochemical tracers in the groundwater relative to the seawater. In other words, the concentration of a solute in the receiving water body is attributed to inputs of that component derived only from groundwater (Moore, 1996; Cable et al., 1996a,b; Porcelli and Swarzenski, 2003). A second approach is the use of vertical profiles of the geochemical compositions in sediment pore waters under the assumption that its distribution can be described by a vertical, one-dimensional advection–diffusion model (e.g., Cornett et al., 1989; Vanek, 1993). However, this is usually limited to the case of homogeneous media.

Over the past few years, several studies used natural radium isotopes and  $^{222}\text{Rn}$  to assess groundwater discharge into the ocean (Burnett et al., 1990, 1996; Ellins et al., 1990; Moore, 1996; Rama and Moore, 1996; Cable et al., 1996a,b, 2004; Moore and Shaw, 1998; Corbett et al., 1999; Hussain et al., 1999; Corbett et al., 2000; Moore, 2000; Krest et al., 2000; Charette et al., 2001; Kelly and Moran, 2002; Kim and Hwang, 2002; Burnett et al., 2002; Burnett and Dulaiova, 2003; Garrison et al., 2003; Krest and Harvey, 2003; Crotwell and Moore, 2003; Moore and Wilson, 2005). Ideally, in order to provide a detectable signal, a groundwater tracer should be greatly enriched in the discharging groundwater relative to coastal marine waters, conservative, and easy to measure. Radium isotopes and radon have been shown to meet these criteria fairly well and other natural tracer possibilities exist which may be exploited for groundwater discharge studies. In applying geochemical tracing techniques, several criteria must be assessed or defined, including boundary conditions (i.e., area, volume), water and constituent sources and sinks, residence times of the surface water body, and concentrations of the tracer. Sources may include ocean water, river water, groundwater, precipitation, in situ production, horizontal water column transport, sediment resuspension, or sediment diffusion. Sinks

may include in situ decay or consumption, horizontal water column transport, horizontal or vertical eddy diffusivity, and atmospheric evasion. Through simple mass balances or box models incorporating both sediment advection and water column transport, the geochemical approach can be quite useful in assessing SGD.

Radium isotopes are enriched in groundwater relative to surface waters, especially where saltwater is coming into contact with surfaces formally bathed only in freshwaters. Moore (1996) showed that waters over the continental shelf off the coast of the southeastern USA were enriched in  $^{226}\text{Ra}$  with respect to open ocean values. The radium concentrations also showed a distinct gradient being highest in the near-shore waters. By using an estimate of the residence time of these waters on the shelf and assuming steady-state conditions, one can calculate the offshore flux of the excess  $^{226}\text{Ra}$  (Fig. 8). If this flux is supported by SGD along the coast, then the SGD can be estimated by dividing the radium flux by the estimated  $^{226}\text{Ra}$  activity of the groundwater. A convenient enhancement to this approach is that one may use the short-lived radium isotopes,  $^{223}\text{Ra}$  and  $^{224}\text{Ra}$ , to assess the water residence time (Moore, 2000).

Moore (1996 and elsewhere) has suggested the following general strategy to determine the importance of oceanic exchange with coastal aquifers: (1) Identify tracers derived from coastal aquifers that are not recycled in the coastal ocean; map their distribution and evaluate other sources. (2) Determine the exchange rate of the coastal ocean with the open ocean. (3) Calculate the tracer flux from the coastal ocean to the open ocean, hence the tracer flux from the aquifer to the coastal ocean. (4) Measure the average tracer concentration in the coastal aquifer to calculate fluid flux. (5) Use the concentrations of other components (nutrients, carbon, metals) in the aquifer or their ratios to the tracer to estimate their fluxes.

Hwang et al. (2005) developed a geochemical model for local-scale estimation of SGD. If the system under

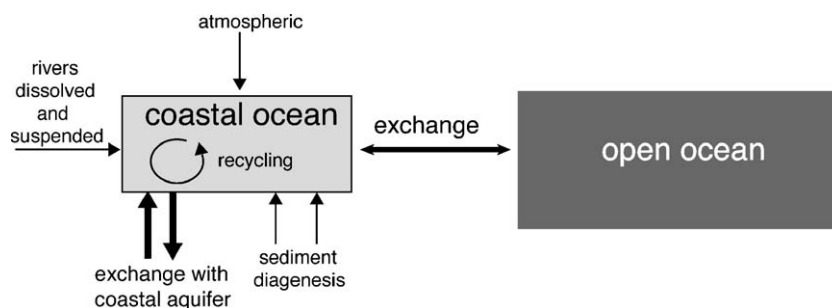


Fig. 8. Box model showing how radium isotopes can be used to investigate exchange between the coastal and open ocean.



study is steady state, than radium additions are balanced by losses. Additions include radium fluxes from sediment, river, and groundwater; losses are due to mixing and, in the case of  $^{223}\text{Ra}$  and  $^{224}\text{Ra}$ , radioactive decay. Using a mass balance approach on a larger scale with the long-lived isotopes  $^{226}\text{Ra}$  and  $^{228}\text{Ra}$ , Kim et al. (2005) determined that SGD-derived silicate fluxes to the Yellow Sea were on the same order of magnitude as the Si flux from the Yangtze River, the fifth largest river in the world.

A steady-state mass balance approach may also be used for  $^{222}\text{Rn}$  with the exception that atmospheric evasion must also be taken into account (Burnett et al., 2003c). The main principle of using continuous time-series radon measurements to decipher rates of groundwater seepage is that if we can monitor the inventory of  $^{222}\text{Rn}$  over time, making allowances for losses due to atmospheric evasion and mixing with lower concentration waters offshore, any changes observed can be converted to fluxes by a mass balance approach (Fig. 9). Although changing radon concentrations in coastal waters could be in response to a number of processes (sediment resuspension, long-shore currents, etc.), advective transport of groundwater (pore water) through sediment of Rn-rich solutions is often the dominant process. Thus, if one can measure or estimate the radon concentration in the advecting fluids, the  $^{222}\text{Rn}$  fluxes may be easily converted to water fluxes.

Although radon and radium isotopes have proven very useful for assessment of groundwater discharges, they both clearly have some limitations. Radium isotopes, for example, may not be enriched in freshwater discharges such as from submarine springs. Radon is

subject to exchange with the atmosphere which may be difficult to model under some circumstances (e.g., sudden large changes in wind speeds, waves breaking along a shoreline). The best solution may be to use a combination of tracers to avoid these pitfalls.

New and improved technologies have assisted the development of approaches based on radium isotopes and radon. The measurement of the short-lived radium isotopes  $^{223}\text{Ra}$  and  $^{224}\text{Ra}$ , for example, used to be very tedious and time-consuming until the development of the Mn-fiber and delayed coincidence counter approach (Moore and Arnold, 1996). Now it is routine to process a sample (often 100–200 L because of very low environmental activities) through an Mn-fiber adsorber, measure the short-lived isotopes the same day by the delayed coincidence approach, and then measure the long-lived isotopes ( $^{226}\text{Ra}$  and  $^{228}\text{Ra}$ ) at a later date by gamma spectrometry. Burnett et al. (2001a) developed a continuous radon monitor that allows much easier and unattended analysis of radon in coastal ocean waters. The system analyses  $^{222}\text{Rn}$  from a constant stream of water delivered by a submersible pump to an air–water exchanger where radon in the water phase equilibrates with radon in a closed air loop. The air stream is fed to a commercial radon-in-air monitor to determine the activity of  $^{222}\text{Rn}$ . More recently, an automated multi-detector system has been developed that can be used in a continuous survey mode to map radon activities in the coastal zone (Dulaiova et al., 2005). By running as many as six detectors in parallel, one may obtain as many as 12 readings per hour for typical coastal ocean waters with a precision of better than 10–15%.

Another approach consists of application of in situ gamma-ray spectrometry techniques that have been recognized as a powerful tool for analysis of gamma-ray emitters in sea-bed sediments, as well as for continuous analysis of gamma-ray emitters (e.g.,  $^{137}\text{Cs}$ ,  $^{40}\text{K}$ ,  $^{238}\text{U}$  and  $^{232}\text{Th}$  decay products) in seawater (e.g., Povinec et al., 2001). In situ gamma-ray spectrometers have been applied for continuous stationary and spatial monitoring of radon (as well as thoron, i.e.,  $^{220}\text{Rn}$ ) decay products in seawater, together with salinity, temperature and tide measurements, as possible indicators of SGD in coastal waters of SE Sicily and at the Ubatuba area of Brazil (Levy-Palomo et al., 2004).

Methane ( $\text{CH}_4$ ) is another useful geochemical tracer that can be used to detect SGD. Both  $^{222}\text{Rn}$  and  $\text{CH}_4$  were measured along the Juan de Fuca Ridge as a means of estimating heat and chemical fluxes from the hydrothermal vents of that area (Rosenberg et al., 1988). Both  $^{222}\text{Rn}$  and  $\text{CH}_4$  were used to evaluate SGD in studies performed in a coastal area of the northeastern

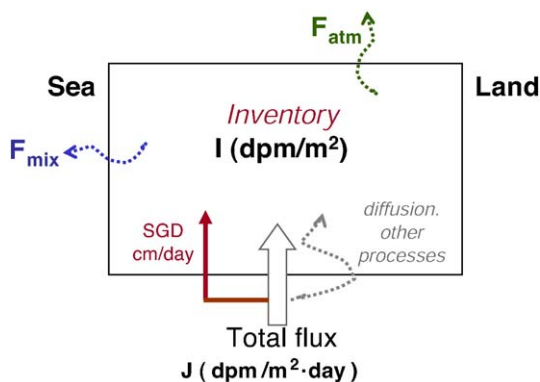


Fig. 9. Conceptual model of use of continuous radon measurements for estimating SGD in a coastal zone. The inventory refers to the total amount of excess  $^{222}\text{Rn}$  per unit area. Losses considered include atmospheric evasion and mixing with offshore waters. Decay is not considered because the fluxes are evaluated on a very short time scale relative to the half-life of  $^{222}\text{Rn}$  (Burnett and Dulaiova, 2003).

Gulf of Mexico (Cable et al., 1996a). Tracer ( $^{222}\text{Rn}$  and  $\text{CH}_4$ ) inventories in the water column and seepage rates measured using a transect of seepage meters were evaluated over several months within a shallow water location. The linear relationships between tracer inventories and measured seepage fluxes were statistically significant (Fig. 10). These investigators found that inventories of  $^{222}\text{Rn}$  and  $\text{CH}_4$  in the coastal waters varied directly with groundwater seepage rates and had a positive relationship (95% C.L.). In addition, water samples collected near a submarine spring in the same area displayed radon and methane concentrations inversely related to salinity and considerably greater than those found in surrounding waters. In a related study, Bugna et al. (1996) demonstrated that groundwater discharge was an important source for  $\text{CH}_4$  budgets on the inner continental shelf of the same region. In another example, Tsunogai et al. (1999) found methane-rich plumes in the Suruga Trough (Japan) and postulated that the plume was supplied from continuous cold fluid seepage in that area. Another technological advance, the “METS” sensor (Capsum Technologies GmbH, Trittau, Germany), can now automatically and continuously measure methane at environmental levels in natural waters (Kim and Hwang, 2002).

Several other natural radioactive ( $^3\text{H}$ ,  $^{14}\text{C}$ , U isotopes, etc.) and stable ( $^2\text{H}$ ,  $^3\text{He}$ ,  $^4\text{He}$ ,  $^{13}\text{C}$ ,  $^{15}\text{N}$ ,  $^{18}\text{O}$ ,  $^{87/88}\text{Sr}$ ,

etc.) isotopes and some anthropogenic atmospheric gases (e.g., CFC's) have been used for conducting SGD investigations, tracing water masses, and calculating the age of groundwater. Uranium may be removed to anoxic sediments during submarine groundwater recharge (SGR). Moore and Shaw (submitted for publication) used deficiencies of uranium concentration (relative to expected concentrations based on the U/salinity ratio in seawater) to estimate SGR in several southeast US estuaries. Stable isotope data can help to evaluate groundwater–seawater mixing ratios, important for the estimation of the SGD in coastal areas (Aggarwal et al., 2004). Seawater and the fresh groundwater end-members often have specific signatures due to different tracers/isotopes. Under good circumstances, such differences between end-members would allow calculation of the percent groundwater contribution. This may be especially useful when mixing is occurring between more than two end-members including saline groundwater.

Besides the mixing ratio calculations, each tracer can be used for interpretation of various groundwater characteristics. In mixed waters, the selection of the related fresh groundwater end-member is an important issue that may be addressed via use of stable isotopes. For example, oxygen and hydrogen isotopes generally carry valuable information about recharge conditions. Such information may include recharge elevation, temperature, and degree of evaporation.

Other variables that change the characteristics of the groundwater component in the mixture are the hydrodynamic properties of the aquifer because of change in length of flow paths, groundwater velocity, and flow conditions (e.g., diffuse or conduit flow). Such hydrodynamic characteristics of the aquifer are important for the chemically reactive (e.g.  $^{13}\text{C}$ ) and radioactive (e.g.  $^3\text{H}$ ) tracers/isotopes. Such processes have to be taken into account in the interpretation of water mixture calculations (Aggarwal et al., 2005).

For evaluating freshwater fluxes, salinity anomalies are useful for estimation of SGD. However, to assess brackish and saline fluxes, which in many cases have more impact on the coastal environment; isotopes have an added advantage over chemical techniques. Various aspects of coastal hydrology could be addressed by investigations using a combination of stable, long-lived, and short-lived isotopes along with other complementary techniques.

In addition to geochemical tracers, geophysical tracers such as groundwater temperature can be used to estimate groundwater discharge rates. Two basic methods are used when using temperature as a tracer: (1)

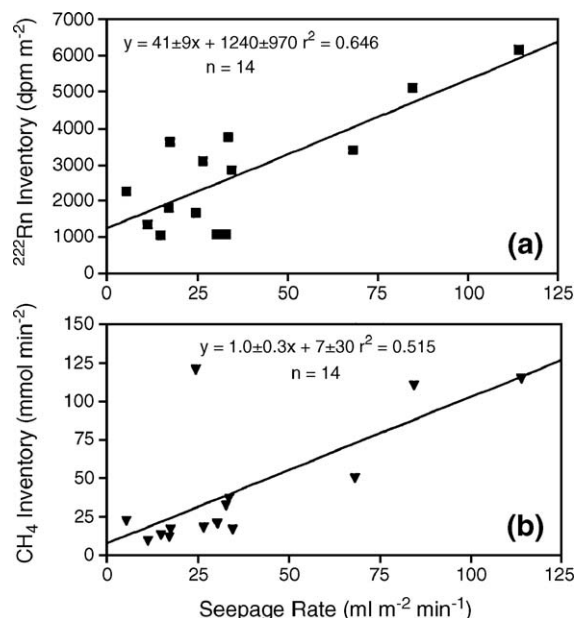


Fig. 10. Relationship between (a)  $^{222}\text{Rn}$  and (b)  $\text{CH}_4$  inventories in the overlying water column and groundwater fluxes measured at one station by seepage meters in the coastal Gulf of Mexico (Cable et al., 1996a).

temperature–depth profiles under the assumption of conservative heat conduction–advection transport; and (2) temperature differences in the groundwater–surface water system as a qualitative signal of groundwater seepage using techniques such as infrared sensors or other remote sensing methods.

Temperature–depth profiles in boreholes have been widely used to estimate groundwater fluxes because heat in the subsurface is transported not only by heat conduction but also by heat advection due to groundwater flow (Taniguchi et al., 2003b). Bredehoeft and Papadopoulos (1965) developed the type curves method for estimating one-dimensional groundwater fluxes based on a steady state heat conduction–advection equation derived from Stallman (1963). This method has been widely used to estimate one dimensional vertical groundwater fluxes (e.g., Cartwright, 1979; Boyle and Saleem, 1979), one-dimensional horizontal groundwater fluxes (e.g., Sakura, 1977), and one-dimensional vertical groundwater fluxes with the effect of horizontal groundwater fluxes (Lu and Ge, 1996). Simultaneous movement of one-dimensional transient heat and steady water flow were analyzed observationally (Sillman and Booth, 1993; Constantz et al., 1994), numerically (Lapham, 1989), and theoretically (Suzuki, 1960; Stallman, 1965; Taniguchi, 1993, 1994). The relationship between two-dimensional subsurface temperature and groundwater flux was theoretically analyzed by Domenico and Palciauskas (1973) and Smith and Chapman (1983). More recently, surface warming caused by global warming and urbanization (Taniguchi et al., 1999a) or deforestation (Taniguchi et al., 1999b) was used as a tracer to detect groundwater fluxes (Fig. 11). Fisher et al. (1999) analyzed thermal data from the upper 150 m of sediment below the seafloor, which were collected during Ocean Drilling Program (ODP) Leg 150. They suggested that the observed thermal data indicated recent warming of the shallow slope bottom water off New Jersey. Borehole temperature data near the coast was also used for estimations of SGD into Tokyo Bay, Japan (Taniguchi et al., 1998) and a saltwater–freshwater interface in Toyama Bay, Japan (Taniguchi, 2000). In a recent application of borehole temperature data, Martin et al. (2006) estimated the magnitude of the saline SGR/SGD component exchanging within the sediments using heat flux calculations to aid in evaluating the fresh component of groundwater discharge. Moore et al. (2002) reported cyclic temperature variations 4 m below the seabed that were in phase with the tidal signal during the summer. They used this relationship

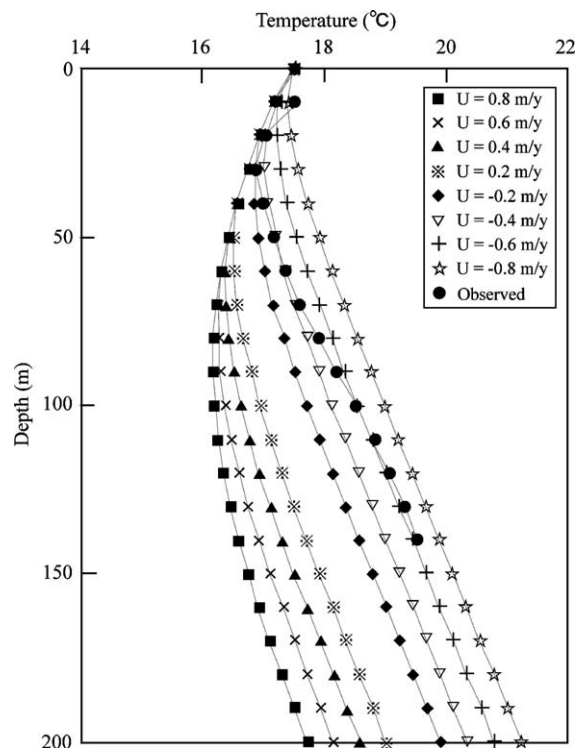


Fig. 11. Observed and calculated temperature–depth profiles using a heat conduction–convection equation to estimate upward groundwater fluxes (groundwater discharge rates) near Tokyo Bay (Taniguchi et al., 1999a).

to estimate SGD fluxes. All of these studies suggest that groundwater temperature–depth profiles in the coastal zone can be used as a valuable tracer to evaluate SGD.

In order to evaluate regional-scale influence of SGD by using surface temperature as a tracer, infrared sensors have been used in many areas (Fischer et al., 1964; Roxburgh, 1985; Banks et al., 1996; Bogle and Loy, 1995). However, SGD values were not evaluated quantitatively though the locations of SGD influence were documented. These detectable locations are attributed to the spatial and temporal variation of both seawater and groundwater temperatures, which requires intensive field calibration. The use of remote sensing technologies to identify and quantify SGD is clearly an area for future research exploitation.

Another geophysical tracer, the bulk ground conductivity of seafloor and beach sediments can be employed to investigate the spatial distribution of saline and fresh porewater. Using these methods, preferential flowpaths of fresh, terrestrially-derived groundwater such as submarine paleochannels can be readily identified from their conductivity signature (Stieglitz, 2005; Stieglitz et al., submitted for publication).

### 3.4. Water balance approaches

The water balance equation for a basin has also been used to estimate fresh SGD and may be described as follows:

$$P = E_T + D_S + D_G + dS \quad (2)$$

where  $P$  is precipitation,  $E_T$  is evapotranspiration,  $D_S$  is surface discharge,  $D_G$  is fresh groundwater discharge, and  $dS$  is the change in water storage. Over extended periods (i.e., years),  $dS$  is usually assumed to be negligible. Therefore, one needs to know precisely the precipitation, evapotranspiration and surface runoff for an accurate estimation of  $D_G$  by this approach.

Basin-scale estimations of fresh SGD via a water balance method have been performed in many places, e.g., Perth, Australia ( $1.0 \times 10^8$  m<sup>3</sup>/year; Allen, 1976), Santa Barbara ( $1.2 \times 10^5$  m<sup>3</sup>/year; Muir, 1968), Long Island, New York ( $2.5 \times 10^7$  m<sup>3</sup>/year; Pluhowski and Kantrowitz, 1964), and in the Adriatic Sea ( $1.7 \times 10^{11}$  m<sup>3</sup>/year; Sekulic and Vertacnik, 1996). When both the area and volume of SGD are known, one can calculate the fresh SGD flux. For example in the case of the Adriatic Sea (Sekulic and Vertacnik, 1996), the mean fresh SGD flux of 0.68 m/year is calculated from the estimated fresh SGD volume and the discharge area. More typically, the area over which SGD occurs is unknown. Therefore, the SGD volume or sometimes “volume of SGD per unit length of shoreline” (Robinson, 1996; Sellinger, 1995) is used for water balance studies, making it difficult to compare with the observed (local) SGD estimates shown as Darcy’s flux (e.g., cm<sup>3</sup>/cm<sup>2</sup> s, cm/s, m/year).

Water budget calculations, while relatively simple, are typically imprecise for fresh groundwater discharge estimations because uncertainties associated with values used in the calculations are often of the same magnitude as the discharge being evaluated. For instance in the global water budget constructed by Garrels and MacKenzie (1971), the estimated fresh SGD is about 6% of estimated evaporation from the land, which is about the same order as the uncertainty of the evaporation rate. Moreover, these estimates do not include the saltwater that mixes into the aquifer and often comprises a significant fraction of total SGD.

In a study designed to test the effects of climate change on groundwater discharge, Oberdorfer (1996) concluded that use of a water budget is an adequate first approach for assessing expected changes in simple groundwater basins. On the other hand, numerical modeling provides a better quantitative estimate of climate change perturbations when dealing with basins

characterized by multiple sources and sinks. Another water balance approach using a budget based on the change in soil moisture has been performed for Tomales Bay, California (Oberdorfer et al., 1990). Their result was comparable to the result obtained by more traditional water balance estimations.

### 3.5. Hydrograph separation techniques

The hydrograph separation technique is based on the assumption that the amount of fresh groundwater entering streams can be obtained via a hydrograph separation and this estimate may be extrapolated to the coastal zone. This technique was used by Zektser and Dzhamalov (1981) for the Pacific Ocean rim, by Boldovski (1996) in eastern Russia, by Williams and Pinder (1990) in the local coastal plain stream in South Carolina, and by Zektser et al. (1973) for global-scale estimation of fresh SGD. Two approaches were used to separate the hydrograph for estimating the fresh groundwater flow component. The first method is simply to assign a base flow due to the shape of the hydrograph. This technique can be performed several ways including the unit graph method (Bouwer, 1978; Zektser et al., 1973). However, a problem with this simple approach is evaluating baseline conditions; often the baseline changes depending on time, space, and prevailing hydrological conditions. The hydrograph separation technique for large-scale SGD estimates applies only to coastal areas with well-developed stream networks and to zones of relatively shallow, mainly freshwater aquifers.

As with the water balance method, the uncertainties in the hydrograph separation terms are often on the same order of magnitude as the discharge being evaluated. For instance, the estimation of groundwater discharge in central and eastern European countries showed the average of estimated fresh groundwater discharge (6% of total water flow) is about 12% of the estimated evaporation (Zektser and Loaiciga, 1993). This estimate is close to the uncertainty usually assigned to evaporation estimates.

The second method of hydrograph separation is the use of geochemical end-member concentrations. Usually, water and geochemical mass balances in a river are shown as follows:

$$D_T = D_S + D_G \quad (3)$$

$$C_T D_T = C_S D_S + C_G D_G \quad (4)$$

where  $D$  and  $C$  are the discharge rate and geochemical concentrations, respectively, and subscripts T, S and G represent the total, surface water and groundwater



components. From those two equations, measured  $D_T$ ,  $C_T$ ,  $C_S$ , and  $C_G$ , we can solve for the two unknown values,  $D_S$  and  $D_G$ .

Recently, not only surface water–groundwater separation (Fritz et al., 1976), but also the separation of three water components, namely groundwater, surface water and soil water, has been studied by using three different compositions of these end-members (Tanaka and Ono, 1998). This method may also be applicable for separation of SGD into the fresh, mixing, and seawater components of SGD if one can identify tracers with sufficient sensitivity and resolution.

Another problem of the hydrograph separation for estimating direct groundwater discharge into the ocean is that gauging stations for measuring the discharge rate in rivers are always located some finite distance upstream from the coast to avoid tidal effects. Therefore, the groundwater discharge downstream of the gauging station is excluded (Buddemeier, 1996).

### 3.6. Theoretical analysis and numerical simulations

Offshore seepage rates were described by an exponentially decreasing function, as explained by McBride and Pfannkuch (1975), who investigated the distribution of groundwater seepage rate through lakebeds using numerical models. Bokuniewicz (1992) questioned the use of such an exponentially decreasing function and developed an analytical solution for SGD as follows:

$$q = (Ki/\pi k)\ln[\coth(\pi xk/4l)] \quad (5)$$

where  $q$  is vertical groundwater seepage flux,  $K$  is vertical hydraulic conductivity (assumed constant),  $i$  is hydraulic gradient,  $k$  is the square root of the ratio of the vertical to the horizontal hydraulic conductivity,  $l$  is aquifer thickness and  $x$  is the distance from the shoreline. The author concluded that a single exponential function underestimated the analytical solution of SGD both near-shore and far from shore, and overestimated the SGD at intermediate distances. Further details concerning the derivation and use of this equation may be found in Bokuniewicz (1992). This relationship between an exponential approximation and analytical solution is similar to the contrast between an exponential representation and the numerical examples calculated by McBride and Pfannkuch (1975).

Fukuo and Kaihotsu (1988) made a theoretical analysis of groundwater seepage rates for areas with a gentle slope into surface water bodies by use of conformal mapping techniques. They used the  $x$ -axis along with the slope (the  $x$ -axis in Bokuniewicz, 1992 is

horizontal), and found that in an unconfined aquifer most of the groundwater flows through a near-shore interface between surface water and groundwater. Equipotential and streamlines in the near-shore vicinity of the aquifer and the distribution of specific discharge through the sediment with different slopes demonstrate this point (Fig. 12a; Fukuo and Kaihotsu, 1988). Analytical solutions indicate that SGD decreases exponentially with distance from the coast and that the rate of decrease is greater when a gentler slope is present (Fig. 12b). Interactions between surface waters and groundwaters also have been studied numerically by Winter (1983, 1986, 1996), Anderson and Chen (1993) and Nield et al. (1994). Linderfelt and Turner (2001) numerically evaluated the net advected groundwater discharge to a saline estuary while Smith and Turner (2001) numerically evaluated the role of the density-driven re-circulation component in the overall groundwater discharge to the same saline estuary.

Although modeling approaches using packages such as MODFLOW (McDonald and Harbaugh, 1984) are widely used for the analysis of basin-scale groundwater hydrology, all of these techniques have certain limitations. For example, aquifer systems are usually heterogeneous, and it is difficult to obtain sufficient representative values such as hydraulic conductivity and porosity to adequately characterize this heterogeneity. Hydraulic conductivity often varies over several orders of magnitude within short distances. Spatial and temporal variations for boundary conditions are also required for hydrological modeling, but this information is often hampered by our ability to acquire adequate field data within the time frame of a typical study.

When estimating nutrient transport by groundwater, it is important to evaluate the groundwater capture zone at near-shore zones. Taniguchi et al. (1999c) analyzed the groundwater seepage rate into Lake Biwa, Japan, to evaluate the capture zone of groundwater entering a surface water body. Transient numerical simulations were made using a two-dimensional (2-D) unsaturated–saturated model with three-layered sediments. They concluded that calculated values agreed well with observed groundwater seepage rates when the thickness of the aquifer was estimated to be 110 m. This model also agreed with the capture zone results estimated by stable isotope data ( $\delta^{18}\text{O}$  and deuterium). It is clear that aquifer thickness and hydraulic conductivity values are the most important factors for reliable estimates of groundwater seepage rates by theoretical and numerical analysis.

All the above described numerical models simulate groundwater flow. A complementary numerical



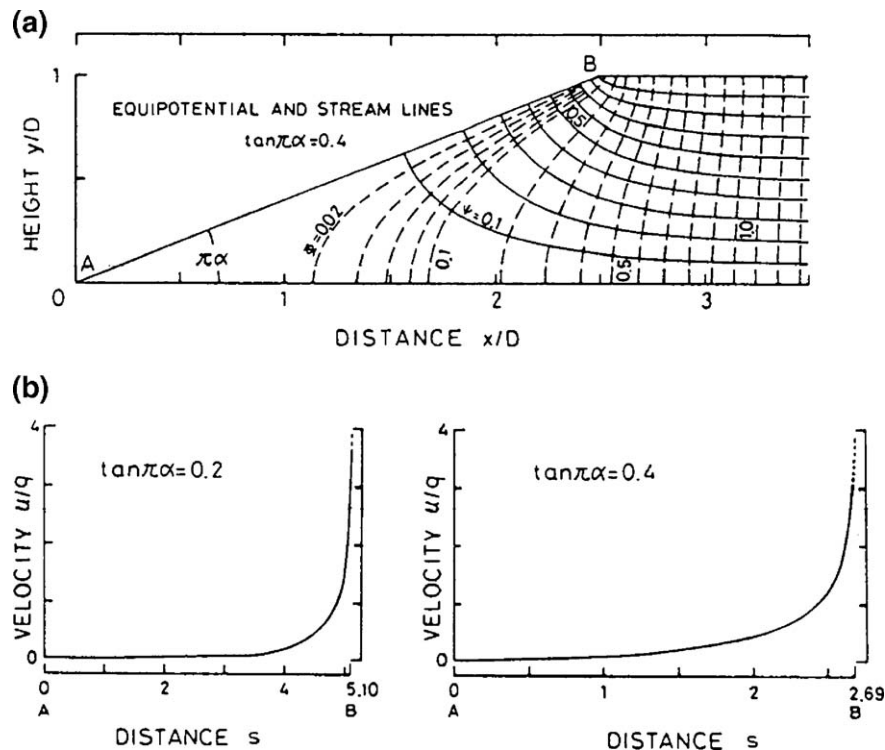


Fig. 12. (a) Equipotential and streamlines near the sediment surface; and (b) distribution of specific discharge on the sediment surface with a gentle slope (Fukuo and Kaihotsu, 1988).

approach is proposed in which the salinity distribution in the *surface water body* is simulated by a three-dimensional (3-D) numerical model to determine the location and strength of SGD. Measurements of the salinity field (or another typical parameter) are needed in the region of the SGD source. One example of such a model is PCFLOW3D, a 3-D, non-linear baroclinic numerical model originally developed to simulate the hydrodynamic circulation and transport and dispersion of different contaminants such as mercury (Rajar et al., 2000) or radionuclides (Četina et al., 2000). The basic idea is to assume a location and strength of the SGD, simulate the salinity distribution, and compare it with the measured distribution. The final information on SGD is obtained by a trial and error procedure. The possibility of the model application was shown with the SGD measurements in Sicily (see Section 5.2).

#### 4. Coastal zone management implications of SGD

Groundwater seepage into the coastal zone may be important for coastal area management for at least three reasons: (1) dissolved solutes that result in chemical and ecological effects in the receiving waters; (2) saltwater

intrusion and associated hydrologic aspects involving water resources; and (3) geotechnical aspects (as sediment stability) of the shoreline. SGD may have significant environmental consequences as groundwaters in many areas have become contaminated with a variety of substances (e.g., nutrients, metals, organics). Because the slow, yet persistent seepage of groundwater through sediments will occur almost anywhere, almost all coastal zones are subject to flow of terrestrially driven groundwater either as submarine springs or disseminated seepage (Johannes, 1980; Church, 1996; Moore, 1996). In addition, significant amounts of recirculated seawater pass through permeable sediments as a result of tidal pumping, topographically induced flow, and other marine processes (see Drivers of SGD). The potential for discharging groundwaters to have a significant impact on surface waters is greatest in regions where fluids may seep into a body of water having limited circulation.

Because groundwaters typically have higher concentrations of dissolved solids than most terrestrial surface waters, SGD often makes a disproportionately large contribution to the flux of dissolved constituents, including nutrients and pollutants. In addition,

discharging groundwater interacts with and influences the recirculation of seawater, which can affect coastal water quality and nutrient supplies to near-shore benthic habitats, coastal wetlands, breeding and nesting grounds. Thus, one of the more important implications for coastal zone managers concerns nutrient (or other solute) loading to near-shore waters. Impacts in the coastal zone from these inputs could be the basis for land-use planning and may place limits on development.

Hwang et al. (2005) estimated SGD using a variety of tracers including  $^{222}\text{Rn}$  and radium isotopes into Bangdu Bay, a semi-enclosed embayment on the Korean volcanic island, Jeju. Their estimated SGD inputs of  $120\text{--}180\text{ m}^3\text{ m}^{-2}\text{ year}^{-1}$  are much higher than those reported from typical continental margins. The nutrient fluxes from SGD were about 90%, 20%, and 80% of the total input (excluding inputs from open ocean water) for dissolved inorganic nitrogen, phosphorus, and silica, respectively. The authors concluded that these excess nutrient inputs from SGD are the major sources of “new nutrients” to this bay and could contribute to eutrophication.

From a management standpoint, a key issue will be the determination of whether SGD is of actual or probable importance in an area of interest. Furthermore, managers must consider the relative importance of SGD among the multiple factors considered in management activities. In this respect, coastal managers face the following problems: (1) they may not be aware of the growing realization of the importance of SGD; (2) if they are aware, they may not know how to decide whether or not SGD is relevant to their situation; and (3) if they do decide this is important, they may not know how to quantify it.

Since SGD is essentially “invisible,” the problem that arises, from both a management and scientific standpoint, is determining how to avoid the error of ignoring an important process on the one hand, and wasting valuable resources on an unimportant issue on the other. Where terrestrially driven SGD is a significant factor in maintaining or altering coastal ecosystems, coastal zone managers will need to consider management of water levels and fluxes through controls on withdrawal or alterations in recharge patterns, as well as groundwater quality management (e.g., through controls on land use, waste disposal, etc.). Such major interventions in the coastal zone management system require a sound scientific justification and technical understanding that does not currently exist.

How can a manager tell if SGD may be important in a particular area? Several potential, indirect indicators of freshwater submarine discharge have been suggested

but not yet widely applied. Its color, temperature, salinity, or some other geochemical fingerprint might distinguish the water itself. Escaping groundwater, for example, might be stained red by the oxidation of iron or colored by tiny gas bubbles. Because groundwater tends to exist at the average annual temperature, cold-water anomalies in the open water during the summer and warm water anomalies during the winter, as might be detected by infrared aerial photography, or a person walking barefoot on the beach, can be an indicator of SGD. Salinity anomalies have also long been used to identify subsea freshwater seeps, and can also be used at a variety of scales from regional water budgets to vertical profiles at specific locations.

Particular site conditions may also provide clues to the occurrence of SGD. The presence of coastal ponds or unconsolidated coastal bluffs, which may maintain a high hydraulic head near shore, may be other indicators. Growths of freshwater coastal vegetation may indicate regions of high SGD offshore. It has also been suggested that the presence of barite, oxidized shells, or beach rock may indicate the occurrence of groundwater discharges. In Great South Bay (New York, USA), there occurs a phenomenon known as “anchor ice,” in which the bay floor freezes while the saline open waters of the bay are still ice-free. This is attributed to the presence of freshwater in the sediments maintained by SGD. It is also reported to occur in the Baltic. Alternatively, in coastal areas that are covered with ice in the water, like the Schlei estuary in northern Germany, ice-free spots, called “wind-spots,” are found above the SGD of relatively warm freshwater. In Eckernförde Bay (southeast Baltic Sea) pockmarks in the fine-grained sediments of the sea floor have been identified as bathymetric expressions of groundwater seeps (Schluter et al., 2000). If the SGD is great enough, the water itself can be domed and “boiling” such at Crescent Beach Spring off Florida (Swarzenski et al., 2002).

Managers must consider the relative relationships and priorities of SGD among the multiple factors considered in management activities. This presents at least two ways that current approaches to the study of groundwater discharge will need to be modified for such studies to be useful to managers: (1) The scale of emphasis would be that of management areas — probably tens to hundreds of kilometers. By contrast, scientists are typically performing investigations at the lower end of this scale (although some tracer investigations work at scales of 10–100 km). (2) Scientists may study one area for years, often reflecting the typical 2–3 year grant cycle. Managers,

on the other hand, will need relatively simple and rapid diagnostic and assessment tools to evaluate the local importance and management issues related to SGD in specific settings. The concerns could be either natural processes or human impacts (which may be extreme in some cases).

## 5. The UNESCO/IAEA joint SGD intercomparison activities

Five SGD assessment intercomparison exercises were organized over the course of the UNESCO/IAEA project (Table 1). The results of each of these experiments are summarized below. Measured seepage rates are provided in a series of tables for each site with the values given as integrated flow rates ( $\text{m}^3/\text{m day}$ ) in all cases except for the measurements at the Brazilian site (given as  $\text{cm}^3/\text{cm}^2 \text{ day}$  or  $\text{cm/day}$ ) where there was so much variability that the width of the seepage face could not be reliably estimated.

### 5.1. Cockburn Sound, Australia

#### 5.1.1. Introduction

We performed our first intercomparison experiment (November 25–December 6, 2000) within the Northern Harbor area (Jervoise Bay) of Cockburn Sound, located in the southwest margin of continental Australia, near metropolitan Perth and Fremantle (Fig. 13). Cockburn Sound is a marine embayment protected from the open Indian Ocean by reefs, a chain of islands, and a man-made causeway. Recently, the area has been the subject

of extensive environmental assessment in order to address strategic environmental concerns and the management of waste discharges into Perth's coastal waters.

Cockburn Sound itself is flanked on its eastern margin by a low-lying sandy coastal plain. Much of Perth's commercial and industrial activity is focused along the southern metropolitan coastline and includes the shoreline of Cockburn Sound. Influx of pollutants to the near-shore marine environment from these activities has been a point of major concern in recent years, and SGD has been recognized as an important pathway for contaminants. Accordingly, a significant amount of baseline environmental information has been gathered over the past 20 years. The primary site for the SGD assessment intercomparison was along an open beach in the Northern Harbor area.

Over 20 scientists from Australia, USA, Japan, Sweden, and Russia participated in this experiment. Several types of SGD assessment approaches, including hydrogeologic measurements, manual and automated seepage meter readings, and tracer measurements were collected during the 10-day intensive experiment.

#### 5.1.2. Seepage meters

Several manual seepage meter measurements were made each day of the experiment for each of eight “Lee-type” meters deployed along two transects (four meters on each transect) set up normal to shore and extended out to a distance of  $\sim 100$  m. Each day, after several measurements were taken, the results were pooled as a

Table 1

Locations, dates, and various characteristics of the five sites used for SGD assessment intercomparison experiments

| Number, site                              | Dates of assessment intercomparison | Geologic/oceanographic settings  | Tidal characteristics, climate   | SGD assessment methods   |
|---|-------------------------------------|--|--|--|
| (1) Cockburn Sound, Western Australia     | November 25–December 6, 2000        | Coastal plain; marine embayment  | Diurnal ( $\sim 1$ m) temperate, semi-arid; occasional high on-shore winds                   | Seepage meters; Ra isotopes; Rn; hydrologic modeling             |
| (2) Donnalucata, southeastern Sicily      | March 18–24, 2002                   | Volcanic with limestone veneer; small boat basin and up to few km offshore | Semidiurnal ( $\sim 0.2$ m); semi-arid; winds calm to strong ( $> 10$ m/s) during experiment | Seepage meters; Ra isotopes; Rn; numerical modeling              |
| (3) Shelter Island, Long Island, New York | May 18–24, 2002                     | Glacial moraine; protected embayment (West Neck Bay)                       | Semidiurnal ( $\sim 1.2$ m); temperate wet   | Seepage meters; Ra isotopes; Rn; previous hydrogeologic modeling |
| (4) Ubatuba, Sao Paulo State, Brazil      | November 16–22, 2003                | Fractured crystalline rocks; marine embayment                              | Semidiurnal ( $\sim 1$ m), subtropical, wet (rain $\sim 1800$ mm/year)                       | Seepage meters; Ra isotopes; Rn; artificial tracers              |
| (5) Mauritius Islands (Indian Ocean)      | March 19–26, 2005                   | Volcanic island; partially enclosed (barrier reef) lagoon                  | Semidiurnal ( $\sim 0.5$ m); tropical, very wet (rain up to 4000 mm/year)                    | Seepage meters; Ra isotopes; Rn; water balance                   |

Further details are provided in the following sections.

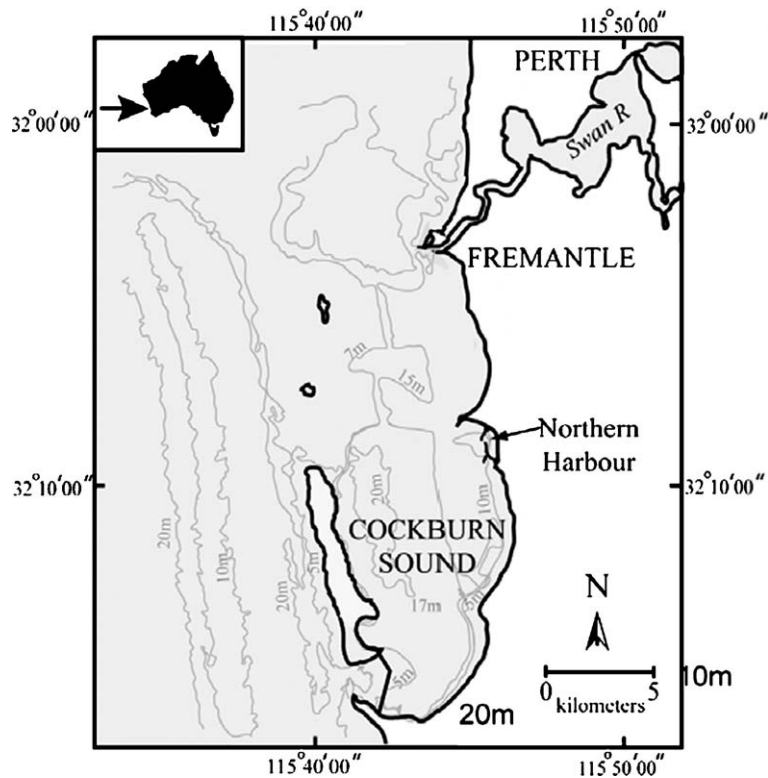


Fig. 13. Location map of Cockburn Sound, Western Australia. The SGD assessment intercomparison was run mainly off the beach in the Northern Harbor area.

“daily average” and integrated by distance offshore to obtain estimates of total seepage per day per meter of shoreline (Fig. 14).

#### 5.1.3. Radium isotopes

The Ra isotope data in Cockburn Sound does not follow a predictable pattern of steadily decreasing

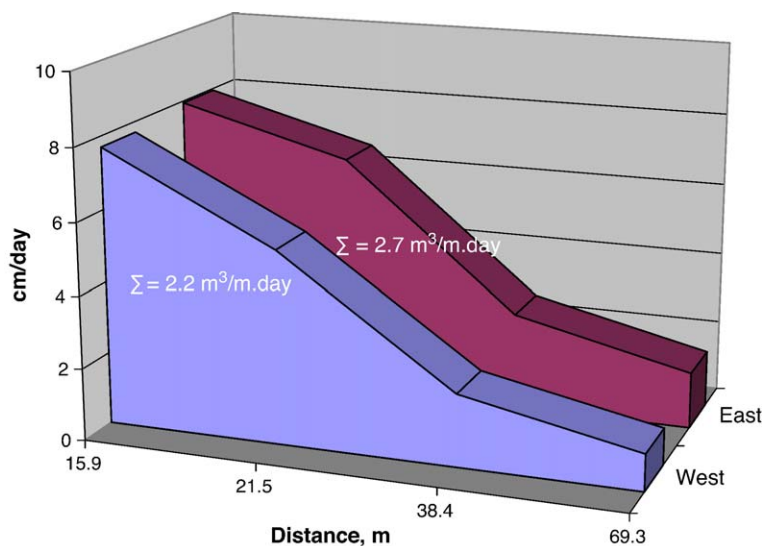


Fig. 14. Manual seepage meter results for November 28, 2000, Cockburn Sound. The two trends correspond to the west (integrated flux =  $2.2 \text{ m}^3/\text{m day}$ ) and east ( $2.7 \text{ m}^3/\text{m day}$ ) transects, respectively.

activities with distance from shore. Instead there are regions of higher activity occurring at considerable distances from shore. We conclude that SGD fluxes occur throughout the Sound, not just at the shoreline. Because of the irregular pattern of enrichments, a simple one-dimensional model cannot be used to interpret the data.

Loveless (2006) used a  $^{226}\text{Ra}$  mass-balance approach based on a model of Charette et al. (2001) to determine the quantity of groundwater input into Cockburn Sound. The residence time of the waters in the system was estimated based on the  $^{224}\text{Ra}/^{226}\text{Ra}$  activity ratios in the harbor compared to pre-discharge groundwaters. The derived estimate of 3.3 days is comparable with a summer value of 2.8–3 days, determined using a Lagrangian water particle tracking model (Wright, 2000). Using the calculated residence time to account for dilution of  $^{226}\text{Ra}$ , the activity in excess of the benthic sediment and ocean end-member sources is attributed to the groundwater source. Oceanic values were taken from Parmelia Bank sampling stations. A reported literature value of  $0.044 \text{ dpm/m}^2 \text{ day}$  was used to account for the contribution of  $^{226}\text{Ra}$  from benthic sediment particles (Charette et al., 2001). Normalized to the area of the harbor, this is a benthic sediment flux of  $3.4 \times 10^4 \text{ dpm/day}$ . It must be recognized that the value given in Charette et al. (2001) was a maximum value intended to demonstrate that little  $^{226}\text{Ra}$  was entering their study area from sediments. However, when extrapolated to the area of Cockburn Sound, this flux is a considerable component of the  $^{226}\text{Ra}$  input to the Sound.

Seepage water concentrations of  $^{224}\text{Ra}$  and  $^{226}\text{Ra}$  were used to represent the SGD activities following procedures outlined earlier in this paper and in Moore (1996), Moore (2000), and Charette et al. (2001). To support the  $^{226}\text{Ra}$  in the surface waters required an “excess” of  $2.51 \times 10^7 \text{ dpm/day}$  of  $^{226}\text{Ra}$  over that activity calculated to be supported from marine and local sediment sources. Using a pre-discharge  $^{226}\text{Ra}$  activity  $0.46 \text{ dpm/L}$ , this excess represents a total SGD input of  $50 \times 10^3 \text{ m}^3/\text{day}$ . It is expected that during the period of the intercomparison (December), the groundwater aquifer displayed a higher recharge condition (peak recharge normally occurs at the end of winter: September–October). Extrapolating to the total shoreline length (16 km) provides an estimated discharge of  $3 \text{ m}^3/\text{m day}$  into Cockburn Sound. This estimate of SGD based on radium isotopes falls nicely in the middle of the reported upper and lower recharge estimate determined by flow net analysis (Smith et al., 2003). However, it must be recognized that the flow net

analysis estimates only fresh SGD, while  $^{226}\text{Ra}$  estimates total SGD. Since the seepage water was near seawater salinity, total SGD must be considerably greater than fresh SGD. It is likely that the  $^{226}\text{Ra}$  model underestimated total SGD because the value taken for the sedimentary input was too large.

#### 5.1.4. Radon

One of the stations in a central portion of the experimental area was equipped with a continuous radon monitor (Burnett et al., 2001b). Grab samples of seawater were also collected from the same location at various times and analyzed by conventional radon emanation techniques with results very close to those provided by the continuous monitor. The radon data showed a pattern generally similar to that of an automated seepage meter deployed by M. Taniguchi with higher radon concentrations and higher seepage rates during the lowest tides, a feature that has been observed elsewhere. Both the radon record and the seepage meter results are suggestive of a strong tidal influence on the transient magnitude of the SGD flux. The estimated flow based on modeling the radon record as described in Burnett and Dulaiova (2003) ranged from  $2.0$  to  $2.7 \text{ m}^3/\text{m day}$ .

#### 5.1.5. Summary

A summary of all the seepage flux estimates from the intercomparison shows that there was good agreement at this site (Table 2). Both the radium isotopes and radon models fall within the range of the seepage meter estimates and the hydrological modeling. This was not the case in a preliminary intercomparison experiment in Florida, where the radiotracers and seepage meters agreed closely, but the modeling showed much lower values (Burnett et al., 2002). The somewhat higher estimate seen by the radium isotopic approach than radon may be a consequence of differences in scale. The radium samples were collected over distances of several

Table 2  
Estimated integrated SGD ranges (daily averages) via four different approaches for Cockburn Sound, Australia (November 25–December 6, 2000)

| Estimated groundwater discharge ( $\text{m}^3/\text{m day}$ ) |                 |         |                       |
|---|-----------------|---------|-----------------------|
| Seepage meters  | Radium isotopes | Radon   | Modeling <sup>a</sup> |
| 2.5–3.7   | 3.2             | 2.0–2.7 | 2.5–4.8               |

The seepage meter, radium isotopes, and radon measurements were all made during the same period. The modeling was performed later for average conditions.

<sup>a</sup> Spatially averaged SGD via a distributed groundwater flow model (Smith and Nield, 2003).



kilometers, from the near-shore out to the mouth of Cockburn Sound. In addition, the radium data suggests that SGD is occurring throughout the Sound, not just along the shoreline where the radon monitor and seepage meters were deployed. The radon estimates were based on continuous measurements at one location near the beach. The seepage meter estimates may be expected to be somewhat higher because the measurements were all made during the day, which happened to coincide with the low tide (higher seepage) intervals.

## 5.2. Donnalucata, Sicily

### 5.2.1. Introduction

Two expeditions were carried out (June 2001 and March 2002) in collaboration with the University of Palermo, Italy, to sample groundwater, seawater, and sediment along the south-eastern Sicilian coast. The studied area (Fig. 15) belongs to a structure, noted in the literature as the Hyblean Plateau that represents one of the principal structural elements of eastern Sicily, which is considered geologically as part of the African continental crust (thickness over 30 km). The western sector, where Donnalucata is found, has an aquifer in the calcarenite sands of Pleistocene origin (an average depth from 50 to 100 m). The second aquifer is in the Ragusa Formation, confined by the marls of the Tellaro Formation. Along the coast, the carbonate aquifers

directly discharge their waters into the sea producing numerous springs observed on beaches. The groundwater also flows through the faults directly to the sea forming submarine springs, locally called “bugli” (Aureli, 1994). Well-known submarine springs are located in the port of Donnalucata (where our intercomparison study was done), in the inlet of Ognina and in the mouth of the River Cassibile called “Balatone.” Further to the east, near Syracuse city, the Aretusa spring has been well known from mythology.

### 5.2.2. Study area and geophysical characterization

The study area for the intercomparison was in the small town of Donnalucata in the province of Ragusa along the southeastern coast of Sicily. Many springs are known to occur in this area, both on-shore and offshore. Our original main goal was to assess SGD along a several kilometer stretch of coastline in this area. Unfortunately, high wind and surf conditions prevented us from making many measurements along the open coastline. However, a protected boat basin (Fig. 16) allowed us to conduct a series of measurements for assessing SGD.

A portable, geo-electric instrument based on time domain electromagnetic sounding technology was used during the 2002 experiment in Donnalucata to obtain subsurface information. The analysis of 3-D structures of geo-electrical data shows the presence of several

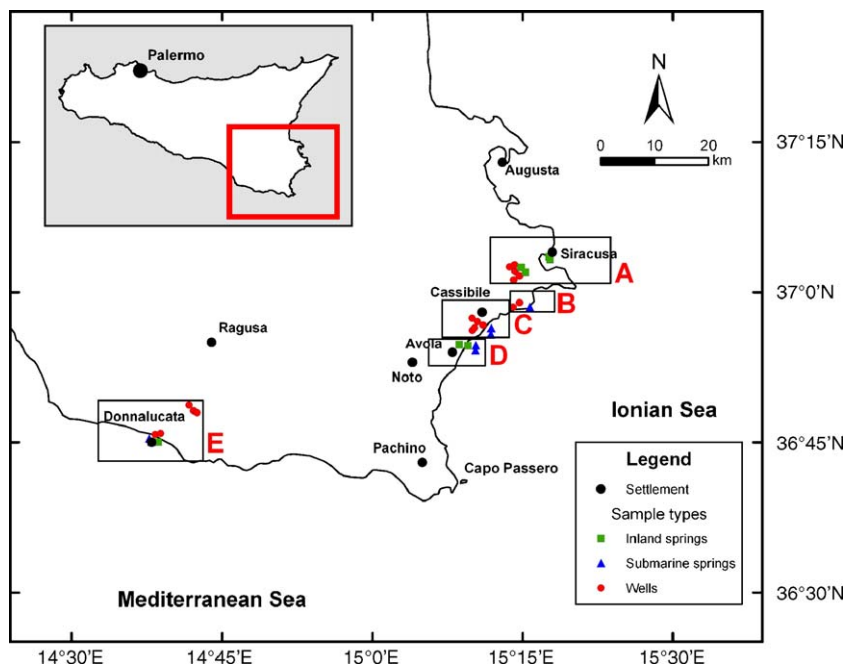


Fig. 15. Areas in southeastern Sicily where SGD studies have been undertaken as part of the IAEA–UNESCO project on SGD. The area around Donnalucata (E) was where the detailed intercomparison studies were performed.

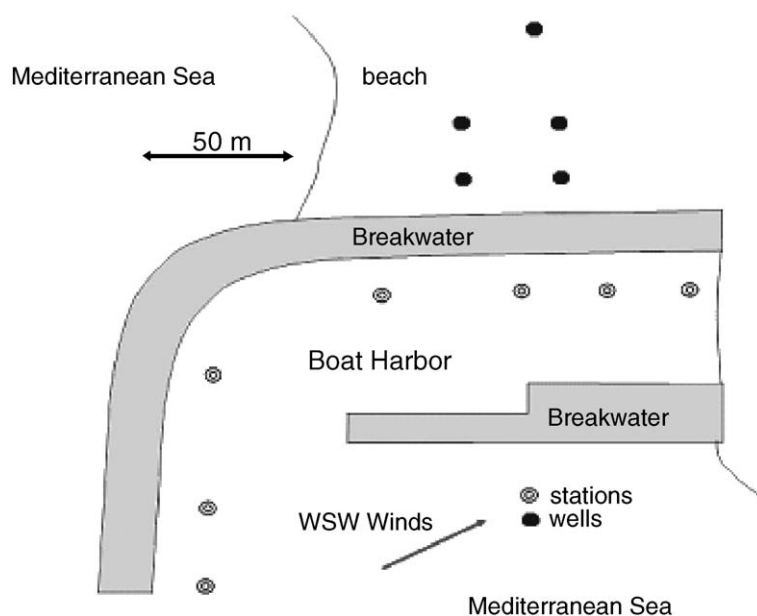


Fig. 16. Sketch diagram of the Donnalucata boat basin.

layers with different formation resistivities. The top 50 m represents a freshwater saturated zone (formation resistivity above 50  $\Omega$  m) with water flowing towards the sea. However, closer to the pier (Fig. 16) a saltwater intrusion can be observed. The pier acts as a barrier for the transport of freshwater to the sea; i.e., it has blocked a superficial drain. The saltwater horizon is located at the depth between about 50 and 80 m, at the east corner of the pier with a formation resistivity between 3 and 30  $\Omega$  m. Below the 80 m layer a freshwater horizon is seen again, which may represent a deeper freshwater aquifer.

### 5.2.3. Isotopic analyses

Stable isotope data shows that the fresh groundwater and some springs discharging groundwater lie close to the Mediterranean meteoric water line, and are depleted in  $\delta^{18}\text{O}$  (from about  $-4.5\text{‰}$  to  $-6\text{‰}$ ) with respect to Vienna Standard Mean Ocean Water (Fig. 17). In contrast, the seawater samples are highly enriched in  $\delta^{18}\text{O}$  (from about  $0\text{‰}$  to  $2\text{‰}$ ). The SGD waters have  $\delta^{18}\text{O}$  values from about  $-2\text{‰}$  to  $-3\text{‰}$ , and fall on a mixing line between groundwater and seawater. These samples may consist of about 40% to 50% fresh groundwater, implying high SGD fluxes into the coastal waters off Sicily. The seawater samples have  $\delta^{18}\text{O}$  values from about  $1.5\text{‰}$  to  $0\text{‰}$ , and fall on the right end of the curve. The tritium content of collected seawater and groundwater samples varied from 1.5 to 4.1 TU. The residence time of groundwater in the limestone

formations of south-eastern Sicily, estimated using the  $^3\text{H}/^3\text{He}$  method and CFC measurements ranges from 2 to 30 years.

### 5.2.4. SGD evaluations

Quantitative assessments of SGD made by seepage meters, radon, and radium isotopes are given in Table 3. The seepage meter and radon estimates were only made within the boat basin while the radium isotope evaluation of groundwater discharge was based on measurements made within a few kilometers offshore of the boat harbor. The SGD estimate per unit shoreline made by radium isotopes, thought to be conservative, is

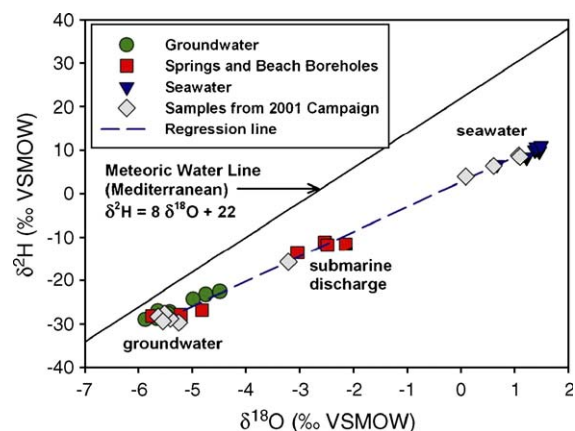


Fig. 17. Isotopic composition ( $\delta^2\text{H}$  and  $\delta^{18}\text{O}$ ) of groundwater and seawater samples from southeastern Sicily.

Table 3

Estimated SGD discharge rates into the boat basin at Donnalucata, Sicily via seepage meters, and radon

|  | Seepage meters | Radon     | Radium |
|--|----------------|-----------|--------|
| Boat basin ( $\text{m}^3/\text{day}$ )                 | 300–1000       | 1200–7400 | –      |
| Shoreline flux ( $\text{m}^3/\text{m}^2 \text{ day}$ ) | 10–30          | 30–200    | 1000   |

The shoreline fluxes were determined from offshore sampling of radium isotopes and by normalizing the seepage meter and radon estimates to the width of the boat basin.

Seepage meter data from Taniguchi et al. (2006); radon estimates from Burnett and Dulaiova (2006); and radium results from Moore (2006).

much higher than either the radon or seepage meter measurements (Moore, 2006). The lower shoreline flux inside the harbor may be because the presence of springs was lower inside the boat basin. Alternatively, it may be that the offshore data was responding more to SGD created by wave set up (e.g., Li et al., 1999) on the beach and this effect was damped in the protected environment of the boat basin.

The proposed numerical method (PCFLOW3D) was applied using parameters measured in the Donnalucata boat basin. For the purpose of numerical simulations measured SGD inflow velocity was assumed to be constant in each region A to E (Fig. 18) using seepage rates determined via seepage meters with the values of: 2.2; 35.7; 2.8; 2.0; and 15.1 cm/day respectively (Taniguchi et al., 2006). The initial value for salinity was 38.2 and the salinity of the inflow SGD sources was assumed to be 1. Wind from WSW, with the velocity of 6 m/s was taken into account. The hydrodynamic and salinity fields were simulated with these data. Tidal elevation changes were below 20 cm and were not taken into account in this case. Simulated and measured salinity distribution is presented in Fig. 18. Generally, the simulation results confirmed the observations and suggest possible future applications of numerical modeling in SGD studies.

### 5.3. Shelter Island, New York

#### 5.3.1. Introduction

Shelter Island is located in Peconic Bay between the north and south forks of Long Island, New York (Fig. 19). The island is composed of upper Pleistocene glaciofluvial deposits consisting of outwash sands (fine, medium, and coarse) and gravel, cobbles, boulders, clay, and silt (drift/till). There are no major streams or creeks on the island and, therefore, groundwater that enters the aquifer primarily discharges through the coastline into the surrounding coastal waters. Freshwater on Shelter Island is restricted to the unconfined Upper Glacial aquifer. Two clay units lie below the Upper Glacial. Water sampled from these lower units was previously determined to be saltwater. The clay layers overlie two deeper, unconsolidated aquifers. The deepest aquifers rest on Precambrian crystalline bedrock.

The intercomparison experiment was conducted May 18–24, 2002, in West Neck Bay, located in the southwestern portion of Shelter Island. The bay and its associated creek comprise a total area of approximately 1.6 km<sup>2</sup>, with a mean tidal volume of 3.7 million cubic meters. The tidal range is approximately 1.2 m and water depths are generally less than 6 m. With the exception of sheet runoff, no surface waters discharge into the bay. The average salinity of the bay is approximately 26. Since 1985, West Neck Bay has been affected by nuisance algal blooms of *Aureococcus anophagefferens*, referred to as “brown tide”.

#### 5.3.2. Seepage meters

Various types of seepage devices including manual or “Lee-type” meters (Lee, 1977), constant heat (Taniguchi and Iwakawa, 2001), ultrasonic (Paulsen et al., 2001), and a dye-dilution meter (Sholkovitz et al., 2003) were deployed at distances up to ~50 m

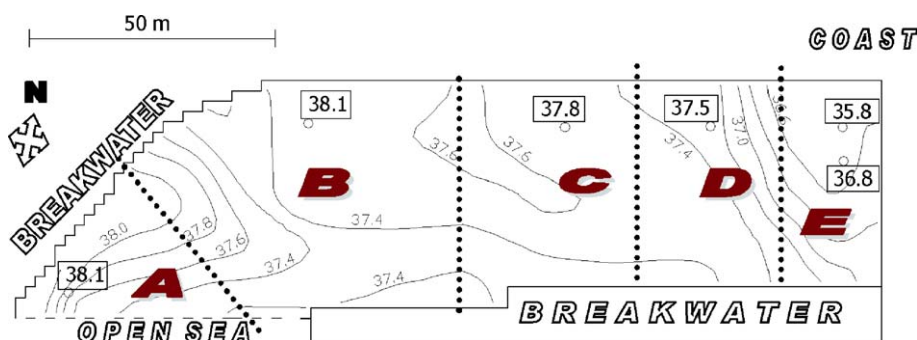


Fig. 18. A comparison of simulated salinity distributions (isolines) with measured salinity (numbers in rectangles) on March 22, 2002.

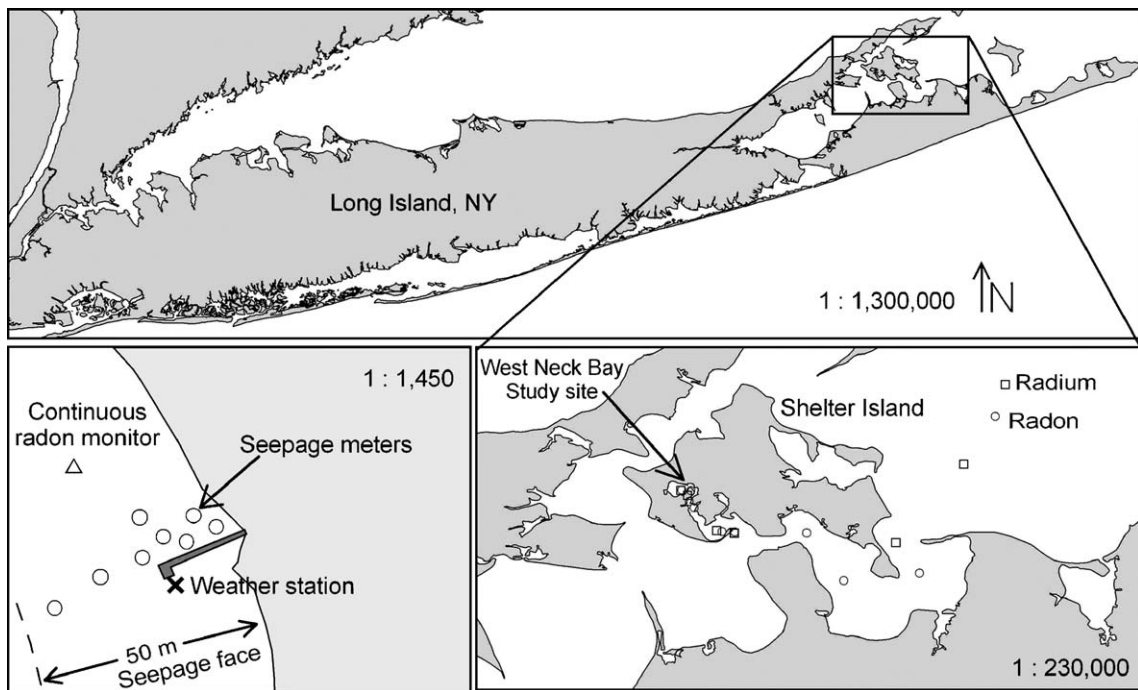


Fig. 19. Location map of West Neck Bay, the study site located at the eastern end of Long Island, New York. The symbols refer to station locations for collection of water samples for geochemical tracers.

from the shoreline. Although SGD is expected to decrease offshore, this pattern is not always found. A pattern of SGD decreasing uniformly offshore was not found at this site. In fact, seepage devices measured rates ranging from less than 10 cm/day to almost 200 cm/day at a similar distance off shore (Fig. 20). This variation was attributed to the influence of a pier that ran perpendicular to the shoreline past the seepage devices. As corroborated by conductivity measure-

ments, the pilings of the pier had apparently pierced a shallow aquitard, allowing local (artesian) discharge of groundwater. Estimated integrated seepage rates for the different types of seepage meters show a total range from 2 to 16 m<sup>3</sup>/m day (Table 4). The ultrasonic and Lee-type meters produced generally higher values than the other types due to the influence of locally high seepage rates near the pier where they were located.

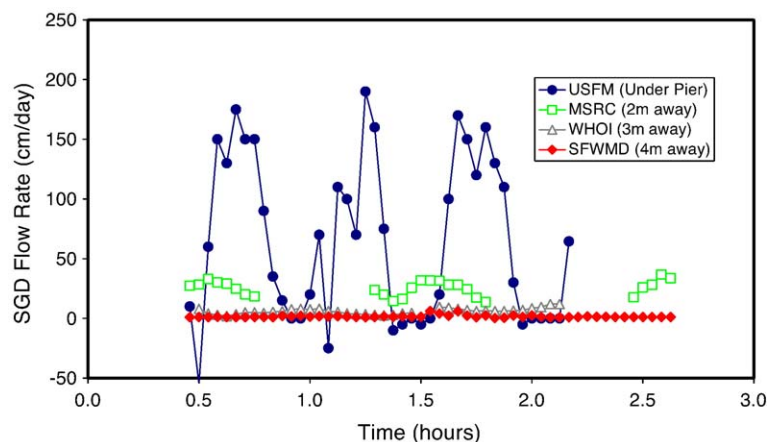


Fig. 20. Variation of SGD at approximately the same distance from shore but at increasing distance from a pier, Shelter Island, New York. The apparent differences in seepage rates were caused by the influence of pilings from the nearby pier that intercepted an aquitard and artificially enhanced seepage.

Table 4

Estimated integrated SGD (daily averages when ranges are shown) via several different types of seepage meters deployed at the Shelter Island intercomparison (May 18–24, 2002)

| Seepage meters estimated groundwater discharge (m <sup>3</sup> /m day) |                           |                                   |                        |                         |
|--|---------------------------|-----------------------------------|------------------------|-------------------------|
| Manual<br>(Lee-type)   | Heat pulse<br>(KrupaSeep) | Continuous<br>heat<br>(Taniguchi) | Dye-dilution<br>(WHOI) | Ultrasonic<br>(Paulsen) |
| 11.5 <sup>a</sup><br><i>n</i> =3 <sup>b</sup>                          | 0.4–0.8<br><i>n</i> =2    | 2.5<br><i>n</i> =1                | 3.4<br><i>n</i> =2     | 17.5<br><i>n</i> =6     |

<sup>a</sup> Using an average flux of 23.2 cm/day.

<sup>b</sup> The *n* in the last row refers to the number of positions each type of meter occupied during the intercomparison.

### 5.3.3. Radon and radium isotopes

The radiotracers produced results (Table 5) that were overlapping but generally higher than the seepage meter results. The radon model shows two ranges based on how the mixing term is evaluated. One way involves inspecting the calculated radon fluxes after corrections for atmospheric evasion and tidal changes. We assumed that the maximum negative fluxes, representing a loss of radon from the system, would be a lower estimate of the mixing loss because greater losses could be masked by concurrently higher inputs. A second approach involves estimating the mixing via inspection of both short-lived radium isotopes and <sup>222</sup>Rn along a transect away from the study site. Multiplying the derived horizontal mixing coefficient ( $K_h$ ; Moore, 2000) by the linear gradient of the <sup>222</sup>Rn and the average depth produces an offshore flux. This result can then be converted to a seabed flux that is equivalent to how the fluxes are expressed in the radon model. The two mixing loss estimates agreed very well at 670 dpm/m<sup>2</sup> h and 730 dpm/m<sup>2</sup> h via inspection of the Rn fluxes and use of radium isotopes, respectively. The integrated seepage rate based solely on radium isotopes overlaps the radon model and the results from the ultrasonic seepage meter.

The integrated discharge calculated from the geochemical techniques was near the upper range of the measurements made with the seepage devices. One possible reason that the radiotracer estimates may tend to be higher than the seepage meter results is that the tracers, measured in the water column, integrate a larger area than the seepage meters. For example, the gradient for <sup>223</sup>Ra, which was used to calculate the mixing and the residence time in West Neck Bay, was based on a transect from the study site in the interior of the bay out to the bay's mouth, over 4 km from the seepage meter site. In addition, results from the WHOI dye-dilution seepage meter, which continuously records the salinity of the seepage fluid, and resistivity profiling both

indicate that a significant portion of the near-shore SGD was as freshwater. Therefore, because of the limited scale of the seepage meter study, the seepage meters may have missed a key component of the total SGD flux at this site; i.e., the seepage meters were responding mostly to near-shore freshwater flow while the radiotracers reflected total (fresh + saline) flow. This suggests that, regionally, there are other areas of high seepage (in addition to the high seepage under the pier) that were not sampled by the meters, but contributed to the SGD measured with geochemical tracers.

There were no modeling estimates made of SGD during the Shelter Island intercomparison. However, a consultant's report concerning the flushing time of West Neck Harbor (DiLorenzo and Ram, 1991) included an estimate of "freshwater inflow" that we assume would be all via groundwater discharges. That report estimated the long-term mean inflow at 1.07 cfs (0.03 m<sup>3</sup>/s) and the maximum inflow at 6.56 cfs (0.19 m<sup>3</sup>/s). We estimated the shoreline length of the bay at 11.3 km. That results in an estimated mean freshwater seepage rate of only 0.23 m<sup>3</sup>/m day and 1.4 m<sup>3</sup>/m day as a maximum inflow. A later USGS study (Schubert, 1998) estimated freshwater inflow into West Neck Bay at 198,000 cfd (0.065 m<sup>3</sup>/s) via a water balance approach. Again normalizing to our estimated shoreline length of 11.3 km, we derive an integrated seepage rate of 0.5 m<sup>3</sup>/m day. All these estimates are lower than the direct measurement approaches. These differences may be attributed to one or more of the following: (1) the models underestimate the groundwater discharge; (2) the seepage meters and tracers are recording higher

Table 5

Estimated integrated SGD ranges (daily averages) via four different approaches for the Shelter Island intercomparison

| Estimated groundwater discharge (m <sup>3</sup> /m day) |   |                 |  |
|---|---|-----------------|--|
| Seepage meters<br>(all types)                           | Radon                                   | Radium isotopes | Modeling   |
| 0.4–17.5  | 8–16 <sup>a</sup><br>18–20 <sup>c</sup> | 16–26           | 0.23–1.4 <sup>b</sup><br>0.5 <sup>d</sup><br>10 <sup>e</sup> |

The seepage meter and isotopic measurements were made during the same period. The modeling was performed by other investigators for average and extreme conditions.

<sup>a</sup> Mixing losses of Rn based on inspection of calculated Rn fluxes.

<sup>b</sup> Based on estimate of mean fresh water discharge into West Neck Harbor (DiLorenzo and Ram, 1991).

<sup>c</sup> Mixing losses of Rn based on short-lived radium isotopes.

<sup>d</sup> Based on a water budget estimate of Shelter Island (Schubert, 1998).

<sup>e</sup> Based on a MODFLOW model of West Neck Bay (O'Rourke, 2000).



flows due to large amounts of recirculated seawater; or (3) the intercomparison exercise was conducted during an atypical period relative to the long term averages that the model-derived fluxes are based upon.

#### 5.3.4. Geophysical studies

Concurrent to the direct measurements of seepage rates, the bulk ground conductivity of seafloor sediments was mapped near a pier at the study site. A shallow sediment layer was identified to provide confinement for lower aquifer units. The conductivity and seepage rate data indicate that pilings of the pier apparently pierce this shallow sediment layer, producing a comparatively high seepage rate driven by the hydraulic head of the (semi)confined aquifer, resulting in a substantial increase in SGD in the immediate vicinity of the pier.

#### 5.3.5. Summary

While there is obviously some uncertainty about the “best” integrated seepage values to apply at the Shelter Island site, some of the comparisons produced some very encouraging results. For example, a comparison of calculated radon fluxes with measured seepage rates via the WHOI dye-dilution seepage meter, and water levels (Fig. 21) shows a great deal of similarity in the derived patterns. During the period (May 17–20) when both devices were operating at the same time, there is a clear and reproducible pattern of higher fluxes during the low tides. There is also a suggestion that the seepage spikes slightly led the radon fluxes, which is consistent with the notion that the groundwater seepage is the source of the radon.

The excellent agreement in patterns and overlapping calculated advection rates (seepage meter = 2–37 cm/day; radon model = 0–34 cm/day, average =  $12 \pm 7$  cm/day) by these two completely independent assessment tools is reassuring. An important lesson from this site was the significance, even dominance, of anthropogenic influences as seen in the elevated SGD at the pier pilings.

#### 5.4. Ubatuba, Brazil

##### 5.4.1. Introduction

The intercomparison in Brazil (November 16–22, 2003) was carried out mainly in Flamengo Bay, one in a series of small embayments near the city of Ubatuba, São Paulo State (Fig. 22). Besides Flamengo Bay (where there is a marine laboratory of the University of São Paulo that served as a base of operations), these embayments included Fortaleza Bay, Mar Virado Bay and Ubatuba Bay. The study area also included the northernmost part of São Paulo Bight, southeastern Brazil, a tropical coastal area. The geological/geomorphologic/hydrogeological characteristics of the area are strongly controlled by the presence of fractured crystalline rocks, especially the granites and migmatites of a mountain chain locally called Serra do Mar (altitudes up to 1000 m), which reaches the shore in almost all of the study area, and limits the extension of the drainage systems and of the Quaternary coastal plains (Mahiques, 1995). The mean annual rainfall is about 1800 mm, the maximum rainfall rates usually occurring in February. Sea level varies from 0.5 to 1.5 m, the highest values occurring in months August/

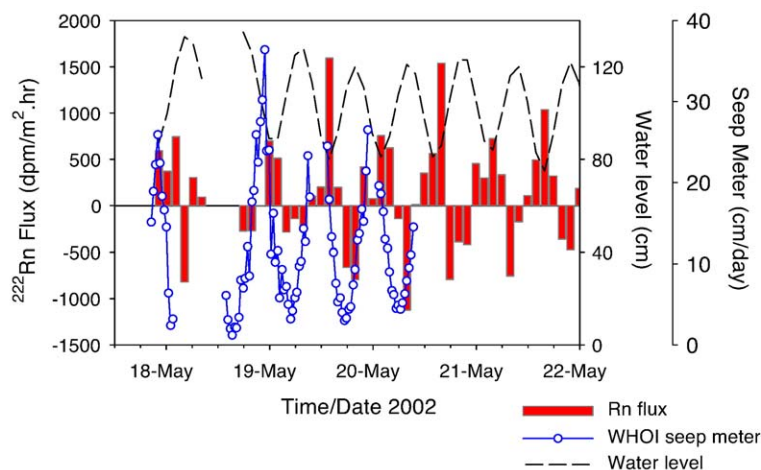


Fig. 21. Plot comparing variations in seepage based on a dye-dilution seepage meter developed at Woods Hole Oceanographic Institution (Sholkovitz et al., 2003), radon fluxes, and water level. Negative Rn fluxes interpreted as being due to mixing losses.

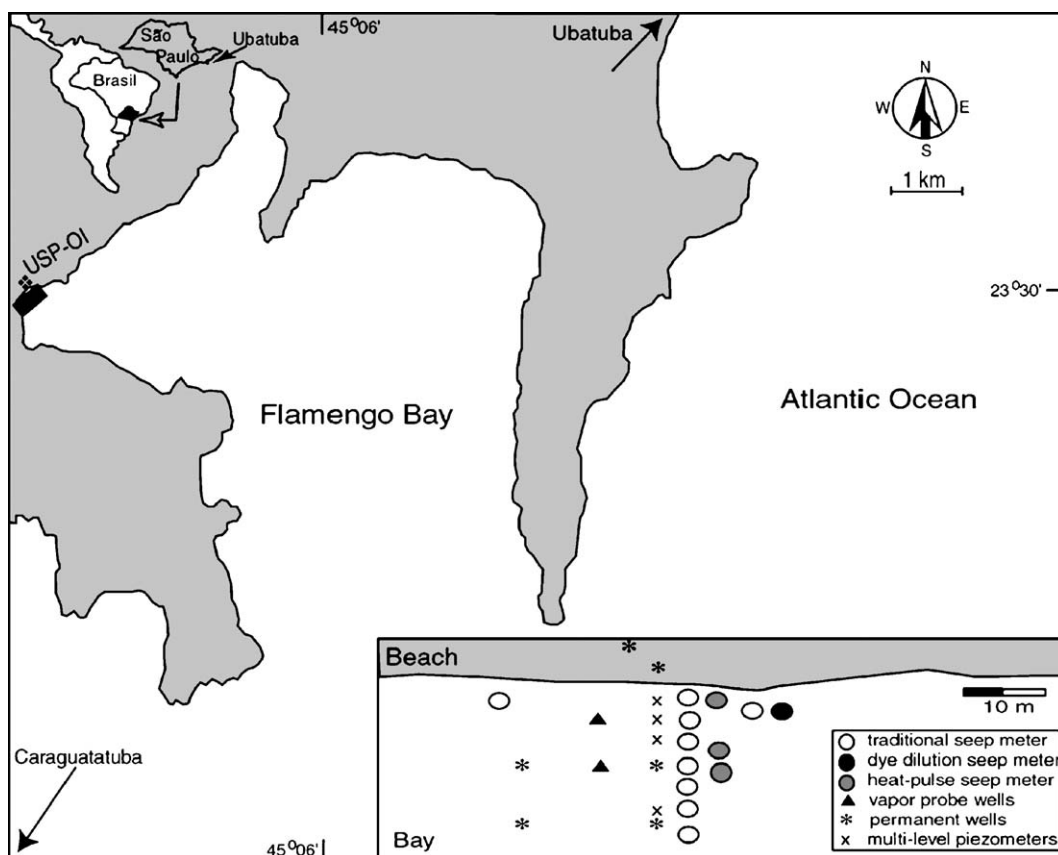


Fig. 22. Field intercomparison of near-shore techniques were performed at the University of Sao Paulo Oceanography Institute (USPOI), near Ubatuba, Brazil. Transects were set up normal to the shoreline for Lee-type seepage meters (open circles), heat-pulse seepage meters (gray circles), and one dye-dilution seepage meter (black circle). In addition, multi-level piezometers (small x's) were installed along a pre-existing transect of wells (stars) or parallel (black triangles) to this well transect.

September due to greater volume of warm waters of Brazil Current (Mesquita, 1997). Despite the small drainage basins between the mountain range and the shore, freshwater discharge is sufficient to reduce the salinity of coastal waters.

#### 5.4.2. Geophysical studies

Preliminary subsurface conductivity/resistivity investigations were run to reveal the structure of the flow field of the freshwater component of SGD. Such measurements allow for predictions of entry points of

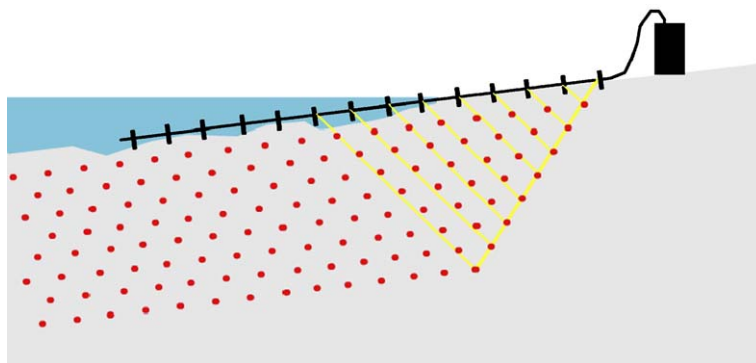


Fig. 23. Schematic diagram showing principle of remote sensing of resistivity (conductivity). The system shown portrays the case where electrodes are only mounted on the surface. Depth of penetration and resolution are dependent upon spacing between these electrodes.

fresh SGD. While it is not possible to derive absolute SGD fluxes from such geoelectric measurements, the relative distribution of SGD can be investigated in great detail, especially where seepage or discharge follows preferential flow paths (Stieglitz, 2005).

Both conductivity and resistivity were measured with electrode arrays, either directly by deploying an electrode array in the ground, or by inverse modeling of remotely sensed resistivity measured on electrodes deployed only on the surface (Fig. 23). The high-resolution transect (Fig. 24a) was interpolated from 130

single-point measurements recorded on electrodes inserted into the ground at different locations along a transect. The significantly reduced ground conductivity close to the sediment surface at around 23–25 m distance suggests a greater influence of fresh SGD at this location than along other parts of the transect. A manual seepage meter, which was deployed at this location subsequent to the conductivity investigations, confirmed both the highest flow rate and lowest salinity discharge along the transect. Without the conductivity investigations, only the seepage meters at 20 m and

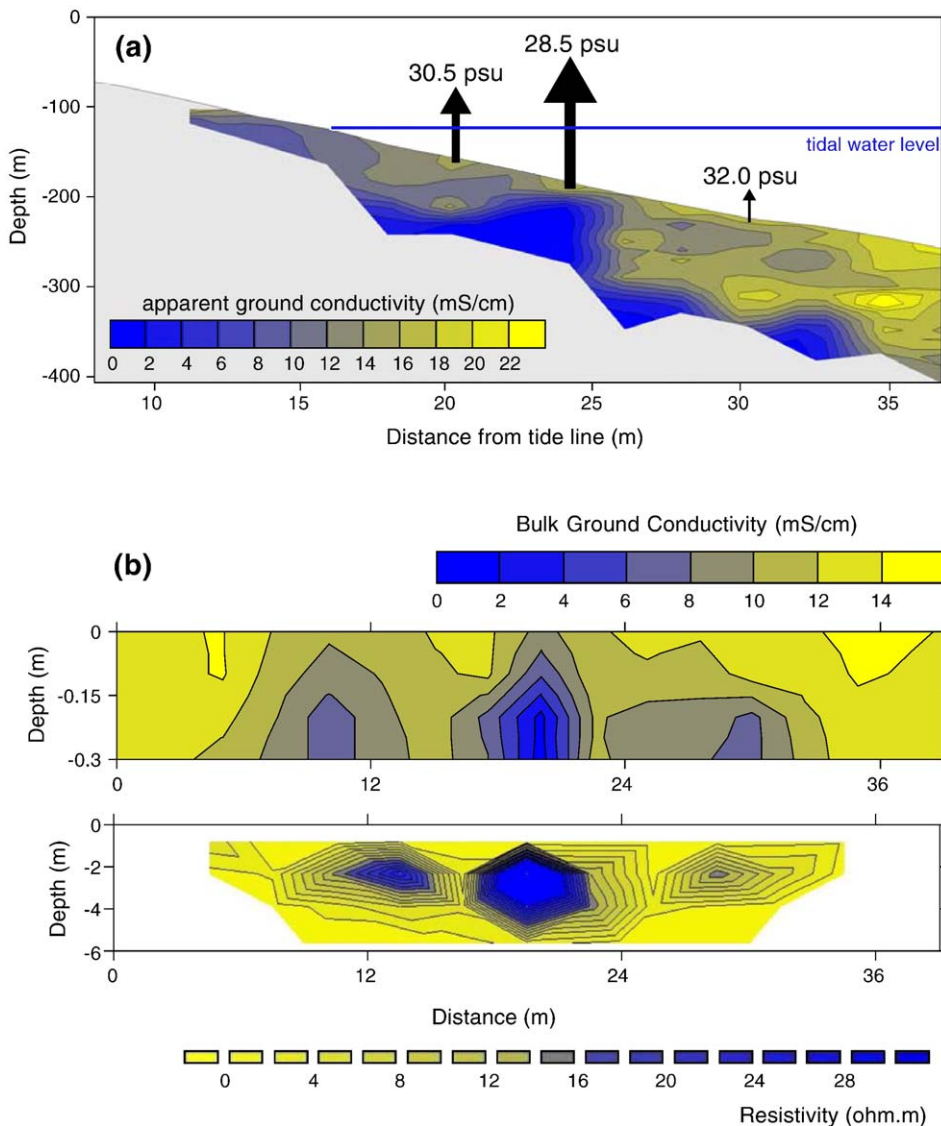


Fig. 24. (a) Ground conductivity shore-normal transect of Flamingo Bay Beach. The arrows at 20 m, 24 m and 31 m distance mark the locations of manual seepage meters deployed along the transect. The length of the arrows is proportional to the average flux of SGD at these sites together with the average salinity. (b) Shore-parallel transects of ground conductivity and resistivity at Fazenda Beach. (top) apparent ground conductivity in the top 30 cm of beach sediment across a shallow creek (center of transect); (bottom) resistivity in the top 5.6 m of beach sediment.

31 m distance would have been deployed, and thus the total flow rate would have been significantly underestimated (Stieglitz et al., submitted for publication).

Simultaneously recorded conductivity and resistivity transects at Fazenda Beach reveal similar features of the subsurface distribution of seawater and freshwater (Fig. 24b). Despite the very different spatial scales of operation of the methods (centimeter vs. meter scale), both methods detected the general features of three low conductivity/high resistivity regions along the beach-parallel profile. The good agreement between the two methods suggests that the results do not suffer from significant artifacts. The transect was recorded across a dry creek on the beach. The low conductivity/high resistivity central region of the transect likely represents the alluvial aquifer of the creek.

#### 5.4.3. Seepage meters

Seven manual seepage meters were deployed along a transect perpendicular from shore at a small beach at the marine laboratory. The shoreward device was exposed at low tide. The other six devices were placed at distances out to 44 m from the low-tide shoreline. Two other devices were placed at the low tide shoreline 19 m east and 14 m west of the transect.

The highest rates of SGD were found at the low tide shoreline, but they were not uniform. The device to the east recorded flow rates as high as 268 cm/day, and collection bags with a capacity of about 6 L had to be replaced every 10 min, whereas at other locations flow rates were often sufficiently low that collections every hour or two were adequate. A tidal modulation was not detected in the results of the manual seepage meters, but

this lack of evidence of tidal influence seems to be an artifact of the sampling interval; continuously recording devices did resolve tidal changes.

The dye-dilution seepage meter was deployed for 3 days (hourly resolution for seepage) at a near-shore location along the beachfront of the marine lab. The meter recorded a pattern of flow that was closely correlated with tidal stage (Fig. 25). Seepage rates ranged from a minimum of 2 cm/day for the high tide on the morning of November 18th to 110 cm/day for the low tide on the morning of November 20th. The average seepage rate for the 3-day deployment was 15 cm/day. The salinity inside the seepage chamber ranged from ~26 to 31. Given an ambient bay water salinity of ~31, the lower salinities suggest that a portion of the SGD included freshwater. The pattern of gradual freshening of the water inside the seepage housing is likely explained by the replacement of bay water (which is trapped inside the housing upon installation of the meter) with fresh/brackish groundwater. The rate at which this bay water is replaced is a function of the seepage rate and the headspace volume inside the seepage chamber. If we assume a headspace volume of ~5 L, a flow rate of ~16 cm/day would be required to explain the gradual freshening inside the seepage chamber from November 18 to 20, which is in excellent agreement with the average flow rate of our dye-dilution method.

SGD was continuously recorded with continuous heat automatic seepage meters every 10 min at three locations along a transect line. The averaged SGD rates were 260 cm/day, 4.2 cm/day, and 356 cm/day at these stations. The averaged conductivities at these same sites

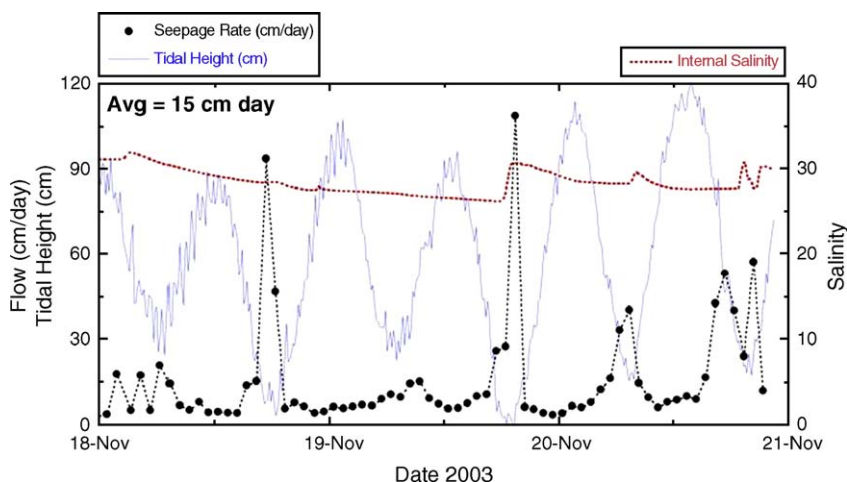


Fig. 25. Water level, seepage rate, and salinity as measured by a dye-dilution seepage meter in a near-shore area off the beach at the marine laboratory, Ubatuba, Brazil (November 18–21, 2003).



were 48.7, 48.9 and 39.9 mS/cm. Semi-diurnal variations of SGD using these automated seepage meters were observed at two of the three stations.

#### 5.4.4. Artificial tracer approach

Multi-level pore water samplers (“multisamplers”) were installed from 2 m below low tide range to about 50 m offshore in the same area as the seepage devices above. Artificial tracers (fluorescein dye saturated with SF<sub>6</sub>) were injected into one of the deeper subsurface ports of the multisamplers and the other ports were sampled at a later time in order to estimate vertical

advective velocities. Based on tracer arrivals at shallower ports than where the tracer was injected, the calculated flow rates ranged from 28 to 184 cm/day.

#### 5.4.5. Radon and radium isotopes

Continuous radon measurements of coastal waters (~2–3 m water depth) were made at a fixed location from a float about 300 m off the marine lab from the afternoon of November 15 to about noon on November 20. There was a short period on November 16 when the system was down for maintenance. The record of radon concentrations showed that they generally range from

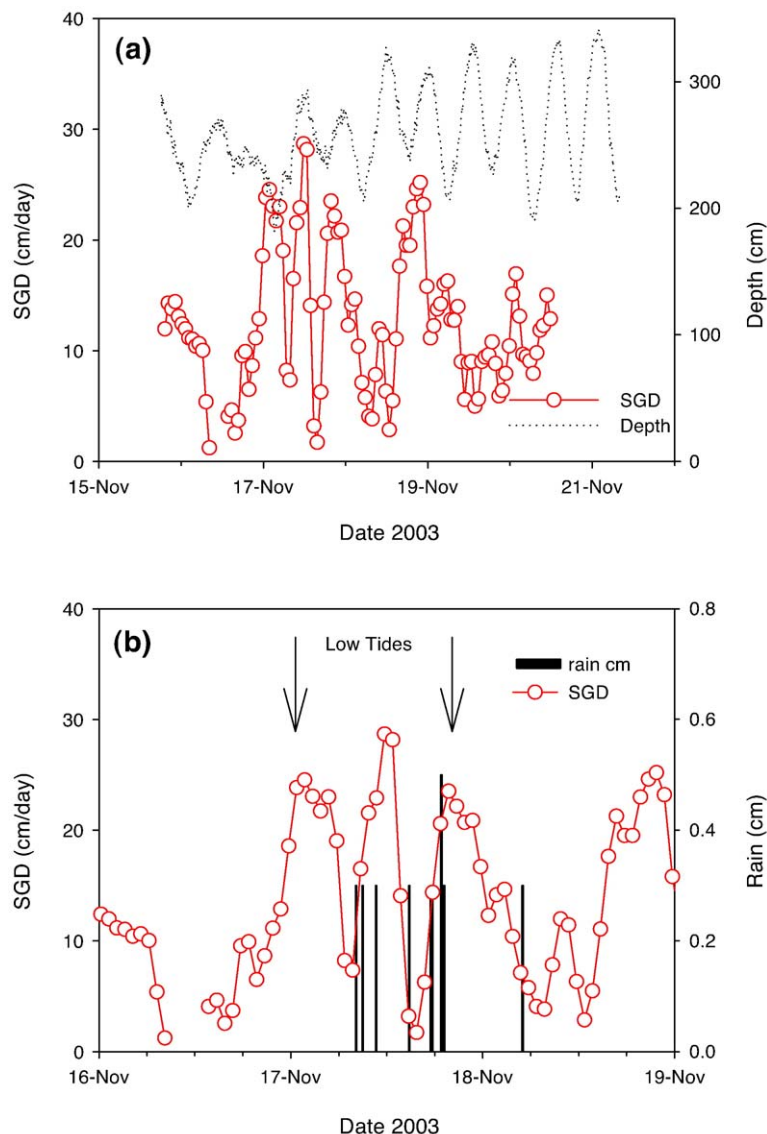


Fig. 26. (a) Calculated SGD rates based on continuous radon measurements at a fixed location about 300 m off the marine laboratory together with water level fluctuations. (b) A portion of the same record showing that the SGD peak that did not correspond to a low tide may have been related to a rain event at that time. Hourly rainfall amounts are shown by the vertical lines (Burnett et al., submitted for publication).

about 2 to 6 dpm/L and showed the highest activities at the lowest tidal stages. Furthermore, the radon maxima tend to have a period of 24-h corresponding to the lowest low tide each day in this semidiurnal, mixed tidal environment. There is one exception to this observation in the early morning of November 17, when an “extra” peak occurred at about the highest tide that day.

We estimated SGD rates from the continuous  $^{222}\text{Rn}$  measurements as described in detail in Burnett and Dulaiova (2003). These rates (Fig. 26a) had a somewhat similar pattern as seen by some of the manual and automated seepage meters deployed at the same time. Over a 109-h period, the estimated SGD based on the radon measurements ranged from 1 to 29 cm/day with an average of  $13 \pm 6$  cm/day. The average seepage rate is very close to the average calculated from the dye-dilution seepage meter of 15 cm/day although that device indicated a much broader range — from about 2 up to over 100 cm/day for short periods during the lowest tides. Most of the seepage spikes that were observed occurred during the lowest tides, with the exception of that one peak around noon on November 17th. Inspection of the rainfall record shows that this was also a period when there was a significant amount of rain (Fig. 26b).

A direct comparison of continuous  $^{222}\text{Rn}$  measurements and advection rates measured by the dye-dilution seepage meter shows some interesting patterns (Fig. 27). It is important to note that these observations showed that the tidal modulation of SGD can be strongly non-linear. While the two instruments only overlapped about 2.5 days during the weeklong experiment, there are clear indications that both measurements were responding to

either tidally induced or modulated forcing. The main peaks in both data sets have a 24-h period and correspond to the lowest low tide each day. The seepage peaks led the peaks in the radon by an hour or two as was also seen in the data from Shelter Island. There are also indications in both records of secondary peaks occurring at the higher low tide. This is more obvious in the seepage meter record, but the radon does show a clear shoulder during the evening low tide on November 19th. It is encouraging that these two completely independent tools respond in such a similar manner to the same process. The seepage meter measured flow directly from a small portion of seabed close to shore while the radon was measured in the overlying water a few hundred meters away and presumably with a much larger sphere of influence.

The Ra isotope studies at Ubatuba revealed inputs of radium occurring in Flamengo Bay at considerable distances from shore. Moore and de Oliveira (submitted for publication) calculated apparent ages of water within Flamengo Bay and used an age vs. distance plot to estimate a water residence time of the order of 10 days. They then developed a mass balance of  $^{228}\text{Ra}$  based on measured values in then seepage bags, Flamengo Bay waters, and offshore waters. They concluded that near-shore SGD as measured by seepage meters can support only 10% of the total SGD to these coastal waters. Most of the SGD must be originating from fracture systems that discharge offshore.

#### 5.4.6. Summary

A summary of the shoreline groundwater discharge estimates, expressed as specific discharge, is given in

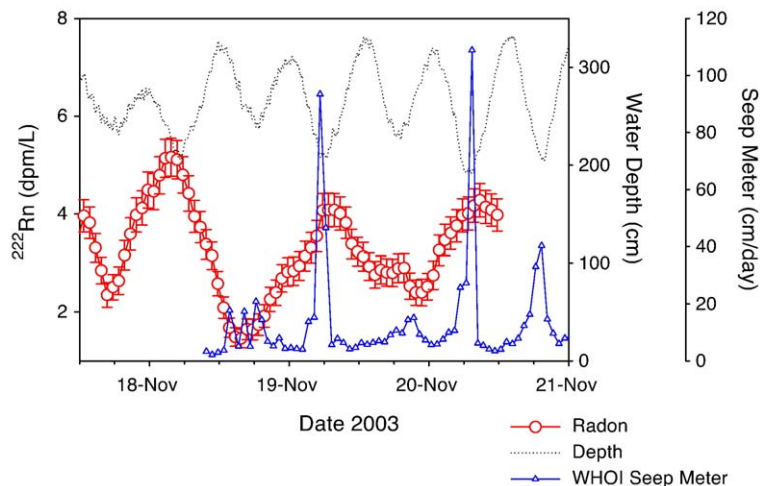


Fig. 27. Combined data sets from the dye-dilution seepage meter (triangles), radon concentration (circles), for the time period when both instruments were running. The water level record (dots) is also shown.

Table 6

Ranges and mean values of specific discharge measurements made during the Brazil intercomparison (November 16–22, 2003) by different approaches

|                | Seepage meters |                               |              | Other            |                     |
|----------------|----------------|-------------------------------|--------------|------------------|---------------------|
|                | Manual meters  | Continuous heat               | Dye-dilution | Continuous radon | MLS SF <sub>6</sub> |
| Range (cm/day) | 5–270          | 0–360                         | 2–109        | 1–29             | 28–184 <sup>a</sup> |
| Mean (cm/day)  |                | 1A: 260<br>3A: 3.1<br>4A: 190 | 15 ± 19      | 13 ± 6           | 88 ± 84             |

All values are given as units of cm/day (cm<sup>3</sup>/cm<sup>2</sup> day) from various locations in the near-shore zone off the marine laboratory in Flamengo Bay. Note that the standard deviations reported reflect the actual variation of the measured seepage and do not reflect an uncertainty of the reported value.

<sup>a</sup> SF<sub>6</sub> tracer-derived seepage rates are minimums.

**Table 6.** We postulate that the irregular distribution of SGD seen at Ubatuba is a characteristic of fractured rock aquifers. The bay floor sediments were sandy and not noticeably different from place to place in the study area. However, bedrock is exposed at the shoreline and an irregular rock surface was encountered at shallow depths offshore. For example, investigators could drive probes to a depth of a few meters in some places but less than half a meter at adjacent locations. The water feeding the SGD is supplied to the bottom of the thin blanket of unconsolidated sediment through a fractured system and concentrated (or dispersed) along the irregular surface of the buried rock. Presumably, this is fresh groundwater working its way seaward through the fractured rock (Fig. 28). The relatively high salinity in the pore water of the sediment blanket, despite high discharge rates, must be due to some efficient mixing process in the surficial sediments themselves, perhaps a combination of gravitational, free convection, and wave pumping (Bokuniewicz et al., 2004).

It is clear from all these results that the advection of pore water fluids across the seabed in Flamengo Bay is

not steady state but episodic with a period that suggests non-linear tidal forcing. This is very similar to observations reported from other environments (e.g., Burnett et al., 2002; Sholkovitz et al., 2003; Taniguchi et al., 2002).

### 5.5. Mauritius

#### 5.5.1. Introduction

One setting was not investigated in a previous intercomparison: volcanic terrain. Volcanic areas, especially islands, may be of particular interest in terms of SGD. The total groundwater discharge to the world oceans estimated by the “combined hydrological and hydrogeological method” (Zektser, 2000) is 2400 km<sup>3</sup>/year (river flow ~35,000–40,000 km<sup>3</sup>/year, so this global SGD estimate represents 6–7% of the world’s river discharge). Of this total flow, Zektser estimates that 1485 km<sup>3</sup>/year is derived from continents and 915 km<sup>3</sup>/year from “major islands.” Thus, the flow from large islands is estimated to be more than one-third of the total global SGD. Recent studies by Kim et al. (2003) and Hwang et al. (2005) on the volcanic island of Jeju, off Korea, have also shown much higher SGD rates than typically observed on continental areas.

The observation that oceanic islands apparently account for such a disproportionately high amount of SGD is likely a combination of several factors. The largest islands (New Guinea, Java, Sumatra, Madagascar, West Indies, etc.) are located in humid tropical regions with high rainfall. In addition, large islands are often characterized by high relief, high permeability of fractured volcanic rocks, and an “immature” landscape with poorly developed river drainage systems. All of these factors contribute to the potential for high groundwater discharges.

We thus decided to investigate a volcanic area for the final intercomparison exercise. While data specifically on SGD in Mauritius (Fig. 29) was not available, reports

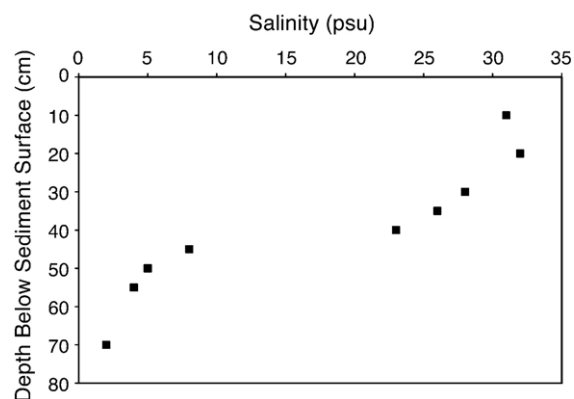


Fig. 28. Porewater salinity profile, located 2 m offshore from the high tide line and measured at high tide. A hard, fine-grained layer was encountered around 42 cm.

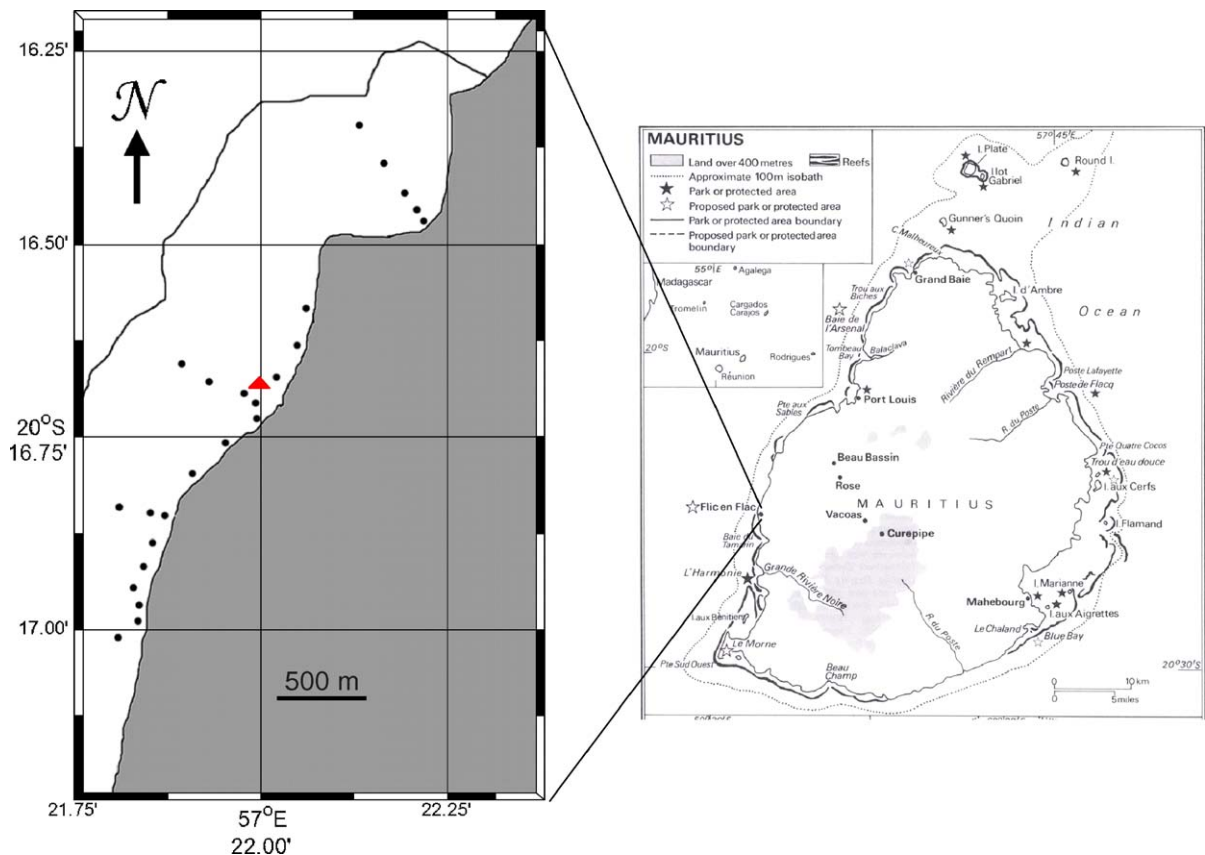


Fig. 29. Map of the island of Mauritius together with a detailed view of the locations of the intercomparison experiments near the town of Flic-en-Flac on the southwest coast. The circles show the locations of manual seepage devices. The triangle denotes the location of a submarine spring.

suggested that substantial groundwater discharges in the lagoons from the volcanic aquifers. In addition to the reports of considerable seepage and large submarine springs, the lagoons are experiencing enhanced nutrient loading and eutrophication. While not documented, SGD likely plays an important role here. The rainfall is high (up to 4000 mm in the mountains), and it has all the other characteristics of areas that have elevated SGD.

##### 5.5.2. Water balance estimate

Mauritius relies heavily upon groundwater to meet both potable water demand (about 56% of that demand is satisfied by groundwater; Ministry of Public Works, 2003) and agricultural demand, primarily for the sugarcane industry. Because of this, a network of monitoring wells, stream gauging stations, and meteorological stations has been established on the island to collect a variety of data related to both groundwater and surface water. These data provide the basis for an estimate of freshwater SGD.

The Curepipe Aquifer extends from the high plateau in the center of the island to the western shoreline,

approximately 15 km to the west. The total area is approximately 95 km<sup>2</sup>. It consists of highly permeable, Recent (1.5 Ma to 25 ka) lava flows with a saturated thickness of 10 to 20 m (Giorgi et al., 1999) and a range of transmissivity of 10<sup>-5</sup> to 10<sup>-2</sup> m<sup>2</sup>/s.

Seasonal rainfall on Mauritius varies from an average maximum of 310 mm/month during the rainy season (December to April) to an average minimum of 75 mm/month during the dry season. For the Curepipe Aquifer, rainfall is about 4000 mm/year near the groundwater divide on the central plateau and decreases with topography to about 800 mm/year near Flic-en-Flac (Giorgi et al., 1999). Surplus rainfall (rainfall in excess of evapotranspiration) is about 70 mm/year along the coast (Medine meteorological station), 840 mm/year halfway inland (Vacoas meteorological station), and 2160 mm/year on the central plateau (Union Park meteorological station) (Proag, 1995). This excess rainfall would go either to surface runoff or groundwater recharge.

The Curepipe aquifer is covered with highly permeable Recent flows and consequently has almost



no surface runoff. The majority of the water infiltrates through the permeable geologic materials, and there are no streams large enough to gauge within the ground-water basin. Because of this, surface runoff can be neglected from the water budget calculation, and the excess rainfall described above is considered to go entirely to groundwater recharge.

The rate of groundwater extraction is known with the least certainty. The Mauritius Water Resources Unit provided data on groundwater pumping for five of the major water supply wells within the basin. The extraction rate for these five wells for 2004 was  $2.4 \times 10^6$  m<sup>3</sup>/year (Zeadally, personal communication). An additional 36 wells are identified as being in use in the basin (Ministry of Public Works, 2003). Assuming similar pumping rates for these additional wells, a total of  $2.0 \times 10^7$  m<sup>3</sup>/year is pumped from the aquifer.

Subtracting the groundwater pumping from the estimated recharge leaves an estimated freshwater discharge at the shoreline of  $7.5 \times 10^7$  m<sup>3</sup>/year. Dividing this discharge rate by the 8 km of shoreline yields an estimated discharge rate of 9400 m<sup>3</sup>/year/m of shoreline or 26 m<sup>3</sup>/day/m of shoreline. Assuming the discharge takes place over a 40 m zone perpendicular to the coast, an average seepage rate of 64 cm/day is calculated.

### 5.5.3. Seepage meters

The rate and distribution of SGD was measured using vented, benthic chambers on the floor of a shallow lagoon on the west coast of Mauritius Island (Flic-en-Flac). Discharge rates were found as high as 490 cubic centimeters of pore water per square centimeter of sea floor per day (490 cm/day). High SGD rates were associated with low pore water conductivity in the region of a freshwater spring. Large variations in SGD rates were seen over distances of a few meters. We attribute variations to the geomorphologic features of the fractured rock aquifer underlying a thin blanket of coral sands as well as the presence of lava tubes leading to sites of high discharge. Clustering of fractures and the topography of the rock sediment interface might be focusing or dispersing the discharge of groundwater.

Nine seepage meters were placed at a total of 28 locations. Devices were deployed in three shore normal transects (one adjacent to a large submarine spring, one in a cove 1000 m north of the spring, and one about 500 m south of the spring), as well as in a 1500 m shore parallel transect, corresponding to areas of low bulk ground conductivity that was measured previously.

The shore parallel transect consisted of measurements taken at various times from devices all located within 15 m of the low tide line. This transect consisted

of 18 devices that were in place for a period of 10 h to 5 days. Not all measurements along this transect were made simultaneously; however, at least six devices along this transect were measuring SGD throughout the sampling period.

The average flow rate along this shore parallel transect was 54.5 cm/day. If integrated over the entire length of the transect, we estimate a total discharge of  $2.2 \times 10^5$  L/m of shoreline per day (220 m<sup>3</sup>/m day). These measurements probably overestimate SGD because of the very high values near the spring. If the calculation is revised using only the measurements from the offshore transect by the north cove, the integrated SGD would be  $3.5 \times 10^4$  L/m of shoreline per day (35 m<sup>3</sup>/m day). Any evidence of tidal modulation was very weak, but seepage rates at particular sites were seen to abruptly increase (or decrease), and to persist at the new levels, for no obvious reason. Such behavior had also been observed at Ubatuba and, anecdotally, at other sites.

Water collected from the benthic chambers showed freshwater dilution only in the vicinity of the spring. Ambient salinities were about 35, but water samples with salinities as low as 5 were accumulated in the benthic chambers, where an inverse correlation was seen between salinity and SGD rates (Fig. 30).

### 5.5.4. Radon

In the case of the Mauritius experiment, it was not possible to deploy the equipment for a complete tidal cycle at any of the stations investigated. We thus

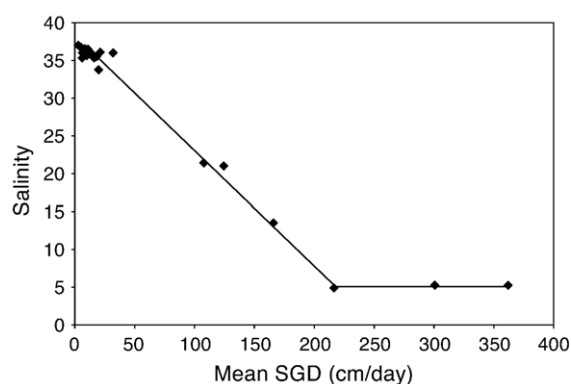


Fig. 30. Mean SGD as measured from each of the 28 locations versus the mean salinity measurements of the water that was discharged through the drum. Below a flow rate of 40 cm/day the seepage device water had virtually the same salinity as ambient seawater. At intermediate salinities between 10 and 20, we find fairly high flow rates (between 100 and 170 cm/day). Above 210 cm/day the salinity of the discharged water was constant at 5. This is the same salinity as measured directly at the spring.

modified our normal approach in the following manner. Time-series plots were constructed of  $^{222}\text{Rn}$  inventories (concentration multiplied by water depth, assuming a well-mixed layer in these shallow coastal waters) against deployment time. Periods when there were systematic increases in radon inventories were then regressed to estimate radon fluxes (slope of the inventory versus time plot). Assuming that these fluxes were due largely to advection of radon-rich pore waters (groundwater), we then estimated flow by dividing the fluxes by measured groundwater concentrations. Samples collected from piezometers and shallow wells showed radon concentrations between 310 and 535 dpm/L.

An example is shown for a deployment near the large submarine spring in the lagoon (Fig. 31). Based on the slopes of the regressions (labeled “a”, “b”, and “c”) and whether the upper (535 dpm/L) or lower (310 dpm/L) groundwater radon concentration estimate is applied, we estimate that seepage rates through the sandy sediments near the spring range from 65 to 140 cm/day. A comparison to the 3 manual seepage meters that were closest to our deployment site (M2, M15, and M6) shows that M2 was lower with an average of 15 cm/day, M15 was much higher at an average of 360 cm/day, and M6 was also higher at about 300 cm/day (Table 7). This high variability was thus observed by both the radon system and seepage meters in this dynamic environment around the submarine spring. The high variability in the

radon record is thought to be a consequence of sampling too close to the groundwater source, resulting in incomplete mixing between high-radon groundwater and low-radon seawater.

Using the same radon approach, we estimated a seepage rate through the sediments at 13–23 cm/day at the south beach site. This compares reasonably well to the manual seepage meter closest to this deployment (M9) that had a range of 2.5–22 cm/day and an average of 8.3 cm/day during the same period. Our final deployment was in a small cove immediately behind the Klondike Hotel. While this was one of the longest deployments, it had to be cut shorter than desired because of a tropical storm that approached the island that day. We calculated a range in seepage of 14–25 cm/day based on the slope of the inventory versus time regression and the radon concentrations in the shallow groundwater. There were no manual seepage meters deployed at this site but the dye-dilution seepage meter was operating nearby at the same time. Their results (5–28 cm/day; average = 10 cm/day; Table 7) closely match the radon rates. That was especially true for the last 3 dye-dilution data points (average = 20 cm/day) that were the closest in timing to the radon measurements.

Measured specific seepage rates (cm/day or  $\text{cm}^3/\text{cm}^2$  day) can be converted to average shoreline fluxes if one knows or can assume a width of the seepage face. Based on the seepage meter measurements, we estimate that

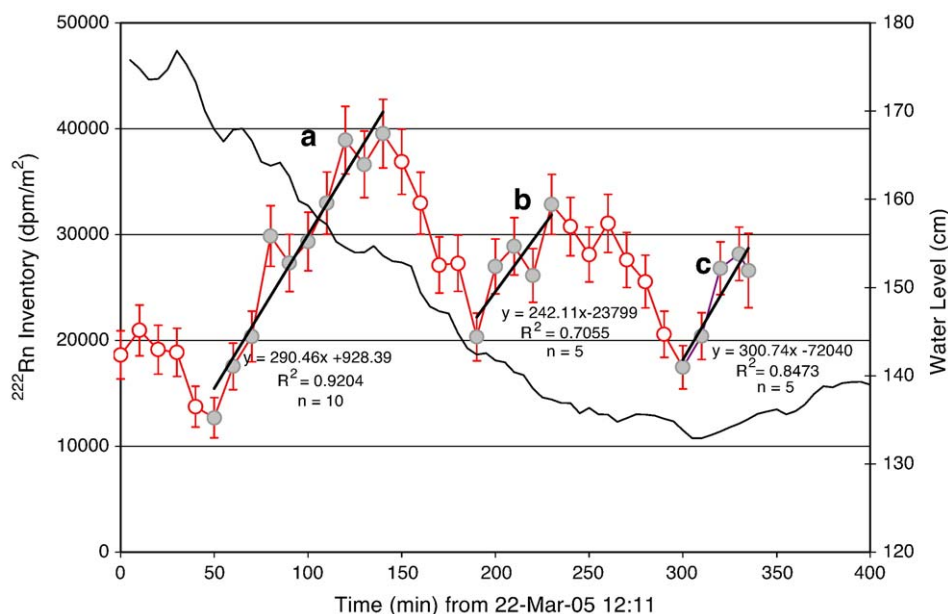


Fig. 31. Time-series radon measurements reported as inventories ( $^{222}\text{Rn}$  activity multiplied by the water depth; circles) just north of the spring on March 22, 2005. The solid line indicates the water level during the same period. Filled circles indicate the points used for regressions (see text for discussion).

Table 7

Estimates of SGD from 3 sites in the lagoon of Mauritius estimated by examination of the trends in  $^{222}\text{Rn}$  inventories compared to discrete seepage meter measurements

| Site           | Approx. time interval for Rn | $^{222}\text{Rn}$ estimate cm/day <sup>a</sup> | Seepage meters    |          |                   |
|----------------|------------------------------|--|-------------------|----------|-------------------|
|                |                              |  | Type <sup>b</sup> | <i>n</i> | cm/day            |
| Spring         | 22-Mar-05<br>13:00–14:30     | (a) 78–130                                     | M2                | 18       | 1–28; av = 15     |
|                |                              | (b) 65–110                                     | M15               | 2        | 360±5             |
|                |                              | (c) 81–140                                     | M6                | 21       | 110–490; av = 300 |
| South Beach    | 23-Mar-05<br>15:00–16:15     | 13–23  | M9                | 12       | 2.5–22            |
|                |                              |  |                   |          | av = 8.3          |
| Klondike Hotel | 24-Mar-05<br>15:00–16:20     | 14–24  | WHOI              | 41       | 5–28              |
|                |                              |  |                   |          | av = 10           |
|                |                              |  |                   |          | last 3 pts = 20   |

<sup>a</sup> The reported range in SGD estimates via this approach is based on upper (535 dpm/L) and lower (310 dpm/L) estimates for the radon concentration in the seepage waters.

<sup>b</sup> The “M” meters are standard manually operated flux chambers (Lee, 1977); the WHOI device is an automatic dye-dilution seepage meter (Sholkovitz et al., 2003).

the width of the seepage area in the lagoon is about 40 m. Using this value, we have calculated the shoreline fluxes for the same three sites as in Table 7 as well as the water balance estimate for the entire lagoon (~8 km; Table 8). We note that the water balance estimate (26 m<sup>3</sup>/m day) is quite close to the seepage meter value (35 m<sup>3</sup>/m day), derived by using the northern meters distant from the large spring.

#### 5.5.5. Summary

Our measurements show significant discharge of groundwater into the Flic-en-Flac Lagoon, Mauritius. This discharge shows large spatial and temporal heterogeneity likely caused by the presence of specialized conduits of groundwater flow created by the coralline basement of the lagoon and occasional lava tubes. Most of the samples collected show no significant

difference between SGD salinity and ambient lagoon salinity, likely due to seawater recirculation and mixing. In the region of a submarine spring, however, SGD was measured to be as high as 490 cm/day and the salinity of SGD was reduced accordingly. The high variability at the spring site was observed by both seepage meters and the radon measurements.

## 6. Overall findings and recommendations

Upon reviewing the results from all the intercomparison experiments, we have come to expect SGD to be fairly ubiquitous in the coastal zone. Rates above 100 cm/day should be considered high while values below 5 cm/day are low (or even marginally detectable). Regardless of location, however, both spatial and temporal variation is to be expected. Measurement strategies should be designed to search for patterns of decreasing SGD with distance from the shore, elevated SGD at submerged springs, and temporal patterns modulated by the tides; not only the diurnal tidal variations but also variations over the spring–neap lunar cycle. Preferential flow paths (the most obvious being submarine springs) are commonly found not only in karstic environments but also in situations that appear more-or-less homogeneous and isotropic. Tidal variations generally appear as higher SGD rates at low tide levels (and lower rates at high tides). However, the modulation is not necessarily linear and the hydrodynamic driving forces are not completely understood. In some situations, the rate of SGD seems to change abruptly without an obvious cause. The composition of SGD will be a mixture of fresh and saline groundwater; recirculated seawater could account for 90% of the discharge or more in some locations.

Table 8

Estimates of SGD on a per unit width of shoreline basis from 3 sites in the Mauritius lagoon

| Area           | Radon estimates<br>(m <sup>3</sup> /m day) | Seepage meter<br>estimates (m <sup>3</sup> /m day) |
|----------------|--|--|
| Spring         | 26–56                                      | 0.4–120  |
| South Beach    | 5.2–9.2                                    | 1–8.8  |
| Klondike Hotel | 5.6–9.6                                    | 2–11   |

#### Large area unit shoreline flux estimates

Water balance estimate = 26 m<sup>3</sup>/m day (Curepipe Aquifer; Oberdorfer, 2005)

Shore parallel seepage meter transect = 220 m<sup>3</sup>/m day (includes spring; Rapaglia et al., 2006)

Shore parallel transect, north area = 35 m<sup>3</sup>/m day (without spring, Rapaglia et al., 2006)

These estimates are based on the specific seepage measurements (Table 7) and assume a 40-m wide seepage face. Also shown are three wide area estimates.

While each study site must be approached individually, we can make a few generalizations for planning purposes. We have reason to believe that all the measurement techniques described here are valid although they each have their own advantages and disadvantages. We recommend that multiple approaches be applied whenever possible. In addition, a continuing effort is required in order to capture long-period tidal fluctuations, storm effects, and seasonal variations.

The choice of technique will depend not only on what is perceived to be the “best” approach, but also by practical considerations (cost, availability of equipment, etc.). For many situations, we think that seepage meters, the only device that measures seepage directly, appear to work very well. These devices provide a flux at a specific time and location from a limited amount of seabed (generally  $\sim 0.25 \text{ m}^2$ ). Seepage meters range in cost from almost nothing for a simple bag-operated meter to several thousands of dollars for those equipped with more sophisticated measurement devices. They are subject to some artifacts but can provide useful information if one is aware of the potential problems and if the devices are used in the proper manner. This seems to be especially true in environments where seepage flux rates are relatively rapid ( $>5 \text{ cm/day}$ ) and ambient open-water currents due to waves and tides are negligible.

Use of natural geochemical tracers involves the use of more costly equipment and requires personnel with special training and experience. One of the main advantages of the tracer approach is that the water column tends to integrate the signal. As a result, smaller-scale variations, which may be unimportant for larger-scale studies, are smoothed out. The approach may thus be optimal in environments where especially large spatial variation is expected (e.g., fractured rock aquifers). In addition to the spatial integration, tracers integrate the water flux over the time-scale of the isotope and the water residence time of the study area. Depending upon what one wants to know, this can often be a great advantage. Mixing and atmospheric exchanges (radon) must be evaluated as described earlier and care must be exercised in defining the end-members. The use of multiple tracers is recommended when possible. As described earlier, the simultaneous measurement of  $^{222}\text{Rn}$  and Ra isotopes can be used to constrain the mixing loss of radon.

Simple water balance calculations have been shown to be useful as a first estimate of the fresh groundwater discharge. Hydrogeologic, dual-density, groundwater modeling can also be done either as simple steady-state

(annual average flux) or non-steady state (requires real-time boundary conditions) methods. Unfortunately, at present, model results usually do not compare well with seepage meter and tracer measurements. Particular problems can be encountered in the proper scaling, both in time and space, and in parameterizing dispersion processes. Apparent inconsistencies between modeling and direct measurement approaches often arise because different components of SGD (fresh and saltwater) are being evaluated or because the models do not include transient terrestrial (e.g., recharge cycles) or marine processes (tidal pumping, wave set up, etc.) that drive part of all of the SGD. Geochemical tracers and seepage meters measure total flow, very often a combination of fresh groundwater and seawater and driven by a combination of oceanic and terrestrial forces. Water balance calculations and most models evaluate just the fresh groundwater flow driven by terrestrial hydraulic heads.

It is important to remember that, although the techniques described here are well-developed, there is as yet no widely accepted “standard” methodology. We can certainly say that if one plans to work in karstic or fractured bedrock environments, heterogeneity must be expected and it would be best to plan on multiple approaches. Rates are likely to be controlled by the presence or absence of buried fracture systems and focused, or dispersed, by the topography of the buried rock surface. In such a situation, integrated SGD might be assessed with dispersed geochemical tracers or described statistically from many, randomly situated, spot measurements. Since the radiometric tracers integrate over time and space, it seems best to avoid making such measurements too close to strong, submarine springs where gradients may be sharp and mixing incomplete. This was a concern, for example, in interpreting the  $^{222}\text{Rn}$  data from near the large spring in the Mauritius. In volcanic aquifers, especially young basalts, the radium signal may be low. This was found to be the case in the Mauritius and in Hawaii. This situation might hamper the application of Ra and Rn tracers in these settings. We suggest in such an environment that one should also confirm the spatial heterogeneity with some preliminary seepage meter deployments and geophysical techniques; and use traditional modeling with caution, as good results will likely have to use more complex models and would require a significant amount of data.

If one plans to work in a coastal plain setting, there likely will be more homogeneous results. These settings can still exhibit pseudo-karstic characteristics, especially where anthropogenic influences modify SGD. Deep



pilings at the Shelter Island site artificially created enhanced SGD. Bulk-headed shorelines, dredged channels that intercept shallow confined aquifers or channelized drainage done to roads or other infrastructure can also introduce karst-like characteristics to otherwise homogeneous aquifers. Seepage meters often work well in such environments and can provide good estimates, especially when there is a distinctive pattern in the results. Such a pattern might, for example, consist of a systematic drop in seepage rates as a function of distance offshore and a correlation between tidal stage and flow. Simple modeling approaches (e.g., hydraulic gradients, tidal propagation, thermal gradients) can often be valuable in this type of environment. Tracers also will work very well in coastal plain environments.

In summary, we make the following suggestions to improve the performance of future SGD assessments:

1. Some geophysical surveying (e.g., resistivity profiling) should be performed prior to the actual assessments so areas prone to high and low SGD can be mapped out in advance.
2. Point discharge measurements are best recorded in units of cm/day. It is often most useful to design measurements to allow for integrated assessments of groundwater flow per unit width of shoreline (e.g., m<sup>3</sup>/m day), the best way to make comparisons and to extrapolate results. For example, seepage meter transects normal to the shoreline that cover the entire seepage face (which can be mapped with the resistivity probes) would fit this requirement.
3. The experimental design should put on a spatial and temporal scale that is appropriate for the methodologies being used.
4. Coordination among groups would ensure that method-to-method intercomparisons could be made. For example, we occasionally had data sets from different devices that only overlap for short periods. Extending these overlapping periods would benefit the evaluation process.
5. Because of the expected complexity and importance of SGD, a continuing effort is strongly recommended; that is, one that can provide measurements of SGD over time periods encompassing the semidiurnal tidal period to seasonal climatic variations.

## Acknowledgments

The authors of this report are grateful for the assistance received from UNESCO's Intergovernmental Oceanographic Commission (IOC) and the International

Hydrologic Program (IHP), through their project "Assessment and Management Implications of Submarine Groundwater Discharge into the Coastal Zone." We also acknowledge support from the International Atomic Energy Agency (IAEA), which financed this activity through their Cooperative Research Project (CRP) entitled "Nuclear and Isotopic Techniques for the Characterization of Submarine Groundwater Discharge (SGD) in Coastal Zones." The IAEA is grateful to the government of the Principality of Monaco for the support provided to the Marine Environment Laboratory in Monaco. Lastly, we wish to thank the many local organizers of the various intercomparison experiments in Australia, Sicily, New York, Brazil, and Mauritius for all their hard work and patience. Without their cooperation, these experiments could not have been conducted.

## References

- Aggarwal PP, Kulkarni KM, Povinec PP, Han L-F, Groening M. Environmental isotope investigation of submarine groundwater discharge in Sicily, Italy. Book of extended synopses. Vienna: IAEA; 2004. p. 222–3.
- Aggarwal PP, Gat JR, Froehlich KFO. Isotopes in the water cycle: past, present and future of a developing science. Dordrecht: Springer; 2005. 381 pp.
- Aureli A. Esperienze e programmi di intervento in materia di ricarica delle falde, per contrastare l'intrusione marina in un acquifero carbonatico sovrassaturato. IV Congr. di Geoingegneria "Difesa e valorizzazione del suolo e degli acquiferi", vol. 3. Torino: Ass. Mineraria Subalpina; 1994. p. 813–8.
- Allen AD. Outline of the hydrogeology of the superficial formations of the Swan Coastal Plain. Western Australia Geol Surv Ann Rep 1976:31–42.
- Anderson MP, Chen X. Long and short term transience in a groundwater/lake system in Wisconsin, U.S.A. *J Hydrol* 1993; 145:1–18.
- Banks W, Paylor R, Hughes W. Using thermal infrared imagery to delineate groundwater discharge. *Groundwater* 1996;34:434–44.
- Barwell VK, Lee DR. Determination of horizontal-to-vertical hydraulic conductivity ratios from seepage measurements on lake beds. *Water Resour Res* 1981;17:565–70.
- Bates RL, Jackson JA. Dictionary of geological terms. NY: American Geological Institute; 1984.
- Baydon-Ghyben W. Nota in verband met de voorgenomen putboring nabij Amsterdam. Koninklyk Instituut Ingenieurs Tijdschrift (The Hague) 1888–1889:8–22.
- Bear JA, Cheng HD, Sorek S, Ouazar D, Herrera I, editors. Seawater intrusion in coastal aquifers — concepts, methods and practices. Dordrecht, the Netherlands: Kluwer Academic Publishers; 1999. 625 pp.
- Belanger TV, Montgomery ME. Seepage meter errors. *Limnol Oceanogr* 1992;37:1787–95.
- Bogle FR, Loy K. The application of thermal infrared thermography in the identification of submerged spring in Chickamauga Reservoir, Hamilton County, Tennessee. Karst Geohazards. Proceedings of the fifth multidisciplinary conference on

- sinkholes and the engineering and environmental impacts of Karst; 1995. p. 415–24. 581pp.
- Bokuniewicz H. Groundwater seepage into Great South Bay, New York. *Estuar Coast Mar Sci* 1980;10:437–44.
- Bokuniewicz HJ. Analytical descriptions of subaqueous groundwater seepage. *Estuaries* 1992;15:458–64.
- Bokuniewicz H, Pavlik B. Groundwater seepage along a barrier island. *Biogeochemistry* 1990;10:257–76.
- Bokuniewicz H, Pollock M, Blum J, Wilson R. Submarine ground water discharge and salt penetration across the sea floor. *Ground Water-Oceans Special Issue* 2004;42:983–9.
- Boldovski NV. Groundwater flow in the coastal zone of the east Sikhote-Alin' volcanogenic belt. *Proc. of Int. Symp. on Groundwater Discharge in the Coastal Zone, Land–Ocean Interactions in the Coastal Zone (LOICZ)*, Moscow, July 6–10; 1996. p. 8–15.
- Boudreau BP, Huettel M, Froster S, Jahnke RA, McLachlan A, Middelburg JJ, et al. Permeable marine sediments: overturning an old paradigm. *EOS* 2001;82:133–6.
- Bouwer H. *Groundwater hydrology*. New York: McGraw-Hill; 1978. 480 pp.
- Boyle DR. Design of a seepage meter for measuring groundwater fluxes in the nonlittoral zones of lakes — evaluation in a boreal forest lake. *Limnol Oceanogr* 1994;39:670–81.
- Boyle JM, Saleem ZA. Determination of recharge rate using temperature depth profiles in wells. *Water Resour Res* 1979; 15:1616–22.
- Bredehoeft JD, Papadopoulos IS. Rates of vertical groundwater movement estimated from the Earth's thermal profile. *Water Resour Res* 1965;1:325–8.
- Brown G, Rogers J, Garbrecht J. Task committee planning: Darcy memorial symposium on the history of hydraulics. *J Hydraul Eng* 2000;126:799–801.
- Buddemeier RW, editor. *Groundwater discharge in the coastal zone: proceedings of an international symposium, Texel, The Netherlands; 1996. LOICZ/R and S/96-8, iv+179 pp. LOICZ.*
- Bugna GC, Chanton JP, Young JE, Burnett WC, Cable PH. The importance of groundwater discharge to the methane budget of nearshore and continental shelf waters of the NE Gulf of Mexico. *Geochim Cosmochim Acta* 1996;60:4735–46.
- Burnett WC. Offshore springs and seeps are focus of working group. *EOS* 1999;80:13–5.
- Burnett WC, Dulaiova H. Estimating the dynamics of groundwater input into the coastal zone via continuous radon-222 measurements. *J Environ Radioact* 2003;69:21–35.
- Burnett WC, Dulaiova H. Radon as a tracer of submarine groundwater discharge into a boat basin in Donnalucata, Sicily. *Cont Shelf Res* 2006;26:862–73.
- Burnett WC, Cowart JB, Deetae S. Radium in the Suwannee River and estuary: spring and river input to the Gulf of Mexico. *Biogeochemistry* 1990;10:237–55.
- Burnett WC, Cable JE, Corbett DR, Chanton JP. Tracing groundwater flow into surface waters using natural  $^{222}\text{Rn}$ . *Proc. of Int. Symp. on Groundwater Discharge in the Coastal Zone. Land–Ocean Interactions in the Coastal Zone (LOICZ)*, July 6–10, Moscow; 1996. p. 22–8.
- Burnett WC, Taniguchi M, Oberdorfer J. Measurement and significance of the direct discharge of groundwater into the coastal zone. *J Sea Res* 2001a;46/2:109–16.
- Burnett WC, Kim G, Lane-Smith D. A continuous radon monitor for assessment of radon in coastal ocean waters. *J Radioanal Nucl Chem* 2001b;249:167–72.
- Burnett WC, Chanton J, Christoff J, Kontar E, Krupa S, Lambert M, et al. Assessing methodologies for measuring groundwater discharge to the ocean. *EOS* 2002;83:117–23.
- Burnett WC, Bokuniewicz H, Huettel M, Moore WS, Taniguchi M. Groundwater and porewater inputs to the coastal zone. *Biogeochemistry* 2003a;66:3–33.
- Burnett WC, Chanton JP, Kontar E, editors. *Submarine groundwater discharge*, vol. 66(1–2). *Spec Issue, Biogeochemistry*; 2003b. 202 pp.
- Burnett WC, Cable JE, Corbett DR. Radon tracing of submarine groundwater discharge in coastal environments. In: Taniguchi M, Wang K, Gamo T, editors. *Land and marine hydrogeology*. Amsterdam: Elsevier; 2003c. p. 25–43.
- Burnett WC, Peterson R, Moore WS, de Oliveira, J. Radon and radium isotopes as tracers of submarine groundwater discharge — results from the Ubatuba, Brazil SGD assessment intercomparison. *Estuar Coast Shelf Sci* submitted for publication.
- Cable J, Bugna G, Burnett W, Chanton J. Application of  $^{222}\text{Rn}$  and  $\text{CH}_4$  for assessment of groundwater discharge to the coastal ocean. *Limnol Oceanogr* 1996a;41:1347–53.
- Cable JE, Burnett WC, Chanton JP, Weatherly GL. Estimating groundwater discharge into the northeastern Gulf of Mexico using radon-222. *Earth Planet Sci Lett* 1996b;144:591–604.
- Cable JE, Burnett WC, Chanton JP, Corbett DR, Cable PH. Field evaluation of seepage meters in the coastal marine environment. *Estuar Coast Shelf Sci* 1997a;45:367–75.
- Cable JE, Burnett WC, Chanton JP. Magnitudes and variations of groundwater seepage into shallow waters of the Gulf of Mexico. *Biogeochemistry* 1997b;38:189–205.
- Cable JE, Martin J, Swarzenski P, Lindenburg M, Steward J. Advection within shallow pore waters of a coastal lagoon. *Ground Water* 2004;42:1011–20.
- Capone DG, Bautista MF. A groundwater source of nitrate in nearshore marine sediments. *Nature* 1985;313:214–6.
- Capone DG, Slater JM. Interannual patterns of water table height and groundwater derived nitrate in nearshore sediments. *Biogeochemistry* 1990;10:277–88.
- Cartwright K. Measurement of fluid velocity using temperature profiles: experimental verification. *J Hydrol* 1979;43:185–94.
- Četina M, Rajar R, Povinec P. Modelling of circulation and dispersion of radioactive pollutants in the Japan Sea. *Oceanol Acta* 2000;23:819–36.
- Chanton JP, Burnett WC, Taniguchi M, Dulaiova H, Corbett DR. Seepage rate variability derived by Atlantic tidal height. *Biogeochemistry* 2003;66:187–202.
- Charette MA, Sholkovitz ER. Oxidative precipitation of groundwater-derived ferrous iron in the subterranean estuary of a coastal bay. *Geophys Res Lett* 2002;29:1444.
- Charette MA, Buesseler KO, Andrews JE. Utility of radium isotopes for evaluating the input and transport of groundwater-derived nitrogen to a Cape Cod estuary. *Limnol Oceanogr* 2001; 46:465–70.
- Cherkauer DS, McBride JM. A remotely operated seepage meter for use in large lakes and rivers. *Ground Water* 1988;26:165–71.
- Church TM. An underground route for the water cycle. *Nature* 1996;380:579–80.
- Considine DM, editor. *Van Nostrand's scientific encyc.* 8th ed. Reinhold: NY Van Nostrand; 1995.
- Constantz J, Thomas CL, Zellweger G. Influence of diurnal variations in stream temperature on streamflow loss and groundwater recharge. *Water Resour Res* 1994;30:3253–64.
- Corbett DR, Cable JE. Seepage meters and advective transport in coastal environments: comments on "Seepage Meters and

- Bernoulli's Revenge" by E.A. Shinn, C.D. Reich, and T.D. Hickey. *Estuaries* 2002;25:126–32. *Estuaries* 2002;26:1383–9.
- Corbett DR, Chanton J, Burnett W, Dillon K, Rutkowski C, Fourqurean J. Patterns of groundwater discharge into Florida Bay. *Limnol Oceanogr* 1999;44:1045–55.
- Corbett DR, Dillon K, Burnett W, Chanton J. Estimating the groundwater contribution into Florida Bay via natural tracers  $^{222}\text{Rn}$  and  $\text{CH}_4$ . *Limnol Oceanogr* 2000;45:1546–57.
- Cornett RJ, Risto BA, Lee DR. Measuring groundwater transport through lake sediments by advection and diffusion. *Water Resour Res* 1989;25:1815–23.
- Crotwell AM, Moore WS. Nutrient and radium fluxes from submarine groundwater discharge to Port Royal Sound, South Carolina. *Aquat Geochem* 2003;9:191–208.
- D'Elia CF, Webb DKL, Porter JW. Nitrate-rich groundwater inputs to Discovery Bay, Jamaica: a significant source of N to local coral reefs? *Bull Mar Sci* 1981;31:903–10.
- Destouni G, Prieto C. On the possibility for generic modeling of submarine groundwater discharge. *Biogeochemistry* 2003;66:171–86.
- DiLorenzo, JL, Ram RV. Flushing-time estimates for West Neck Harbor: a small tidal embayment of the Peconic Bays, New York. Report — Najarian Associates, L.P. Eatontown, New Jersey, 1991. 44 pp.
- Domenico PA, Palciauskas VV. Theoretical analysis of forced convective heat transfer in regional ground-water flow. *Geol Soc Amer Bull* 1973;84:3803–13.
- Dulaiova H, Peterson R, Burnett WC. A multi-detector continuous monitor for assessment of  $^{222}\text{Rn}$  in the coastal ocean. *J Radioanal Nucl Chem* 2005;263(2):361–5.
- Ellins KK, Roman-Mas A, Lee R. Using Rn-222 to examine ground water/surface discharge interaction in the Rio Grande de Manati, Puerto Rico. *J Hydrol* 1990;115:319–41.
- Fanning KA, Byrne RH, Breland JA, Betzer PR, Moore WS, Elsinger RJ, et al. Geothermal springs of the west Florida continental shelf. Evidence for dolomitization and radionuclide enrichment. *Earth Planet Sci Lett* 1981;52:345–54.
- Fellows CR, Brezonik PL. Seepage flow into Florida lakes. *Water Resour Bull* 1980;16:635–41.
- Fischer WC, Moxham RM, Polcyn F, Landis GH. Infrared surveys of Hawaiian volcanoes. *Science* 1964;146:733–42.
- Fisher AT, Von Herzen RP, Blum P, Hoppie B, Wang K. Evidence may indicate recent warming of shallow slope bottom water off New Jersey shore. *EOS* 1999;80:171–3.
- Freeze RA, Cherry JA. *Groundwater*. Englewood Cliffs, NJ: Prentice-Hall Inc.; 1979. 604 pp.
- Fritz P, Cherry JA, Weyer KU, Sklash M. Storm runoff analyses using environmental isotopes and major ions. Interpretation of environmental isotope and hydrochemical data in groundwater hydrology. Vienna: IAEA; 1976. p. 111–30.
- Fukuo Y. Studies on groundwater seepage in the bottom of Lake Biwa. Report for Environmental Sciences by the Ministry of Education, Science and Culture, Japan, 1986, B289-R-12-2, 1–23.
- Fukuo Y, Kaihotsu I. A theoretical analysis of seepage flow of the confined groundwater into the lake bottom with a gentle slope. *Water Resour Res* 1988;4:1949–53.
- Garrels RM, MacKenzie FT. *Evolution of sedimentary rocks*. New York: Norton and Co.; 1971. 397 pp.
- Garrison GH, Glenn CR, McMurtry GM. Measurement of submarine groundwater discharge in Kahana Bay, Oahu, Hawaii. *Limnol Oceanogr* 2003;48:920–8.
- Giorgi L, Borchellini S, Delucchi L. Ile Maurice, Carte Geologique au 1:50 000, Schema hydrogeologique, Geolab, July 1999.
- Glover, R.E. The patterns of fresh-water flow in a coastal aquifer. In: Cooper Jr. HH, Kohout FA, Henry HR, Glover RE, editors. *Sea water in coastal aquifers* (pp. C32–C35). U.S. Geological Survey Water Supply Paper; 1964, p. 1613-C.
- Granier A. Une nouvelle methode pour la mesure du flux de seve brute dans tronc desarbres. *Ann Sci For* 1985;42:81–8.
- Henry HR. Interface between salt water and fresh water in a coastal aquifer. In: Cooper Jr. HH, Kohout FA, Henry HR, Glover RE, editors. *Sea water in coastal aquifers* (pp C35–C70). U.S. Geological Survey Water Supply Paper; 1964, p. 1613-C.
- Herzberg A. Die wasserversorgung einiger Nordseebader. *Journal Gasbeleuchtung und Wasserversorgung* (Munich) 1901; 44: 815–819, 842–844.
- Hubbert MK. The theory of ground-water motion. *J Geol* 1940; 48:785–944.
- Huettel M, Gust G. Solute release mechanisms from confined sediment cores in stirred benthic chambers and flume flows. *Mar Ecol, Prog Ser* 1992;82:187–97.
- Hussain N, Church TM, Kim G. Use of  $^{222}\text{Rn}$  and  $^{226}\text{Ra}$  to trace submarine groundwater discharge into the Chesapeake Bay. *Mar Chem* 1999;65:127–34.
- Huettel M, Ziebis W, Forester S. Flow-induced uptake of particulate matter in permeable sediments. *Limnol Oceanogr* 1996; 41:309–22.
- Hwang DW, Kim G, Lee Y-W, Yang H-S. Estimating submarine inputs of groundwater and nutrients to a coastal bay using radium isotopes. *Mar Chem* 2005;96:61–71.
- Israelsen OW, Reeve RC. Canal lining experiments in the delta area, Utah. *Utah Agr Exp Sta Tech Bull* 1944;313 52pp.
- Jackson JA, editor. *Glossary of geology*. 4th ed. VA: American Geological Institute Alexandria; 1977.
- Johannes RE. The ecological significance of the submarine discharge of groundwater. *Mar Ecol, Prog Ser* 1980;3:365–73.
- Kelly RP, Moran SB. Seasonal changes in groundwater input to a well-mixed estuary estimated using radium isotopes and implications for coastal nutrient budgets. *Limnol Oceanogr* 2002; 47:1796–807.
- Kim G, Hwang DW. Tidal pumping of groundwater into the coastal ocean revealed from submarine Rn-222 and  $\text{CH}_4$  monitoring. *Geophys Res Lett* 2002;29. doi:10.1029/2002GL015093.
- Kim G, Lee KK, Park KS, Hwang DW, Yang HS. Large submarine groundwater discharge (SGD) from a volcanic island. *Geophys Res Lett* 2003;30. doi:10.1029/2003GL018378.
- Kim G, Ryu JW, Yang HS, Yun ST. Submarine groundwater discharge (SGD) into the Yellow Sea revealed by Ra-228 and Ra-226 isotopes: implications for global silicate fluxes. *Earth Planet Sci Lett* 2005;237(1–2):156–66.
- Kitheka JU. Groundwater outflow and its linkage to coastal circulation in a Mangrove-fringed Creek in Kenya. *Estuar Coast Shelf Sci* 1988;47:63–75.
- Kohout FA. Submarine springs: a neglected phenomenon of coastal hydrology. *Hydrology* 1966;26:391–413.
- Krest JM, Harvey JW. Using natural distributions of short-lived radium isotopes to quantify groundwater discharge and recharge. *Limnol Oceanogr* 2003;48:290–8.
- Krest JM, Moore WS, Gardner LR. Marsh nutrient export supplied by groundwater discharge: evidence from radium measurements. *Glob Biogeochem Cycles* 2000;14:167–76.
- Krupa SL, Belanger TV, Heck HH, Brok JT, Jones BJ. Krupaseep — the next generation seepage meter. *J Coast Res* 1998;25:210–3.
- Lapham WW. Use of temperature profiles beneath streams to determine rates of vertical ground-water flow and vertical

- hydraulic conductivity. U S Geol Surv Water Supply Pap 1989; 2337. 35 pp.
- Lapointe BE, O'Connell J. Nutrient-enhanced growth of *Cladophora* prolifera in Harrington Sound, Bermuda: eutrophication of a confined, phosphorus-limited marine ecosystem. *Estuar Coast Shelf Sci* 1989;28:347–60.
- Lapointe B, O'Connell JD, Garrett GS. Nutrient coupling between on-site sewage disposal systems, groundwaters, and nearshore surface waters of the Florida Keys. *Biogeochemistry* 1990;10:289–307.
- LaRoche J, Nuzzi R, Waters R, Wyman K, Falkowski PG, Wallace DWR. Brown tide blooms in Long Island's coastal waters linked to interannual variability in groundwater flow. *Glob Change Biol* 1997;3:397–410.
- Lee DR. A device for measuring seepage flux in lakes and estuaries. *Limnol Oceanogr* 1977;22:140–7.
- Levy-Palomo I, Comanducci JF, Povinec PP. Investigation of submarine groundwater discharge in Sicilian and Brazilian coastal waters using underwater gamma spectrometer. Book of extended synopses. Vienna: IAEA; 2004. p. 228–9.
- Li L, Barry DA, Stagnitti F, Parlange JU. Submarine groundwater discharge and associated chemical input into a coastal sea. *Water Resour Res* 1999;35:3253–9.
- Libelo EL, MacIntyre WG. Effects of surface-water movement on seepage-meter measurements of flow through the sediment–water interface. *Hydrogeol J* 1994;2:49–54.
- Linderfelt WR, Turner JV. Interaction between shallow groundwater, saline surface water and nutrient discharge in a seasonal estuary: the Swan-Canning River and estuary system, Western Australia. Hydrological processes special issue: integrating research and management for an urban estuarine system: the Swan-Canning Estuary, Western Australia. *Hydrol Process* 2001;15:2631–53.
- Loveless AM. Biogeochemical, spatial and temporal dynamics of submarine groundwater discharge in an oligotrophic semi-enclosed coastal embayment. PhD thesis 2006, University of Western Australia, Perth, Australia.
- Lu N, Ge S. Effect of horizontal heat and fluid flow on the vertical temperature distribution in a semiconfining layer. *Water Resour Res* 1996;32:1449–53.
- Mahiques MM. Sedimentary dynamics of the bays off Ubatuba, State of São Paulo. *Bol Inst Oceanogr, São Paulo* 1995;43(2): 111–22.
- Martin JB, Cable JE, Jaeger J, Hartl K, Smith CG. Thermal and chemical evidence for rapid water exchange in the Indian River Lagoon, Florida. *Limnol Oceanogr* 2006;51:1332–41.
- McBride MS, Pfannkuch HO. The distribution of seepage within lakebed. *J Res US Geol Surv* 1975;3:505–12.
- McDonald MG, Harbaugh AW. A modular three-dimensional finite-difference groundwater flow model. US Geol Surv Open-File Report 1984;83–875. 528p.
- Mesquita AR. Marés, circulação e nível do mar na Costa Sudeste do Brasil. São Paulo: Relatório Fundespa; 1997.
- Michael HA, Lubetsky JS, Harvey CF. Characterizing submarine groundwater discharge: a seepage meter study in Waquoit Bay, Massachusetts. *Geophys Res Lett* 2003;30(6). doi:10.1029/GL016000.
- Michael HA, Mulligan AE, Harvey CF. Seasonal oscillations in water exchange between aquifers and the coastal ocean. *Nature* 2005;436:1145–8.
- Ministry of Public Works. Hydrology data book (1995–1999). Mauritius: Water Resources Unit; 2003.
- Moore WS. Large groundwater inputs to coastal waters revealed by  $^{226}\text{Ra}$  enrichments. *Nature* 1996;380:612–4.
- Moore WS. High fluxes of radium and barium from the mouth of the Ganges-Brahmaputra River during low river discharge suggest a large groundwater source. *Earth Planet Sci Lett* 1997; 150:141–50.
- Moore WS. The subterranean estuary: a reaction zone of ground water and sea water. *Mar Chem* 1999;65:111–25.
- Moore WS. Determining coastal mixing rates using radium isotopes. *Cont Shelf Res* 2000;20:1995–2007.
- Moore WS. Radium isotopes as tracers of submarine groundwater discharge in Sicily. *Cont Shelf Res* 2006;26:852–61.
- Moore WS, Arnold R. Measurement of  $^{223}\text{Ra}$  and  $^{224}\text{Ra}$  in coastal waters using a delayed coincidence counter. *J Geophys Res* 1996; 101:1321–9.
- Moore WS, Shaw TJ. Chemical signals from submarine fluid advection onto the continental shelf. *J Geophys Res - Oceans* 1998;103:21543–52.
- Moore WS, Wilson AM. Advective flow through the upper continental shelf driven by storms, buoyancy, and submarine groundwater discharge. *Earth Planet Sci Lett* 2005;235:564–76.
- Moore WS, de Oliveira J. Determination of residence time and mixing processes of the Ubatuba, Brazil, inner shelf waters using natural Ra isotopes. *Estuar Coast Shelf Sci* submitted for publication.
- Moore WS, Shaw TJ. Fluxes and behavior of radium isotopes, barium, and uranium in seven Southeastern US rivers and estuaries. *Mar Chem* submitted for publication.
- Moore WS, Krest J, Taylor G, Roggenstein E, Joye S, Lee R. Thermal evidence of water exchange through a coastal aquifer: implications for nutrient fluxes. *Geophys Res Lett* 2002;29. doi:10.1029/2002GL014923.
- Muir, K.S. Groundwater reconnaissance of the Santa Barbara — Montecito Area, Santa Barbara County, California. U. S. Geol. Surv. Water Supply Pap 1968; 1859-A, 28 pp.
- Nield SP, Townley LR, Barr AD. A framework for quantitative analysis of surface water–groundwater interaction: flow geometry in a vertical section. *Water Resour Res* 1994;30:2461–75.
- Nielsen P. Tidal dynamics in the water table in a beach. *Water Resour Res* 1990;26:2127–34.
- Nixon SW, Ammerman JW, Atkinson LP, Berounsky VM, Billen G, Boicourt WC, et al. The fate of nitrogen and phosphorus at the land–sea margin of the North Atlantic Ocean. *Biogeochemistry* 1996;35:141–80.
- Oberdorfer, J.A. Numerical modeling of coastal discharge: predicting the effects of climate change, Groundwater discharge in the coastal zone, in LOICZ IGBP, 69–75, edited by R.W. Buddemeier, pp. 179, LOICZ, Texel, Netherlands, Russian Academy of Sciences, Moscow, 1996.
- Oberdorfer, J. Fresh groundwater discharge to the coastline of the Curepipe Aquifer, Mauritius. Submarine Groundwater Discharge Assessment Intercomparison Experiment, Mauritius; Report to UNESCO, 2005.
- Oberdorfer JA, Valentino MA, Smith SV. Groundwater contribution to the nutrient budget of Tomales Bay, California. *Biogeochemistry* 1990;10:199–216.
- O'Rourke, D. Quantifying specific discharge into West Neck Bay, Shelter Island, New York using a three-dimensional finite-difference groundwater flow model and continuous measurements with an ultrasonic seepage meter. Master's Thesis, State University of New York at Stony Brook, 2000.
- Paulsen RJ, Smith CF, O'Rourke D, Wong T. Development and evaluation of an ultrasonic ground water seepage meter. *Ground Water* 2001;39:904–11.



- Pluhowski EJ, Kantrowitz IH. Hydrology of the Babylon–Islip Area, Suffolk County, Long Island, New York. US Geol Surv Water Supply Pap 1964; 1768. 128 pp.
- Porcelli D, Swarzenski PW. The behaviour of U- and Th series nuclides in groundwater and the tracing of groundwater. *Rev Mineral Geochem* 2003;52:317–61.
- Povinec PP, La Rosa J, Lee S-H, Mulsow S, Osvath I, Wyse E. Recent developments in radiometric and mass spectrometry methods for marine radioactivity measurements. *J Radioanal Nucl Chem* 2001;248:713–8.
- Proag V. The geology and water resource of Mauritius. Mauritius: Mahatma Gandhi Institute; 1995.
- Rajar R, agar D, Širca A, Horvat M. Three-dimensional modeling of mercury cycling in the Gulf of Trieste. *Sci Total Environ* 2000; 260:109–23.
- Rama, Moore WS. Using the radium quartet for evaluating groundwater input and water exchange in salt marshes. *Geochim Cosmochim Acta* 1996;60:4245–52.
- Rapaglia, J., Beck, A., Stieglitz, T., Bokuniewicz, H., Kontar, E. Submarine groundwater discharge patterns through volcanic fractured rock. Submarine Groundwater Discharge Assessment Inter-comparison Experiment, Mauritius; Report to UNESCO; 2006.
- Reich CD, Shinn EA, Hickey TD, Tihansky AB. Tidal and meteorological influences on shallow marine groundwater flow in the upper Florida Keys. In: Porter JW, Porter KG, editors. *The Everglades, Florida Bay, and coral reefs of the Florida Keys*. Boca Raton: CRC Press; 2002. p. 659–76.
- Riedl R, Huang N, Machan R. The subtidal pump: a mechanism of interstitial water exchange by wave action. *Mar Biol* 1972; 13:210–21.
- Robinson MA. A finite element model of submarine ground water discharge to tidal estuarine waters. PhD dissertation, Virginia Polytechnic Institute; 1996.
- Rosenberg ND, Lupton JE, Kadko D, Collier R, Lilly MD, Pak H. Estimation of heat and chemical fluxes from a seafloor hydrothermal vent field using radon measurements. *Nature* 1988;334:604–8.
- Roxburgh IS. Thermal infrared detection of submarine spring associated with the Plymouth Limestone. *Hydrol Sci J* 1985;30:185–96.
- Sakura Y. The method for estimations of the groundwater velocity from temperature distributions: on the groundwater around Sapporo, Japan. *Stud Water Temp* 1977;21:2–14.
- Sayles FL, Dickinson WH. The seep meter: a benthic chamber for the sampling and analysis of low velocity hydrothermal vents. *Deep-Sea Res* 1990;88:1–13.
- Schubert CE. Areas contributing ground water to the Peconic estuary, and ground-water budgets for the North and South forks and Shelter Island, Eastern Suffolk County, New York. U.S. Geological Survey, Water Resources Investigations Report 97-4136, 1998.
- Schluter M, Suess E, Linke P, Sauter E. SUBGATE — coordination: submarine groundwater fluxes and transport processes from methane-rich coastal environments. In: Suess E, editor. *GEOMAR report*, vol. 97. Germany: Kiel; 2000. p. 119–20.
- Sekulic B, Vertacnik A. Balance of average annual fresh water inflow into the Adriatic Sea. *Water Resour Dev* 1996;12:89–97.
- Sellinger. Groundwater flux into a portion of eastern Lake Michigan. *J Great Lakes Res* 1995;21:53–63.
- Shaw RD, Prepas EE. Anomalous, short-term influx of water into seepage meters. *Limnol Oceanogr* 1989;34:1343–51.
- Shaw RD, Prepas EE. Groundwater–lake interactions: I. Accuracy of seepage meter estimations of lake seepage. *J Hydrol* 1990a; 119:105–20.
- Shaw RD, Prepas EE. Groundwater–lake interactions: II. Nearshore seepage patterns and the contribution of ground water to lakes in central Alberta. *J Hydrol* 1990b;119:121–36.
- Shinn EA, Reich CD, Hickey TD. Seepage meters and Bernoulli's revenge. *Estuaries* 2002;25:126–32.
- Sholkovitz ER, Herbold C, Charette MA. An automated dye-dilution based seepage meter for the time-series measurement of submarine groundwater discharge. *Limnol Oceanogr Methods* 2003;1:17–29.
- Sillman SE, Booth DF. Analysis of time-series measurements of sediment temperature for identification of gaining vs. losing portions of Juday Creek, Indiana. *J. Hydrol* 1993;146:131–48.
- Smith L, Chapman DS. On the thermal effects of groundwater flow: 1. Regional scale system. *J Geophys Res* 1983;88:593–608.
- Smith AJ, Nield SP. Groundwater discharge from the superficial aquifer into Cockburn Sound Western Australia: estimation by inshore water balance. *Biogeochemistry* 2003;66:125–44.
- Smith, A.J., Turner, J.V. Density-dependent surface water–groundwater interaction and nutrient discharge: The Swan-Canning River and estuary system, Western Australia. *Hydrological Processes Special Issue: Integrating Research and Management for an Urban Estuarine System: The Swan-Canning Estuary, Western Australia. Hydrological Processes*, 15, 2595–2616, 2001.
- Smith L, Zawadzki W. A hydrogeologic model of submarine groundwater discharge: Florida intercomparison experiment. *Biogeochemistry* 2003;66:95–110.
- Smith AJ, Turner JV, Herne DE, Hick WP. Quantifying submarine groundwater discharge and nutrient discharge into Cockburn Sound Western Australia. CSIRO Land and Water. Perth; 2003. p. 185.
- Stallman RW. Computation of groundwater velocity from temperature data. US Geol Surv Water Supply Pap 1963;1544-H:36–46.
- Stallman RW. Steady one-dimensional fluid flow in a semi-infinite porous medium with sinusoidal surface temperature. *J Geophys Res* 1965;70:2821–7.
- Stieglitz SE. A dictionary of earth science. NY: PICA Press; 1977.
- Stieglitz T. Submarine groundwater discharge into the near-shore zone of the Great Barrier Reef, Australia. *Mar Pollut Bull* 2005; 51:51–9.
- Stieglitz T, Taniguchi M, Neylon S. Spatial variability of submarine groundwater discharge, Ubatuba, Brazil. *Est Coast Shelf Sci* submitted for publication.
- Suzuki S. Percolation measurements based on heat flow through soil with special reference to paddy fields. *J Geophys Res* 1960;65:2883–5.
- Swarzenski PW, Reich CD, Spechler RM, Moore WS. Using multiple geochemical tracers to characterize the hydrogeology of the submarine spring off Crescent Beach, Florida. *Chem Geol* 2002;179:187–202.
- Talbot JM, Kroeger KD, Rago A, Allen MC, Charette MA. Nitrogen flux and speciation through the subterranean estuary of Waquoit Bay, Massachusetts. *Biol Bull* 2003;205:244–5.
- Tanaka T, Ono T. Contribution of soil water and its flow path to stormflow generation in a forested headwater catchment in central Japan. *IAHS Publ* 1998;248:181–8.
- Taniguchi M. Evaluation of vertical groundwater fluxes and thermal properties of aquifers based on transient temperature–depth profiles. *Water Resour Res* 1993;29:2021–6.
- Taniguchi M. Estimated recharge rates from groundwater temperatures in Nara basin, Japan. *Appl Hydrogeol* 1994;2:7–13.
- Taniguchi M. Change in groundwater seepage rate into Lake Biwa, Japan. *Jpn J Limnol* 1995;56:261–7.

- Taniguchi M. Evaluation of the saltwater–groundwater interface from borehole temperature in a coastal region. *Geophys Res Lett* 2000; 27:713–6.
- Taniguchi M. Tidal effects on submarine groundwater discharge into the ocean. *Geophys Res Lett* 2002;29. doi:10.1029/2002GL014987.
- Taniguchi M, Fukuo Y. Continuous measurements of ground-water seepage using an automatic seepage meter. *Ground Water* 1993; 31:675–9.
- Taniguchi M, Fukuo Y. An effect of seiche on groundwater seepage rate into Lake Biwa, Japan. *Water Resour Res* 1996;32:333–8.
- Taniguchi M, Iwakawa H. Measurements of submarine groundwater discharge rates by a continuous heat-type automated seepage meter in Osaka Bay, Japan. *J Groundw Hydrol* 2001;43:271–7.
- Taniguchi M, Sakura Y, Ishii T. Estimations of saltwater–fresh water interfaces and groundwater discharge rates in coastal zones from borehole temperature data. *Proceeding of Japanese Association of Groundwater Hydrology Meeting*, Tokyo, October; 1998. p. 86–9.
- Taniguchi M, Shimada J, Tanaka T, Kayane I, Sakura Y, Shimano Y, et al. Disturbances of temperature–depth profiles due to surface climate change and subsurface water flow: 1. An effect of linear increase in surface temperature caused by global warming and urbanization in the Tokyo metropolitan area, Japan. *Water Resour Res* 1999a;35:1507–17.
- Taniguchi M, Williamson DR, Peck AJ. Disturbances of temperature–depth profiles due to surface climate change and subsurface water flow: 2. An effect of step increase in surface temperature caused by forest clearing in southwest Western Australia. *Water Resour Res* 1999b;35:1519–29.
- Taniguchi M, Inouchi K, Tase N, Shimada J. Combination of tracer and numerical simulations to evaluate the groundwater capture zone. *IAHS Publ* 1999c;258:207–13.
- Taniguchi M, Burnett WC, Cable JE, Turner JV. Investigations of submarine groundwater discharge. *Hydrol Process* 2002; 16:2115–29.
- Taniguchi M, Turner JV, Smith A. Evaluations of groundwater discharge rates from subsurface temperature in Cockburn Sound, Western Australia. *Biogeochemistry* 2003a;66:111–24.
- Taniguchi M, Burnett WC, Smith CF, Paulsen RJ, O'Rourke D, Krupa S, et al. Spatial and temporal distributions of submarine groundwater discharge rates obtained from various types of seepage meters at a site in the northeastern Gulf of Mexico. *Biogeochemistry* 2003b;66:35–53.
- Taniguchi M, Burnett WC, Dulaiova H, Kontar EA, Povinic PP, Moore WS. Submarine groundwater discharge measured by seepage meters in Sicilian coastal waters. *Cont Shelf Res* 2006;26:835–42.
- Todd DK. *Groundwater hydrology*. 2nd edition. NY: John Wiley and Sons; 1980. 535 pp.
- Tsunogai U, Ishibashi J, Wakita H, Gamo T. Methane-rich plumes in the Suruga Trough (Japan) and their carbon isotopic characterization. *Earth Planet Sci Lett* 1999;160:97–105.
- Vacher HL. Dupuit–Ghyben–Herzberg analysis of strip-island lenses. *Geol Soc Amer Bull* 1988;100:580–91.
- Valiela I, D'Elia C. Groundwater inputs to coastal waters. *Special Issue Biogeochemistry* 1990;10 [328 pp.].
- Valiela I, Teal JM, Volkman S, Shafer D, Carpenter EJ. Nutrient and particulate fluxes in a salt marsh ecosystem: tidal exchanges and inputs by precipitation and groundwater. *Limnol Oceanogr* 1978; 23:798–812.
- Valiela I, Foreman K, LaMontagne M, Hersh D, Costa J, Peckol P, et al. Couplings of watersheds and coastal waters: sources and consequences of nutrient enrichment in Waquoit Bay, Massachusetts. *Estuaries* 1992;15:443–57.
- Valiela I, Bowen JL, Kroeger KD. Assessment of models for estimation of land-derived nitrogen loads to shallow estuaries. *Appl Geochem* 2002;17:935–53.
- Vanek V. Groundwater regime of a tidally influenced coastal pond. *J Hydrol* 1993;151:317–42.
- Webster IT, Norquay SJ, Ross FC, Wooding RA. Solute exchange by convection within estuarine sediments. *Estuar Coast Shelf Sci* 1996;42:171–83.
- Williams MO. Bahrain: port of pearls and petroleum. *Natl Geogr* 1946;89:194–210.
- Williams JB, Pinder III JE. Ground water flow and runoff in a coastal plain stream. *Water Resour Bull* 1990;26:343–52.
- Winter TC. The interaction of lakes with variably saturated porous media. *Water Resour Res* 1983;19:1203–18.
- Winter TC. Effect of ground-water recharge on configuration of the water table beneath sand dunes and on seepage in lakes in the sand hills of Nebraska, U.S.A. *J Hydrol* 1986;86:221–37.
- Winter TC. Numerical simulation analysis of the interaction of lakes and groundwater. *US Geol Survey Prof Paper* 1996;1001 [45 pp.].
- Wright, M.D. The flushing and circulation patterns of Jervoise Bay, Northern Harbour. *BEng Honours Thesis*, University of Western Australia, Perth, 2000.
- Wyatt A. *Challinor's dictionary of geology*. 6th ed. Cardiff: University of Wales Press; 1986. 374 pp.
- Younger PL. Submarine groundwater discharge. *Nature* 1996;382: 121–2.
- Zektser, I.S. Groundwater discharge into the seas and oceans: state of the art. In: Buddemeier RW, editor. *Groundwater discharge in the coastal zone* (pp. 122–123). *LOICZ IGBP, LOICZ, Texel, Netherlands, Russian Academy of Sciences, Moscow*, 1996, 179 pp.
- Zektser IS. *Groundwater and the environment: applications for the global community*. Boca Raton: Lewis Publishers; 2000. 175 pp.
- Zektser IS, Dzhamalov RG. Groundwater discharge to the Pacific Ocean. *Hydrol Sci Bull* 1981;26:271–9.
- Zektser IS, Loaigiga HA. Groundwater fluxes in the global hydrologic cycle: past, present and future. *J Hydrol* 1993;144:405–27.
- Zektser IS, Ivanov VA, Meskheteli AV. The problem of direct groundwater discharge to the seas. *J Hydrol* 1973;20:1–36.